STII

WT-414 (EX)

EXTRACTED VERSION

OPERATION JANGLE

Summary Report: Weapon Effects Tests

c. c. 2
DEFENSE NUCLEAR AGENCY
TECHNICAL LIBRARY
9 JUL 1980

Armed Forces Special Weapons Project
Washington, D.C.

Nevada Proving Grounds
October—November 1951

DNA1.940930.017

DTL-80,0983

NOTICE

This is an extract of WT-414, Operation JANGLE, "Summary Report," which remains classified Secret/Restricted Data as of this date.

Extract version prepared for:
Director
DEFENSE NUCLEAR AGENCY
Washington, D.C. 20305

1 October 1979

Approved for public release; distribution unlimited.

HRE-0716

Unclassified

SECURITY CLASSIFICATION OF THIS PAGE (When Data Entered)

REPORT DOCUMENTATION PAGE		READ INSTRUCTIONS BEFORE COMPLETING FORM
1. REPORT NUMBER WT-414 (EX)	2. GOVT ACCESSION NO	3. RECIPIENT'S CATALOG NUMBER
4. TITLE (and Subtitle) Operation JANGLE - Summary Report: Weapon Effects Tests		5. TYPE OF REPORT & PERIOD COVERED
		6. PERFORMING ORG. REPORT NUMBER WT-414 (EX)
7. AUTHOR(s) M. S. George A. F. Spilhaus		8. CONTRACT OR GRANT NUMBER(s)
9. PERFORMING ORGANIZATION NAME AND ADDRESS Armed Forces Special Weapons Project Washington, D. C.		10. PROGRAM ELEMENT, PROJECT, TASK AREA & WORK UNIT NUMBERS
11. CONTROLLING OFFICE NAME AND ADDRESS		12. REPORT DATE November 1952
		13. NUMBER OF PAGES 153
14. MONITORING AGENCY NAME & ADDRESS(if different from Controlling Office)		15. SECURITY CLASS. (of this report) Unclassified
		15a. DECLASSIFICATION/DOWNGRADING SCHEDULE

16. DISTRIBUTION STATEMENT (of this Report)

Approved for public release; unlimited distribution.

17. DISTRIBUTION STATEMENT (of the abstract entered in Block 20, if different from Report)

18. SUPPLEMENTARY NOTES

This report has had the classified information removed and has been republished in unclassified form for public release. This work was performed by the General Electric Company-TEMPO under contract DNA001-79-C-0455 with the close cooperation of the Classification Management Division of the Defense Nuclear Agency.

19. KEY WORDS (Continue on reverse side if necessary and identify by block number)

Nuclear Effects
Airblast
Craters
Ground Motion
Thermal Radiation
Radiological Effects
Dose Measurements

20. ABSTRACT (Continue on reverse side if necessary and identify by block number)

DD FORM 1 JAN 73 1473 EDITION OF 1 NOV 65 IS OBSOLETE

Unclassified

FOREWORD

This report has had classified material removed in order to make the information available on an unclassified, open publication basis, to any interested parties. This effort to declassify this report has been accomplished specifically to support the Department of Defense Nuclear Test Personnel Review (NTPR) Program. The objective is to facilitate studies of the low levels of radiation received by some individuals during the atmospheric nuclear test program by making as much information as possible available to all interested parties.

The material which has been deleted is all currently classified as Restricted Data or Formerly Restricted Data under the provision of the Atomic Energy Act of 1954, (as amended) or is National Security Information.

This report has been reproduced directly from available copies of the original material. The locations from which material has been deleted is generally obvious by the spacings and "holes" in the text. Thus the context of the material deleted is identified to assist the reader in the determination of whether the deleted information is germane to his study.

It is the belief of the individuals who have participated in preparing this report by deleting the classified material and of the Defense Nuclear Agency that the report accurately portrays the contents of the original and that the deleted material is of little or no significance to studies into the amounts or types of radiation received by any individuals during the atmospheric nuclear test program.

PREFACE

Part One is a general summary of the major findings as applied to operational weapons. Part Two is a resume of the results obtained with the test weapons together with a discussion of the problems involved in extrapolation. This report is based principally on the final project reports of the various agencies participating in the operation. These have been consolidated into 28 volumes and are listed in Appendix A.

It should be pointed out that a preliminary report, "Operation JANGLE, Weapons Effects Tests" was issued by the Armed Forces Special Weapons Project in January, 1952, to satisfy the immediate need for data, which, together with operational considerations, could be used to make decisions relative to the stockpiling of several types of atomic bombs. In general, the conclusions reached in the preliminary report agree with those reported herein with the exceptions indicated below. In view of these and other detailed changes the preliminary report should be disregarded.

a. Comparison of radiological effects for [illegible] underground detonation with those for an [illegible] KT surface detonation have been modified.

b. Fall-out of radioactive debris from the cloud from underground detonations at scaled depths comparable to the JANGLE underground appears to be of greater importance and that from the base surge of less importance than previously indicated.

c. Some but not all of the physical laws governing scaling between HE and nuclear detonations have been demonstrated.

d. Some of the capabilities and limitations of techniques and equipment developed for military operations have been further evaluated.

The JANGLE Operation was carried out under the general direction of Dr. A. C. Graves, Test Director, with Dr. A. F. Spilhaus as Deputy Test Director for Weapons Effects. Field operations at the site were under the general direction of Dr. J. C. Clark, Deputy Test Director. The weapons effects programs were carried out under the direction of Colonel Max S. George, FA, USA, Director of Effects Tests, assisted by Lt.Col. G. M. McHaney, USA.

This report was prepared by members of the staff of the Deputy Test Director for Weapons Effects, consisting of the following individuals: Dr. H. L. Andrews, USPHS; CDR E. J. Hoffman, USN; Lt.Col. E. A. Martell, USA; CDR D. C. Campbell, USN; LCDR J. J. Newman, USN; LCDR L. H. O'Donnell, USN; and 1st Lt. R. A. Burgin, USAF.

Acknowledgement is made of the valuable assistance of Dr. Herbert Scoville, Jr., Mr. Sherwood B. Smith, Mr. Benjamin Sassholz, and other members of the staff of Headquarters, Armed Forces Special Weapons Project. Special mention is made of those, listed below, who reviewed the report in whole or in part and provided much helpful comment:

C. W. Lampson, Ballistic Research Laboratory
G. K. Hartmann, Naval Ordnance Laboratory
Frederick Reines, Los Alamos Scientific Laboratory
D. T. Griggs, University of California
Ernest Plesset, Rand Corporation
John Bugher, Atomic Energy Commission
P. C. Tompkins, U. S. Naval Radiological Defense Laboratory
C. H. Morris, Massachusetts Institute of Technology
Edgar Fey, Armour Research Institute
Arsham Amirikian, Bureau of Yards and Docks, Department of the Navy

CONTENTS

PREFACE iii

CONTENTS v

ILLUSTRATIONS ix

TABLES xi

PART I

JANGLE DATA EXTRAPOLATED TO OPERATIONAL WEAPONS

CHAPTER 1 INTRODUCTION 1

1.1 General 1
1.2 Objectives 1
1.3 Limitations 2
1.4 Scope of Tests. 2
1.4.1 Phenomena Measured 3
1.5 Test Detonations. 3
1.5.1 Specific Objectives of the Shots. 4

CHAPTER 2 ESTIMATES FOR OPERATIONAL WEAPONS. 6

2.1 Weapons 6
2.2 Summary of Estimated Effects 6
2.3 Craters 6
2.4 Air Blast 9
2.5 Ground Shock 11
2.6 Structural Damage 11
2.6.1 Significant Conclusions Drawn from Extrapolations 11
2.7 Thermal Radiation 12
2.8 Radiological Effects. 13
2.8.1 Comparison of [redacted] Underground and [redacted] KT Surface Detonations. 14

CHAPTER 3 CONCLUSIONS AND RECOMMENDATIONS. 21

3.1 Conclusions 21
3.2 Recommendations 22

PART II

RESUME OF JANGLE RESULTS

CHAPTER 4 THE TEST EXPLOSIONS 23

4.1 General. 23
4.2 Surface Detonation 23
4.3 Underground Detonation 24
4.4 HE Bursts. 32
4.5 Craters Produced by the Nuclear Tests. 32

CHAPTER 5 AIR BLAST AND GROUND PHENOMENA. 38

5.1 Pressure Measurements in the Air Above the Burst . 38
5.2 Pressure Measurements Along the Ground 38
5.3 Blast Efficiencies 41
5.4 Ground Accelerations 43
5.5 Ground Pressures 46
5.6 Permanent Displacements. 47

CHAPTER 6 EFFECTS ON STRUCTURES 51

6.1 General. 51
6.2 Surface Structures 51
6.3 Buried Structures. 52
6.4 Shafts 53
6.5 Reinforced Concrete Box. 53
6.6 Missiles 54
6.7 Summary. 54

CHAPTER 7 THERMAL RADIATION 55

7.1 Thermal Radiation vs Distance. 55
7.2 Spectrum of Thermal Radiation - Surface Detonation 55

CHAPTER 8 RADIOLOGICAL EFFECTS 57

8.1 General 57
8.2 Gamma Radiation Dose Rate vs Time 57
8.3 Total Gamma Radiation Dose Measurements. 69
8.4 Radiological Importance of Base Surge 69
8.5 Gamma Energy Measurements. 70
8.6 Beta Radiation Measurements. 70
8.7 Particle Studies 72
8.7.1 Principal Results and Conclusions from Particle Studies 72
8.8 Nature of Residual Contamination 75
8.9 Inhalation Studies 77

8.10 Gamma Depth-Dose Measurements 78
8.11 Sampling Techniques 78

CHAPTER 9 TESTS OF SERVICE EQUIPMENT AND OPERATIONS 79

9.1 Introduction 79
9.2 Evaluation of Military Radiac Equipment 79
9.3 Aerial Radiological Survey Techniques. 80
9.4 Protection and Decontamination of Land Targets and Vehicles 81
9.5 Military Individual and Collective Protection Devices and Clothing 83
9.6 Evaluation of Potential Respiratory Hazards Associated with Tank Operations in a Radioactively Contaminated Area. 83
9.7 Consideration of Radioactive Contamination in Major Overhaul of Aircraft Turbo-jet Engines 84
9.8 Clothing Decontamination and Evaluation of Laundry Methods 84
9.9 Evaluation of U. S. Army Field Water Supply Equipment and Operations 84

CHAPTER 10 INDIRECT BOMB DAMAGE ASSESSMENT. 86

10.1 General. 86
10.2 Method 86
10.3 Underground Detonation 86
10.4 Surface Detonation 86
10.5 Conclusion 86

CHAPTER 11 LONG-RANGE DETECTION 87

11.1 Radiochemical Analyses 87
11.2 Acoustic Detection 87
11.3 Seismic Detection 87

CHAPTER 12 EXTRAPOLATION OF TEST RESULTS TO OPERATIONAL CONDITIONS 89

12.1 Introduction 89
12.2 Influence of Soil 89
12.3 Influence of Meteorology 91
12.3.1 Effect of Wind Velocity on the Distribution of Residual Contamination 91
12.3.2 Effect of Wind Shear 92
12.3.3 Effect of Rain 92
12.3.4 Effect of Delivery Technique 92

12.4 Scaling 93
12.4.1 Craters 93
12.4.2 Air Blast Overpressure 96
12.4.3 Ground Accelerations 96
12.4.4 Ground Pressures 97
12.4.5 Thermal Radiation 97
12.4.6 Radiological Effects 98
12.4.6.1 Dose-rate Scaling 98
12.4.6.2 Total Dose Scaling 98
12.4.7 Reliability of Scaling Radiological Effects 99

CHAPTER 13 CONCLUSIONS AND RECOMMENDATIONS 101

13.1 Conclusions 101
13.2 Recommendations 102

REFERENCES 103

APPENDIX A JANGLE REPORT VOLUMES 104

APPENDIX B CONDITIONS OF NUCLEAR TESTS 112

APPENDIX C BASIC PHYSICAL MEASUREMENTS 116

APPENDIX D RADIOACTIVITY AND BIOMEDICAL MEASUREMENTS INSTRUMENTATION 121

APPENDIX E STRUCTURES TESTS 128

ILLUSTRATIONS

2.1 Penetration vs Impact Velocity [ ] 8
2.2 Air Overpressure Along Ground vs Distance from Zero for [ ] KT Air, [ ] Surface, and [ ] KT Underground Bursts at Sea Level . . 10
2.3 Air Overpressure vs Height Above Zero for [ ] KT Surface and [ ] KT Underground Bursts at Sea Level 10
2.4 Total Gamma Dose for First 10 Seconds vs Distance from Ground Zero at Sea Level 15
2.5 Total Dose in Roentgens at 10 Minutes, [ ] KT Surface Shot. Wind Speed 15 mph 16
2.6 Total Dose in Roentgens at 10 Minutes, [ ] KT Underground Shot. Wind Speed 5 mph 16
2.7 Total Dose in Roentgens at One Hour, [ ] KT Surface Shot. Wind Speed 15 mph 17
2.8 Total Dose in Roentgens at One Hour, [ ] KT Underground Shot. Wind Speed 5 mph 17
2.9 Dose Rates in Roentgens Per Hour, [ ] KT Surface Shot. Wind Speed 15 mph 18
2.10 Dose Rates in Roentgens Per Hour at One Hour, [ ] KT Underground Shot. Wind Speed 5 mph 18
4.1 JANGLE Area Layout 25
4.2 Initial Stages of Surface Nuclear Shot 26
4.3 Early Stages of Underground Nuclear Shot 27
4.4 Formation and Growth of Column and Cloud of Surface Shot . . . 28
4.5 Surface Shot at Approximately One Minute 29
4.6 Formation of Base Surge and Growth of Cloud of Underground Shot 30
4.7 Underground Shot at Plus 2 Minutes 31
4.8 2560 Pounds of High Explosive on Surface of Ground 33
4.9 40,000 Pounds of High Explosive at Same Scaled Depth as Underground Nuclear Shot. 34
4.10 2560 Pounds of High Explosive at 3.7 Times Scaled Depth of Underground Nuclear Shot 35
4.11 Crater and Lip for the Surface Detonation 36
4.12 Crater and Lip for the Underground Detonation 37
5.1 Air Overpressure for Surface and Underground Nuclear Shots from Shock Velocities Measured from Rocket Trails 39
5.2 Air Overpressure Along the Ground vs Distance from Zero for Surface and Underground Shots as Measured by Wiancko Gages and as Calculated from Shock Velocities Using Blast Switches . . . 40
5.3 Comparison of Scaled Air Pressures Along the Ground From Surface Shot and in Free Air From Higher Detonations 42
5.4 Accelerometer Records as a Function of Depth. Records are for vertical accelerations at depths of 10,20, and 30 feet at 1213 feet from zero for the surface and underground shots 44
5.5 A Comparison of Maximum Accelerations Produced by JANGLE Detonations 45

5.6 Permanent Horizontal Displacements about the Underground Zero 48
5.7 Permanent Vertical Displacements about the Underground Zero . 49
7.1 Thermal Energy vs Distance for the Surface Shot 56
8.1 Surface Shot, Dose Rate and Total Dose vs Time, Upwind . . . 58
8.2 Surface Shot, Dose Rate and Total Dose vs Time, Downwind . . 59
8.3 Underground Shot, Dose Rate and Total Dose vs Time, Upwind . 60
8.4 Underground Shot, Dose Rate and Total Dose vs Time, Downwind. 61
8.5 Surface Shot, Gamma Dose Rate Contours at H+1 Hour in Roentgens per Hour (Wind Profile Given in Table B.2) 62
8.6 Underground Shot, Gamma Dose Rate Contours at H+1 Hour in Roentgens per Hour (Wind Profile Given in Table B.2) 63
8.7 Total Gamma Dose in Roentgens for First 10 Seconds vs Distance from Ground Zero 64
8.8 Total Gamma Dose in Roentgens for First 10 Minutes, Surface Shot 65
8.9 Total Gamma Dose in Roentgens for First 10 Minutes, Underground Shot 66
8.10 Total Gamma Dose in Roentgens for First Hour, Surface Shot. . 67
8.11 Total Gamma Dose in Roentgens for First Hour, Underground Shot 68
8.12 Gamma Flux vs Energy, Low and Intermediate Energy Regions, Underground Shot 71
8.13 Per Cent of Total Station Activity Found in Particles of Less Than 75 Microns Diameter vs Distance Downwind, Surface Shot . 74
8.14 Per Cent of Total Station Activity Found in Particles of Less Than 75 Microns Diameter vs Distance Downwind, Underground Shot. 74
8.15 Beta Activity vs Time, Crater Lip Samples 76
D.1 Scintillation Counter Station Pattern, Surface Shot 125
D.2 Scintillation Counter Station Pattern, Underground Shot . . . 126
D.3 Thermal Recipitator and Differential Collector Stations . . . 127
D.4 Fall-out Collector Pattern 127
E.1 Structural Array, Underground Site 134

TABLES

1.1 First HE Series 4
1.2 Second HE Series. 5
2.1 Summary of Estimated Effects of Underground, Surface and Air Bursts 7
2.2 Range of Damage to Surface Structures 12
2.3 Range of Thermal Damage 13
2.4 Estimated Radiological Effects for Operational Weapons at Sea Level 20
6.1 Permanent Displacement of Vertical Shafts Around Underground Zero. 53
8.2 Activity vs Particle Size, Downwind 73
9.1 Decontamination Effectiveness 82
9.2 Vehicle Shielding 82
12.1 Effect of Wind on Gamma Dose and Dose Rate Areas. 93
12.2 Crater Radii Calculations from Lampson's Relationship 94
12.3 Crater Radii Calculations for Operational Weapons 95
B.1 Nuclear Detonations 112
B.2 Meteorological Conditions 113
B.3 Subsoil Characteristics at Zero Points 114
B.4 Density and Seismic Velocities at Zero Points 114
C.1 Summary of Basic Physical Measurements. 116
C.2 Basic Physical Measurements 117
E.1 Structural Test Projects 128

PART I

JANGLE DATA EXTRAPOLATED TO OPERATIONAL WEAPONS

CHAPTER 1

INTRODUCTION

1.1 GENERAL

Operation JANGLE was executed at the Nevada Test Site (now Nevada Proving Grounds) in the fall of 1951 to determine the properties of large surface and underground atomic explosions. It involved the detonation of 13 high explosive charges and two atomic bombs of 1.2 KT yield.

An operation of this nature was conceived soon after the underwater test of Operation CROSSROADS and approved by the Joint Chiefs of Staff in November, 1950. Since weapons of operational size were under consideration, safety considerations dictated that such an operation be done at a site outside the continental United States. The test was scheduled to be conducted on Amchitka Island in the Aleutian chain under the code name WINDSTORM.

A detailed examination of the soil and meteorological conditions on Amchitka indicated that an operation there would produce results of marginal value. Consequently, on 9 May 1952 the Joint Chiefs of Staff indefinitely postponed Operation WINDSTORM and directed the execution of Operation JANGLE at the Nevada Test Site.

The move from Amchitka to Nevada necessitated a change in the weapons to be detonated. The possibility of contaminating a large area limited the yield of the weapons to about 1 KT. 1/ As a result, it has been necessary to extrapolate from the results for the 1 KT weapons to estimate the effects stated herein for weapons of operational size.

1.2 OBJECTIVES

The objectives of Operation JANGLE were considered to be:

a. To determine the military effects of atomic weapons detonated underground and on the ground surface.

b. To determine the relative effectiveness and fissionable material economy of atomic weapons capable of detonation underground and on

the surface for use in establishing the requirements for development and production of such weapons.

c. To determine the physical laws governing shock wave propagation and scaling between conventional high explosive (TNT) and nuclear detonations so that HE experiments can be used to predict the effects of nuclear explosions under varying conditions on a wide variety of targets.

d. To evaluate the suitability of equipment and techniques developed for military operations in which atomic weapons are used.

1.3 LIMITATIONS

It must be emphasized that Operation JANGLE involved the detonation of two 1.2 KT atomic bombs, one on the surface of the ground and the other 17 feet underground, whereas the operational weapons to be compared are quite different in energy release and conditions of detonation. Using the data obtained from the 1.2 KT detonations to estimate results likely to accrue from larger bombs involves extrapolations which can be accepted only with caution.

The results and the predictions reported herein apply with greatest certainty to situations which most nearly duplicate the conditions which prevailed at the Nevada site. The significant variables to be considered are soil and meteorology. The earth in which the test was conducted had a high attenuation to ground shock. There are indications that this attenuation is near the higher limit of the range for common soil types. The shots were detonated in clear, dry, desert weather with about a 5 mile per hour surface wind. These weather conditions were favorable for the study of the spread of radioactivity. Other weather conditions will materially affect the area and intensity of residual contamination.

This report is restricted to a description of the effects which may be anticipated from the use of weapons in wartime and is not concerned with other operational factors. However, in scaling the effects of the test weapons to operational weapons, some limited consideration has been given to factors that are inherently a part of the target, the method of delivery, and the meteorological conditions at the time of delivery.

1.4 SCOPE OF TESTS

Operation JANGLE provides the first experimental data on the military effects of surface and underground detonations of atomic weapons. Prior to this operation estimates were based on theories developed from studies of results from high explosive tests and the underwater deto-

nation of Operation CROSSROADS.

Since the test weapons were considerably lower in yield than presently developed operational weapons, and since the test programs were carried out in only one environment, only marginal basic data on the effects of surface and underground detonations were obtained. These data serve to fill in major gaps in the weapons effects information and permit rough extrapolation of operational weapons and conditions.

1.4.1 Phenomena Measured

Operation JANGLE produced basic data on ground shock, air blast, and on the size and shape of craters from underground and surface bursts. Some information was obtained on missiles and throw-out.

Considerable information was obtained on the loading of and response of structures within the region of elastic structural action. Very little information was obtained for the region of plastic action and such data are necessary for the calculation of ultimate resistance.

Extensive measurements of gamma radiation rate versus time and distance were made. Sampling of fall-out and near-ground dust cloud was carried out over a broad pattern to determine the distribution of residual contamination and provide samples for radiochemical and particle studies. Biological studies were conducted to assess the beta and gamma hazard and possible inhalation hazard.

Extensive photographic records were obtained and have been partially analyzed to provide measurements of transient ground displacements, measurements of air blast, and correlation of visible phenomena with radioactivity records. These pictures will be useful for training and indoctrination.

The operation provided an excellent opportunity to field test various radiological defense measures. Field tests were also made of the techniques of long-range detection, indirect bomb damage assessment, and the vulnerability of various types of military equipment and fortifications.

1.5 TEST DETONATIONS

The following series of shots was fired to achieve the objectives of Operation JANGLE:

a. Thirteen high explosive (HE) shots using several weights of explosive from 177 pounds of pentolite to 40,000 pounds of TNT, fired underground and on the surface of the ground.

b. Surface shot [redacted] above ground, [redacted] 1.2 KT yield, [redacted] fired 19 November 1951.

c. Underground shot, same weapon as the surface shot, 1.2 KT yield center of gravity 17 feet underground, fired 29 November 1951.

1.5.1 Specific Objectives of the Shots

The HE shots listed in Table 1.1 were carried out in Yucca Flat prior to the nuclear explosions to provide a basis for selecting instrument ranges capable of recording data from the nuclear shots. In addition, these HE shots provided a basis for the assignment of equivalent TNT yields for the nuclear shots, and the possible establishment of TNT-nuclear scale relationships. A second series of HE shots, listed in Table 1.2, was fired in Frenchman Flat to provide basic data for base surge studies.

The surface nuclear shot was fired to determine the effect of detonating a weapon on or near the surface of the earth and to determine whether large yield weapons using relatively small amounts of fissionable material would produce underground effects equivalent to those produced by lower yield penetrating weapons using larger amounts of fissionable material. Air pressure information from a surface shot was required to give "0 height" data for height of burst curves.[2]

The underground nuclear shot was fired to provide a basis for the estimation of the effects to be expected from the detonation of a [redacted] penetrating weapon at a depth of approximately 50 feet underground.

TABLE 1.1

First HE Series

Shot	TNT W (pounds)	Depth to Charge Center of Gravity d (feet)	Scaled Depth $\lambda_c = \frac{d}{W^{1/3}}$	Date
HE-1	2560	2.05	0.15	25 Aug
HE-2	40,000	5.13	0.15	3 Sep
HE-3	2560	6.8	0.5	15 Sep
HE-4	2560	-2.05	-0.15	9 Sep

TABLE 1.2

Second HE Series

Shot	TNT W (pounds)	Depth to Charge Center of Gravity d (feet)	Scaled Depth $\lambda_c = \frac{d}{W^{1/3}}$	Date
HE-5	2560 TNT	4.1	0.30	20 Sep
HE-6	2560 TNT	3.0	0.22	2 Oct
HE-7	2560 TNT	2.6	0.19	4 Oct
HE-8*	216 TNT, 177 Pentolite	1.08	0.18	13 Oct
HE-9*	216 TNT, 177 Pentolite	0.84	0.14	14 Oct
HE-10*	216 TNT, 177 Pentolite	3.0	0.5	14 Oct

* Two separate charges fired simultaneously

CHAPTER 2

ESTIMATES FOR OPERATIONAL WEAPONS

2.1 WEAPONS

Two existing weapons have been selected to make comparative estimates of the major effects to be expected from surface and underground detonations of nuclear weapons of operational size.

The presently developed weapon capable of ground penetration is the [redacted] The scaled depth of 17 feet for the 1.2 KT test explosion corresponds to a depth of about 50 feet for the [redacted] The depth of penetration [redacted] will vary with the type of earth in the target area. A penetration of 30-40 feet may be expected in sand, 45-60 feet in loam, and 85-100 feet in plastic clay. The exact penetration in a given soil depends on the attitude and velocity of the bomb on impact.

Implosion type weapons capable of ground penetration have not been developed, but fusing of implosion weapons for detonation at or near the ground surface is practicable and under development. Therefore, the capabilities of such weapons detonated at the ground surface should be compared with those of the [redacted] In this report the [redacted] with an estimated yield of [redacted] KT has been used for comparison. Based on the assumption that 1 kg of plutonium is equivalent to 5 kg of uranium-235, one of these bombs would contain about one-third the equivalent amount of fissionable material in one [redacted] Other implosion weapons could be compared with some change in the relative economy in fissionable material. However, for all weapons with the [redacted] geometry the changes will be minor. The economy figure will be lower (the [redacted] will thus compare more favorably in this respect) for all weapons with the [redacted] geometry.

2.2 SUMMARY OF ESTIMATED EFFECTS

Table 2.1 is a brief summary of the estimated effects of a [redacted] detonated underground, an [redacted] KT surface detonation, and an [redacted] KT air burst fired at 3400 feet—the height of burst to give the maximum area covered by 10 psi air overpressure.

2.3 CRATERS

Results from the JANGLE operation indicate that predictions of

crater formation are reliable. This evaluation of reliability is based on a comparison of HE and nuclear results which is discussed under Crater Scaling, Paragraph 12.4.1.

Crater radii for underground explosions may be calculated from relationships developed in HE experiments [3,4] and from observed ballistic properties [ ] bomb case, which determine its penetration in a given soil [5]. Figure 2.1 shows the penetrations which may be expected for the [ ] weapon and Table 2.1 shows the crater dimensions calculated for several representative situations. The results of the nuclear shots in Nevada and the relationships from earlier HE experiments were used in making the calculations.

If a [ ] bomb were dropped in the center of an airfield runway, and penetrated to about 50-foot depth, it would produce a crater [ ] Reactivation of the runway for use by bombers (a strip of 200-foot mini-

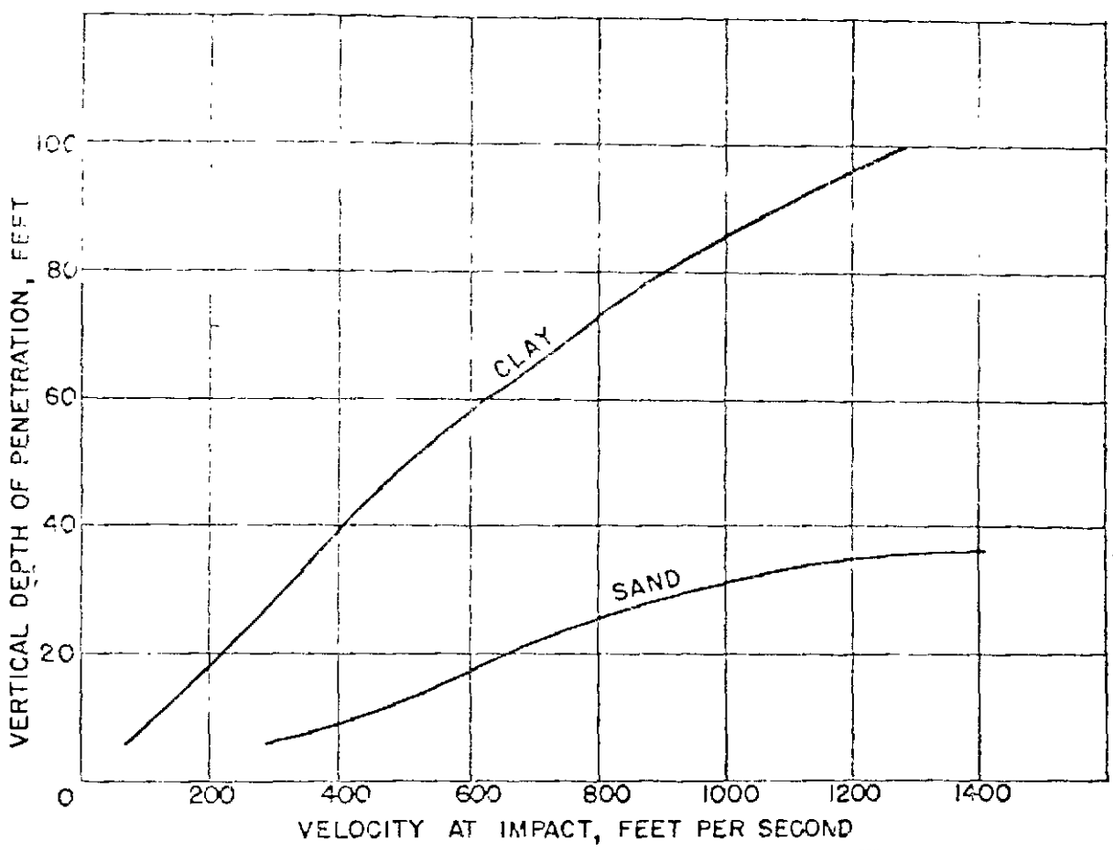

Fig. 2.1 Penetration vs Impact Velocity for [ ] Weapon

mum width) would take about [ ] cubic yards of fill and would require a minimum of about 30 days' work for completion under emergency operating conditions. Unless shielding for equipment operators were provided, it would be impracticable to start work before one or two weeks because of radioactive contamination. Even then, the repair forces must be prepared to provide several replacement crews of equipment operators and other personnel working in the immediate area. If shielding equivalent to 1/2 inch of steel were provided, work could begin within two days with few, if any, radiation casualties. After four weeks, the radiation problem would not seriously hinder construction.

An [ ] KT surface detonation under similar conditions would produce a crater [ ] To replace a 200-foot runway strip would take [ ] cubic yards of fill and would require about one week of work. Radioactive contamination would present about the same problems to the repair crews as in the case of the underground burst.

If atomic weapons are used in mining operations to produce a crater an implosion bomb should be buried deep underground, i.e., hundreds of feet for an [ ] KT bomb.

2.4 AIR BLAST

Air pressure measurements from the underground nuclear test showed characteristics similar to those observed with the scaled HE tests. Therefore, direct scaling for an operational weapon under the Nevada conditions appears justified. The effects for other depths of burial and other soil conditions are not as well established. Heavier soil or greater depths of penetration will reduce the overpressure as compared to JANGLE conditions.

Peak air pressures along the ground for the two operational weapons being considered are compared to the pressures obtained with an [ ] KT air burst in Figure 2.2.

Blast pressures in the air above either a surface or underground burst are a matter of interest for the safety of aircraft in that vicinity. Figure 2.3 gives peak overpressures for the operational weapons under consideration. These curves are scaled from the JANGLE data and corrected to give values at sea level. A correction for the decline in atmospheric pressure with increasing altitude above the surface must be used for any operational situation. These data apply for positions directly above the point of detonation. Further extension of the JANGLE data is required to give information for other positions in space.

2.5 GROUND SHOCK

Insufficient experimental data exist to establish laws which will allow scaling ground pressures and accelerations with their associated time characteristics and displacements to operational size weapons. For these ground phenomena no systematic relationship has been determined between the HE and the nuclear shots. Therefore, the immediate application of these data to operational conditions is impossible.

Comparison of the earth accelerations in the JANGLE HE tests and tests at the Dugway Proving Ground indicates that different soils and geological conditions will alter the distance at which a certain effect takes place by as much as a factor of three or more. In general, damaging effects will be transmitted to much greater distances in saturated soil, particularly wet clay, than in soil having smaller water content. A hard underlayer will reflect the ground effects and increase their range. In this respect it should be pointed out that regions of geologic nonuniformity become more important as the size of the charge increases.

The air blast from a surface or shallow underground explosion produces accelerations and pressures. In general, the highest peak values are produced through this action, but in the case of accelerations the peaks are of such short duration that they will usually be negligible in causing structural damage. The magnitude of these phenomena relative to direct transmitted effects increases with charge size.

2.6 STRUCTURAL DAMAGE

Dynamic model laws were used to extrapolate the test results from 1.2 KT bombs to the effects of operational weapons. The assumption that direct scaling is valid is questionable in several details. However, variation of results within the extremes considered probable will not alter the general picture.

2.6.1 Significant Conclusions Drawn From Extrapolations

Underground or surface weapons are the only effective means presently available for atomic attack on heavy fortifications, sub-pens, or other extremely resistant construction. Structures of this nature in soil similar to that at the Nevada Test Site would probably have to be within the crater to ensure appreciable damage. Table 2.1 indicates that the crater diameter of the [redacted] would be about twice that of the [redacted] KT surface weapon.

Surface structures are damaged primarily by air blast. Table 2.2 indicates that the [redacted] KT surface weapon would have a damage radius two to three times that of the [redacted] at overpressures in excess

of 10 psi. The pattern for severe damage to surface structures is given in Table 2.2. It is based on the criteria for air blast damage given in Reference 2.

The JANGLE tests indicate that the area of appreciable damage to light underground construction is quite limited. From the results of previous tests it appears that this area would be somewhat less than the damage area for heavy surface construction.

Calculations made on the resistance of truss bridges[6] indicate that ground shock is relatively ineffective in producing damage. The bridge piers would have to be virtually within the crater to ensure failure from pier displacement. However, the calculations show that the superstructure of such bridges of 150- to 300-foot span would be destroyed by air blast of 15 to 20 psi intensity. Direct extrapolation of the JANGLE data indicates that the [redacted] would give [redacted] psi at [redacted] yards and the [redacted] KT surface weapon would give this pressure at [redacted] yards.

TABLE 2.2

Range of Damage to Surface Structures

Type of Construction	Damaging Overpressure psi
Heavy Steel Frame Heavy Reinforced Concrete	25
Light Steel Frame Heavy Masonry	10
Light Masonry	5
Light Frame (Dwelling)	3

* Height to maximize area covered by 10 psi air blast overpressure

2.7 THERMAL RADIATION

The effects of thermal radiation from a surface detonation are much less than in the case of an air burst of the same weapon. The thermal energy an any given distance from a surface burst is about one-third that from an air burst. Even so, under good visibility conditions the danger area for thermal radiation to exposed personnel exceeds that of initial gamma radiation. A comparison of the thermal effects from a surface and an air burst is given Table 2.3. It should be noted that

in the case of the surface burst thermal radiation ranges depend much more on flatness of terrain.

Thermal radiation effects decrease greatly with penetration of the weapon into the ground. They will be negligible in the case of weapons fired at depths comparable to the JANGLE underground shot.

TABLE 2.3

Range of Thermal Damage

Effect	Thermal Energy (Cal./cm^2)
Moderate skin burns	3
3rd degree skin burns	9
Cotton twill, khaki or green, destroyed light woolen fabric, khaki, destroyed	15
16 oz. wool jersey or elastique, green, destroyed	30

* Tabulated Values are horizontal distances from ground zero, feet

2.8 RADIOLOGICAL EFFECTS

The radiological effect produced by nuclear weapons detonated on the ground surface or underground is a major one. Just as for the air burst, gamma radiation during the first few seconds following such detonations will produce casualties over a large area. For both the surface and underground detonations, the danger area from this early gamma radiation is comparable to that in which light surface structures receive major damage from air blast.

The radioactive debris from either the surface or the underground detonation is associated with large particles which are deposited at a sufficiently rapid rate to produce significant concentrations of radioactive contamination over extensive areas around and downwind from the zero point. Apart from the change in wind direction with height, the crosswind extent of the area of residual contamination is dependent on the weapon, its method of detonation, and soil conditions. The downwind

extent of the area is largely determined by the wind velocity.

Important radiological hazards associated with contaminating bursts and estimates of effects to be expected for [redacted] underground and for an [redacted] KT surface detonation are presented in Section 2.8.1. Estimates are presented for effects at sea level with an average wind velocity of 5 miles per hour for the [redacted] and 15 miles per hour for the [redacted] KT surface burst. This selection of winds is arbitrary but is considered reasonable since surface shot clouds will rise considerably higher than the underground shot clouds and in general will move in a higher wind speed region.

2.8.1 Comparison of [redacted] Underground and [redacted] KT Surface Detonations

A surface detonation of an implosion weapon is the most economical method in terms of fissionable materials for producing lethal radiation dosages over large areas under all probable wind conditions. The areas receiving lethal dosage within any period of time are not significantly different between surface detonations and underground detonations up to the JANGLE scaled depth for weapons of equal energy release fired under comparable wind conditions.

The most significant factor in determining the area contaminated to any specific radiation level for a given yield is the wind.

The area receiving lethal dosage in the first 10 seconds is considerably greater for an [redacted] KT surface burst than for a [redacted] underground burst. (See Fig. 2.4 and Table 2.4.)

Areas receiving lethal dosage in the first 10 seconds for underground and surface detonations in irregular terrain and in developed areas will be drastically reduced due to shielding. For large air bursts detonated at heights maximizing 10 psi air overpressures the loss in area receiving lethal gamma radiation dose is considerable due to increased slant range. (See Fig. 2.4.) The danger area for initial gamma radiation is greatest for low to intermediate height air bursts where the shielding losses are balanced against slant range losses.

The area receiving lethal dosage in the first 10 minutes is more than twice as great for an [redacted] KT surface burst as that for a [redacted] underground burst. (See Fig. 2.5 and 2.6 and Table 2.4.)

The area receiving lethal dosage in one hour from an [redacted] KT surface burst is about three times that from a [redacted] underground burst. (See Figs. 2.7 and 2.8 and Table 2.4.) In the case of the scaling for one hour dosages involved here, the uncertainties are increased to a factor of about 2 due to the wind influence.

Areas unsafe for troops operating in the open (i.e., area exceeding a dose rate of 300 r/hr at one hour) are extensive for several hours and might be about three times as large for an [illegible] KT surface burst as for a [illegible] underground burst. (See Figs. 2.9 and 2.10 and Table 2.4.) These areas continue to change in shape and size after one hour in a complex manner due to wind and radioactive decay, extending further downwind as a result of later fall-out and shrinking due to decay.

Areas of significant residual contamination (greater than 100 r/hr at one hour) for both surface and underground detonations scale roughly as the yield to the two-thirds power. Uncertainties in the prediction of location and size of areas of contamination due to unreliability of scaling are aggravated by uncertainties to be expected from predicted meteorology.

The base surge associated with underground atomic detonations at the JANGLE scaled depth appears to be secondary in its contribution to transient radiation dosage and in its distribution of residual contamination. The bulk of the activity is initially in the central upper cloud. The base surge associated with the underground detonation deposits some contamination but the relative contribution from base surge and fall-out has not been evaluated from present data.

The contribution of soil induced radioactivity to residual contamination should be small for surface and subsurface detonations in most soils for all weapons except those in which the ratio of escape neutrons to total fissions is markedly increased over the ratio for the JANGLE weapon. The [illegible] would increase the ratio of escape neutrons to total fissions and thus increase the soil induced radioactivity.

The inhalation of radioactive particles constitutes no military hazard* independent of external gamma radiation hazards of more serious consequence.

Long term biological effects from inhaled particles are very doubtful but not ruled out.

Subjecting an urban area to radioactive contamination by either a surface or subsurface burst will not result in denying permanent occupancy of this area. With the exception of the crater and environs, substantial reoccupation may take place within a matter of weeks.

Weapons of yield greater than 1 KT may be fired safely underground and on the surface within the continental United States.

---

* In this report the term "military hazard" is used to imply a reduction in combat effectiveness in a relatively short time (several hours to one week). See Reference 7.

pgs. 15 thru 18 DELET

A[redacted] fired about 50 feet underground at the Nevada Proving Grounds would be less harardous than a tower shot of comparable yield from the point of view of radioactive fall-out outside the immediate test area.

CHAPTER 3

CONCLUSIONS AND RECOMMENDATIONS

3.1 CONCLUSIONS

The military effects of atomic weapons detonated underground and on the surface were determined to be:

a. The creation of large craters.

b. The creation of areas of high air blast overpressures which would damage heavy surface structures.

c. The coupling of considerable energy into the ground which, under favorable circumstances, would probably cause damage to heavy, buried structures and fortifications somewhat beyond the limits of the crater volume.

d. The creation of large areas where the total radiation dosage is above lethal to personnel in the open and which have high levels of residual radioactive contamination.

e. In the case of the surface weapon the creation of thermal radiation which is dangerous to exposed personnel over large areas.

The relative effectiveness of the two weapons compared [detonated underground and an [ ] detonated at the surface) in producing these results of military importance is indicated below. It should be noted that the [ ] uses about three times the amount of fissionable material as that used in the [ ] Any comparison to be made on the basis of economy of fissionable material must weigh the comparisons of effectiveness by this factor.

a. The [ ] is from ten to twenty times as effective in producing volume of crater. It is four to eight times as effective if area at the surface of the crater is selected as the criterion. For crater formation the surface weapon is not sensitive to small heights of burst, i.e., less than 50 feet.

b. The radius of damage to heavy, buried structures and fortifications is more than twice as great for the [ ] as for the [ ]

c. The [ ] will damage heavy, surface structures (25 psi air pressure or greater) at a distance about three times as great as the

[ ]

d. The [ ] may be as much as three times as effective in creating areas of high radioactive contamination as the [ ]

e. Only the [ ] will produce significant thermal effects.

3.2 RECOMMENDATIONS

This test has demonstrated that the [ ] and the surface detonated implosion weapons are special purpose atomic weapons which have significantly greater effectiveness than other types in damaging underground and massive structures, in producing craters, and in distributing radioactive contamination over extensive areas. It is recommended that operational studies to determine the use of these weapons be restricted to situations where these factors are of primary importance.

In the use of these weapons, target intelligence will be particularly important since the radius of the above significant military effects will be markedly altered by the character of the soil, and the meteorology at the time of the drop as well as the method of delivery.

PART II

RESUME OF JANGLE RESULTS

CHAPTER 4

THE TEST EXPLOSIONS

4.1 GENERAL

Data on the weapons, soil and meteorology are presented in Appendix B. Detailed information regarding basic physical measurements, radioactivity and biological measurements and structural tests is given in Appendices C, D and E respectively. A general layout of the JANGLE test area is shown in Figure 4.1.

4.2 SURFACE DETONATION

The visible phenomena observed during the 1.2 KT nuclear surface detonation were, in some respects, similar to those associated with low air bursts. This was particularly true of the later visible form of the detonation consisting of the typical smoke column and mushroom shaped cloud. Differences in form were obviously the result of the column and cloud being heavily loaded with dirt and dust.

Upon detonation there was an emission of very high intensity visible radiation which rapidly diminished to a low irregular configuration of incandescent dirt and dust. Although the luminosity persisted for several seconds, the ball of fire was greatly obscured and diluted when it finally emerged from the surface debris in true spherical shape after about one and a half seconds. At this time the top of the sphere was at a height of approximately 900 feet and the sphere was rising at the rate of about 200 feet per second. These immediate visible phenomena are shown in Figure 4.2.

As the high temperature sphere rose from the surface debris, the latter subsided and joined the surface dust cloud created by the shock wave striking the ground. No base surge was formed. As the sphere cooled and ascended, a chimney effect was noted wherein the trailing column of dust and debris was sucked up from the surface. This later visible form of the column and cloud was very similar to that of a low air burst. At no time, however, was the sphere or upper cloud separated from the visible column. The formation and growth of the column and

upper cloud are presented in Figure 4.3

The upper cloud and column continued to expand and rise for several minutes after formation, gradually drifting downwind and dispersing. Figure 4.4 shows the fully developed form from the surface detonation before being dispersed by winds. The maximum height of the main cloud mass was about 6400 feet.

4.3 UNDERGROUND DETONATION

As anticipated, the visible phenomena observed for the underground nuclear detonation materially differed from those of air, surface, and underwater nuclear bursts. They did not differ, however, except in degree, from those observed for large TNT underground explosions.

High intensity illumination accompanying the underground detonation lasted an extremely short time. No illumination was visible after sixteen hundredths of a second. Large quantities of earth and debris were thrown upward and outward with very high velocity within a very short period of time to form an inverted conical shape. This throw-out reached a height of 900 feet and a diameter of 1200 feet in about one-half of a second after the detonation. These immediate visible phenomena are presented in Figure 4.3.

Approximately 2 seconds after detonation the rate of rise of the throw-out material subsided and large streamers of dirt and dust were expelled from the sides of the inverted cone. These struck the ground and joined the surface dust cloud created by the air blast. A chimney effect was briefly observed at about this time, although it was of short duration and did not materially affect the form of the dust cloud. The central portion of the inverted cone continued to rise as an irregular geometrical shape at a relatively slow rate of about 35 feet per second.

At about 15 seconds after detonation a base surge cloud of fine dust particles appeared at the base of the column. This cloud continued to expand for about 3 minutes, reaching a maximum crosswind radius of about 2200 feet. Large quantities of material continued to fall into the surge after the radial growth of the surge cloud had ceased, increasing the surge height but having little effect on the diameter. The surge height increased continually for about 10 minutes, gradually dispersing in a downwind direction. The above phenomena are shown in Figure 4.6.

A distinct upper cloud, heavily loaded with dirt and attached to a lower and less opaque cloud, continued to rise and expand until more than 3 minutes after detonation, reaching a maximum height of about 5000 feet. Figure 4.7 shows the fully developed form of the

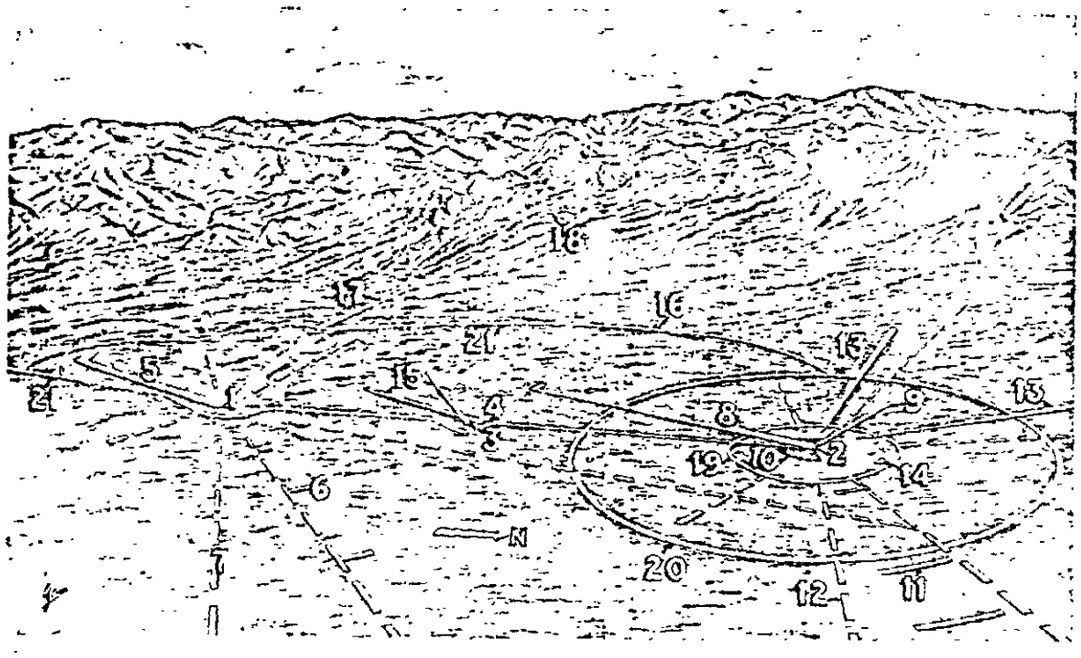

Fig. 4.1 JANGLE Area Layout

1. Zero for surface nuclear shot
2. Zero for underground nuclear shot
3. Zero for HE-1, 3, 4
4. Zero for HE-2
5. Line for blast measurements, surface nuclear shot
6. Stations for exposure of biological specimens for surface shot
7. Lines for gamma radiation measurement and particle collection stations for surface shot
8. Main line for blast measurements, underground nuclear shot
9. Minor line for blast measurements
10. Area for test structures
11. Stations for exposure of biological specimens for underground shot
12. Lines for gamma radiation measurement and particle collection stations for underground shot
13. Missile collection areas
14. Test areas for land decontamination
15. Lines for blast measurements for HE tests
16. Main distribution station for timing signals for the nuclear shot
17. Recording station for gamma intensity measurements
18. Recording station for free air pressure measurements
19. 2000-foot circumferential road
20. One mile circumferential road
21. Approach roads

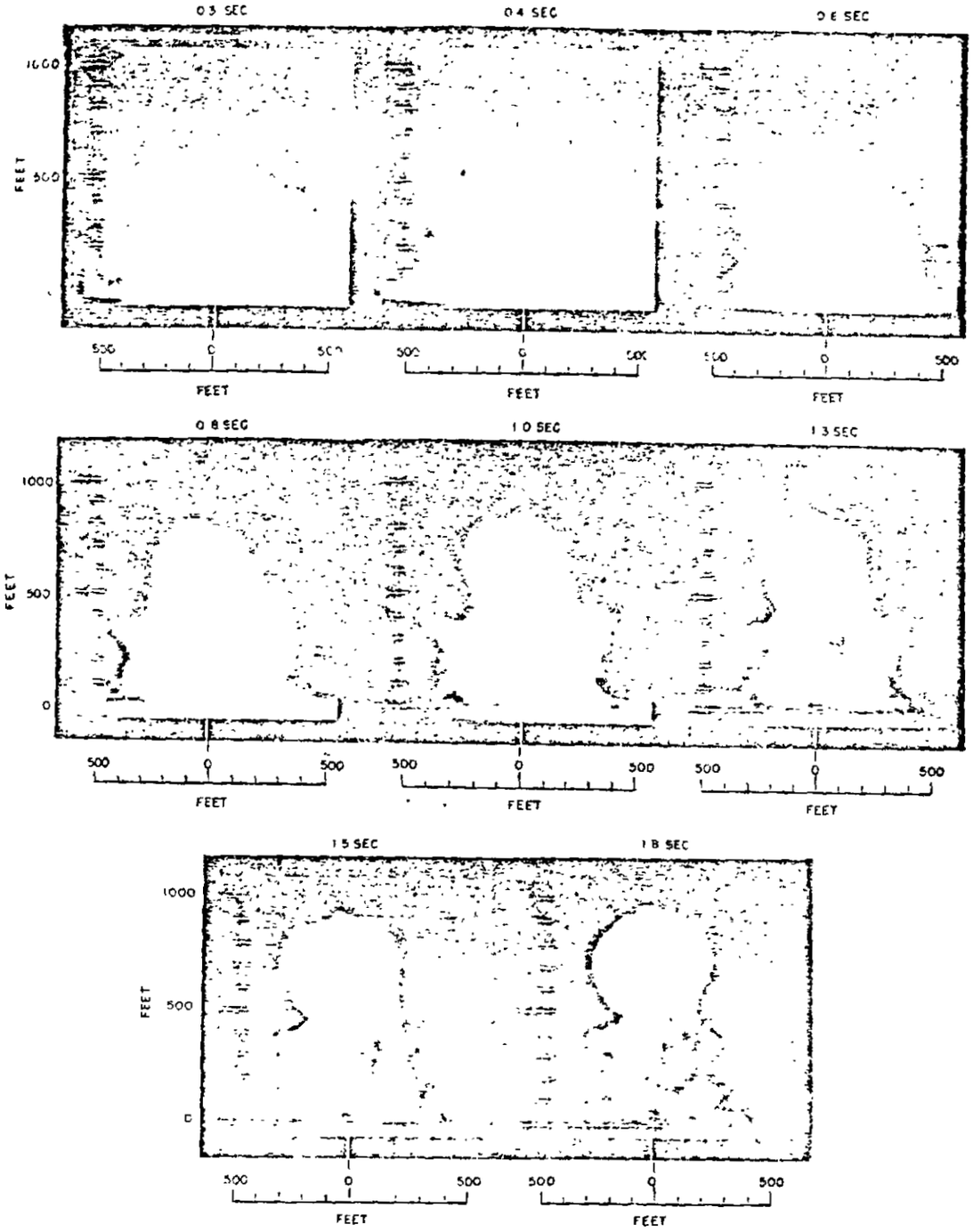

Fig. 4.2 Initial Stages of Surface Nuclear Shot

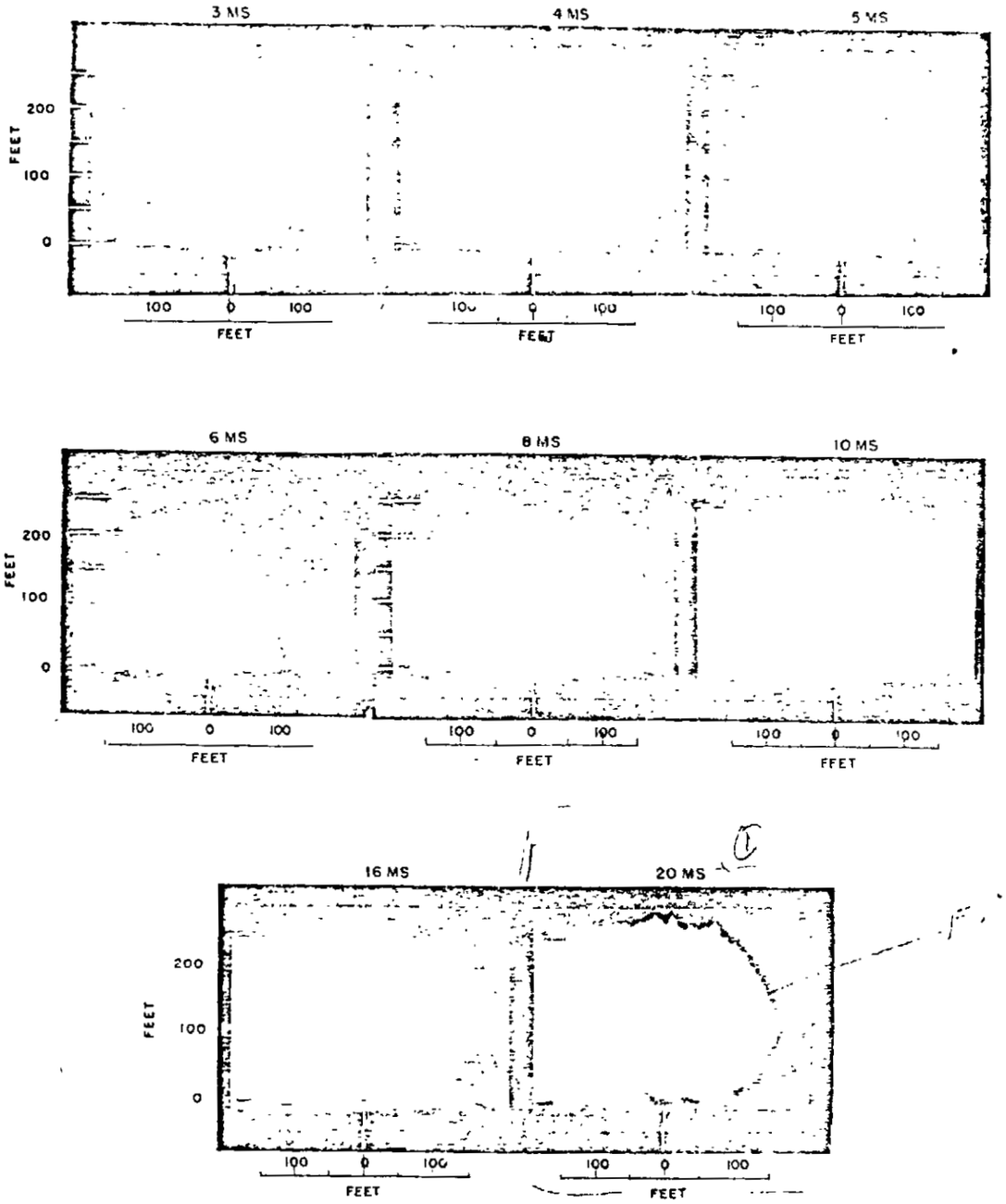

Fig. 4.3 Early Stages of Underground Nuclear Shot

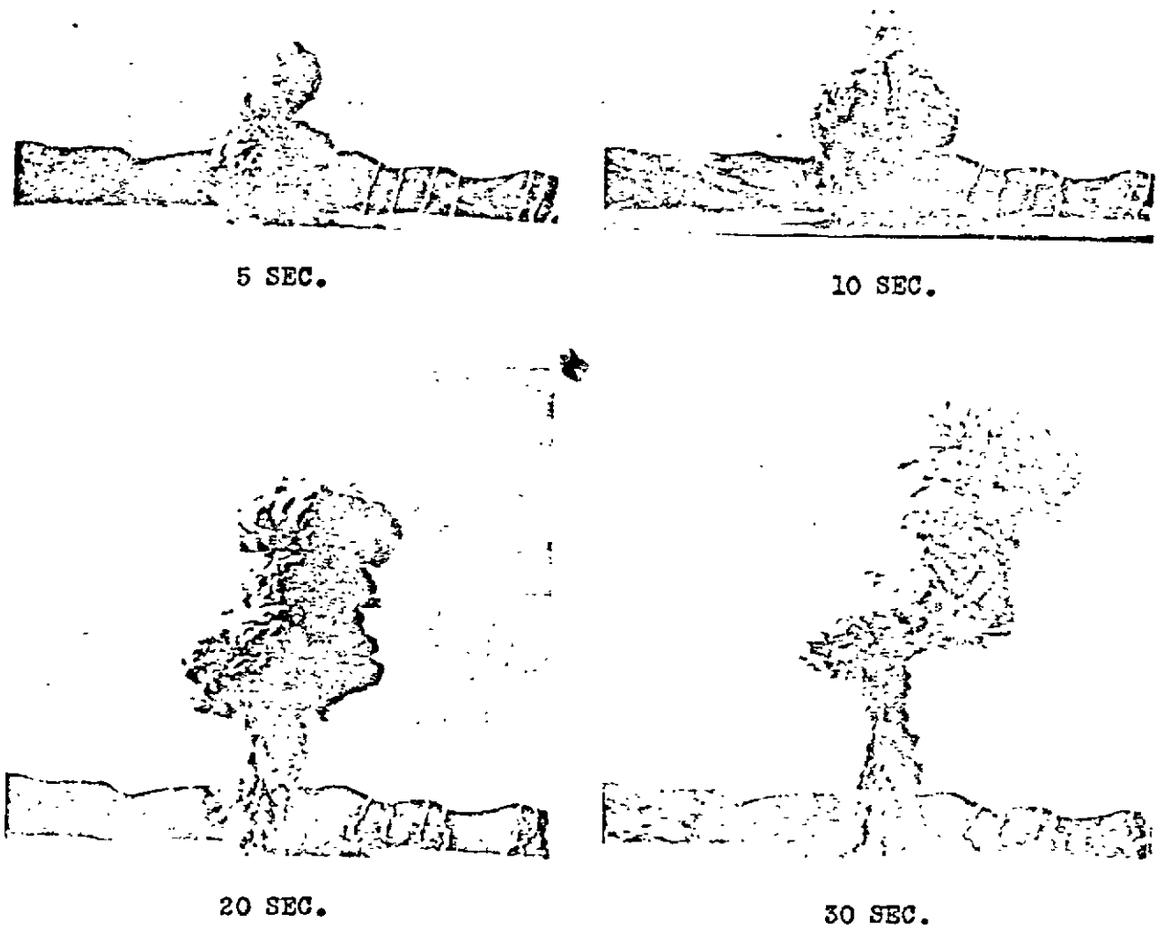

Fig. 4.4 Formation and Growth of Column and Cloud of Surface Shot

Fig. 4.5 Surface Shot at Approximately Plus One Minute

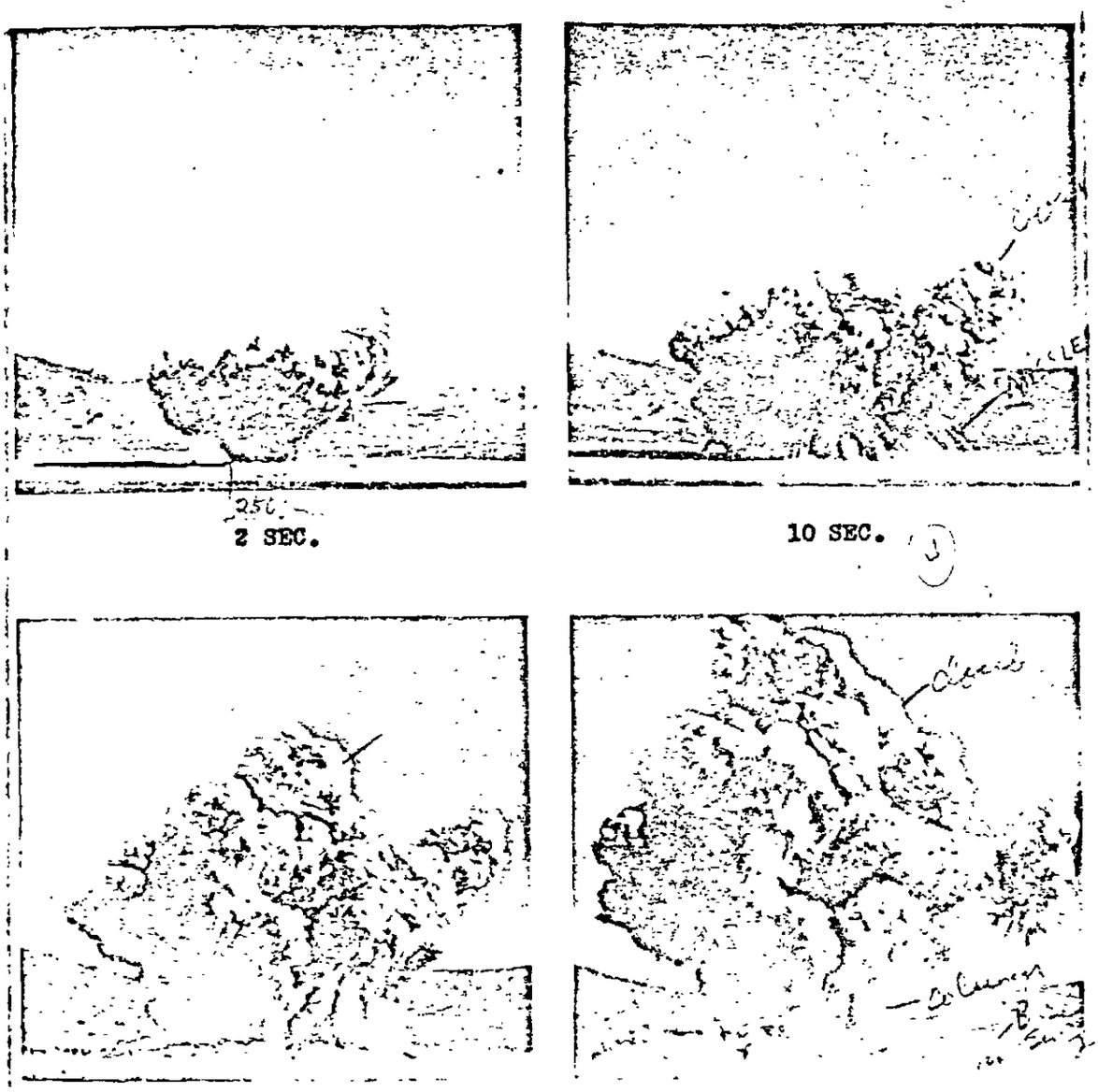

Fig. 4.6 Formation of Base Surge and Growth of Cloud of Underground Shot

Fig. 4.7 Underground Shot at Plus 2 Minutes

underground nuclear detonation.

4.4 HE BURSTS

A series of 13 high explosive shots using several weights of explosives was carried out prior to the nuclear bursts. These shots are discussed under paragraph 1.5.1. A striking similarity of visible phenomena existed between the nuclear and the HE scaled bursts despite the fact that there is considerable uncertainty regarding the physical laws governing scaling between the two.

Photographs of Shot HE-4 which was detonated in the scaled position of the surface nuclear detonation are presented in Figure 4.8. Visible phenomena of the conventional high explosive fired at the scaled depth of the underground nuclear shot, HE-2, are shown in Figure 4.9.

Several conventional high explosive shots were fired to give basic data for base surge studies. The effect of extreme depth of burial on the development of the base surge is shown in Figure 4.10. This series of photographs of the detonation of a conventional high explosive buried at 3.7 times the scaled depth of the underground nuclear shot shows all of the cloud collapsing into the base surge.

4.5 CRATERS PRODUCED BY THE NUCLEAR TESTS

The craters produced by the two nuclear shots are illustrated in Figures 4.11 and 4.12. The surface crater was 90 feet in diameter and 21 feet in depth. The underground crater was 260 feet in diameter and 53 feet in depth. For these shallow depths of burial, there is no difference between the apparent and the true craters.

High-speed photographs of the underground detonation reveal that the resulting crater was formed by a progressive scouring action rather than by ejection of large segments or plugs of earth. The nature of the cratering action is borne out by the essentially unchanged condition of the original soil structure at the face of the crater walls. The original soil structure, consisting of alternating layers of caliche and loose sand, is apparent in Figure 4.12.

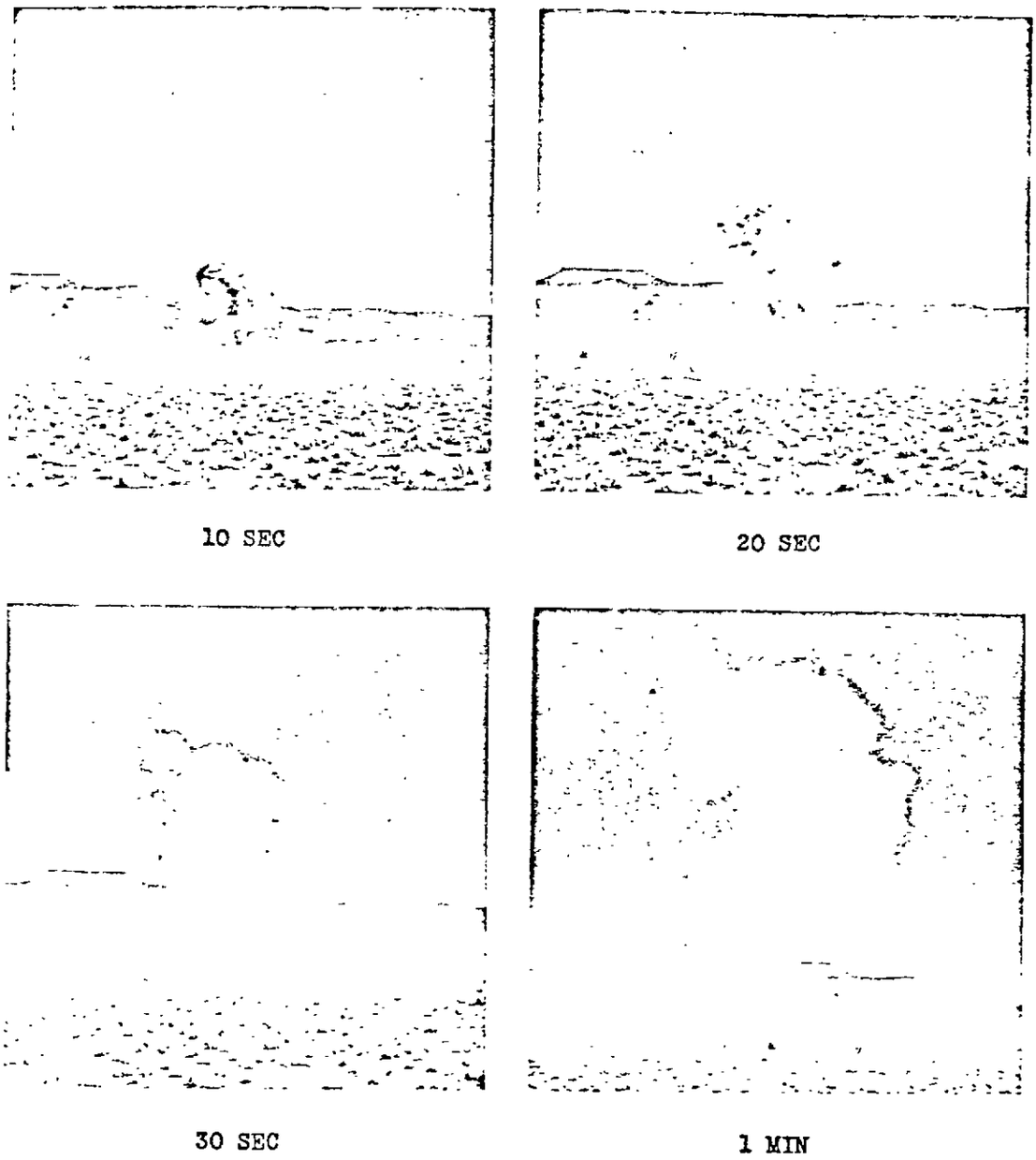

Fig. 4.8 2560 Pounds of High Explosive on Surface of Ground

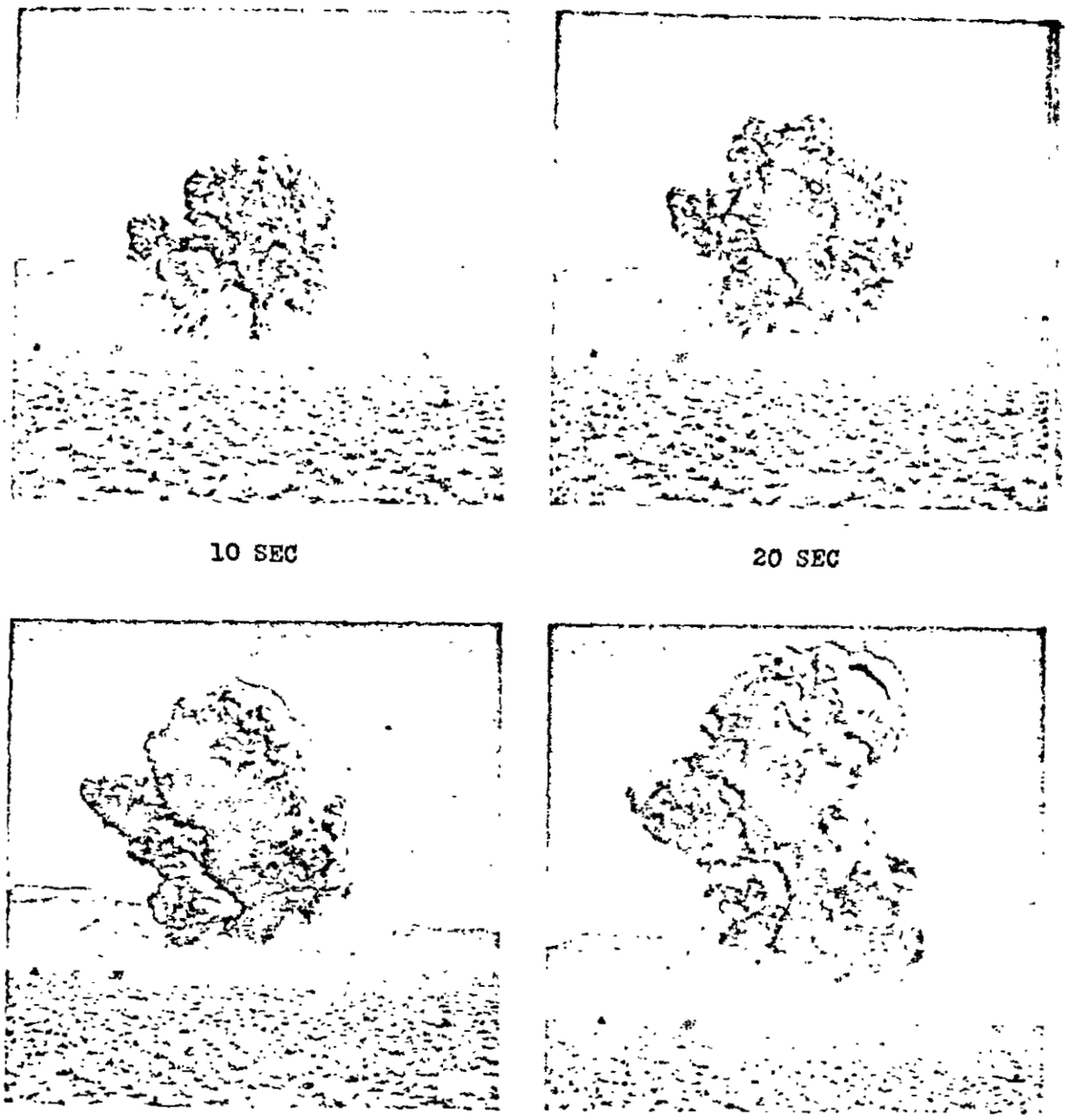

Fig. 4.9 40,000 Pounds of High Explosive at Same Scaled Depth as Underground Nuclear Shot

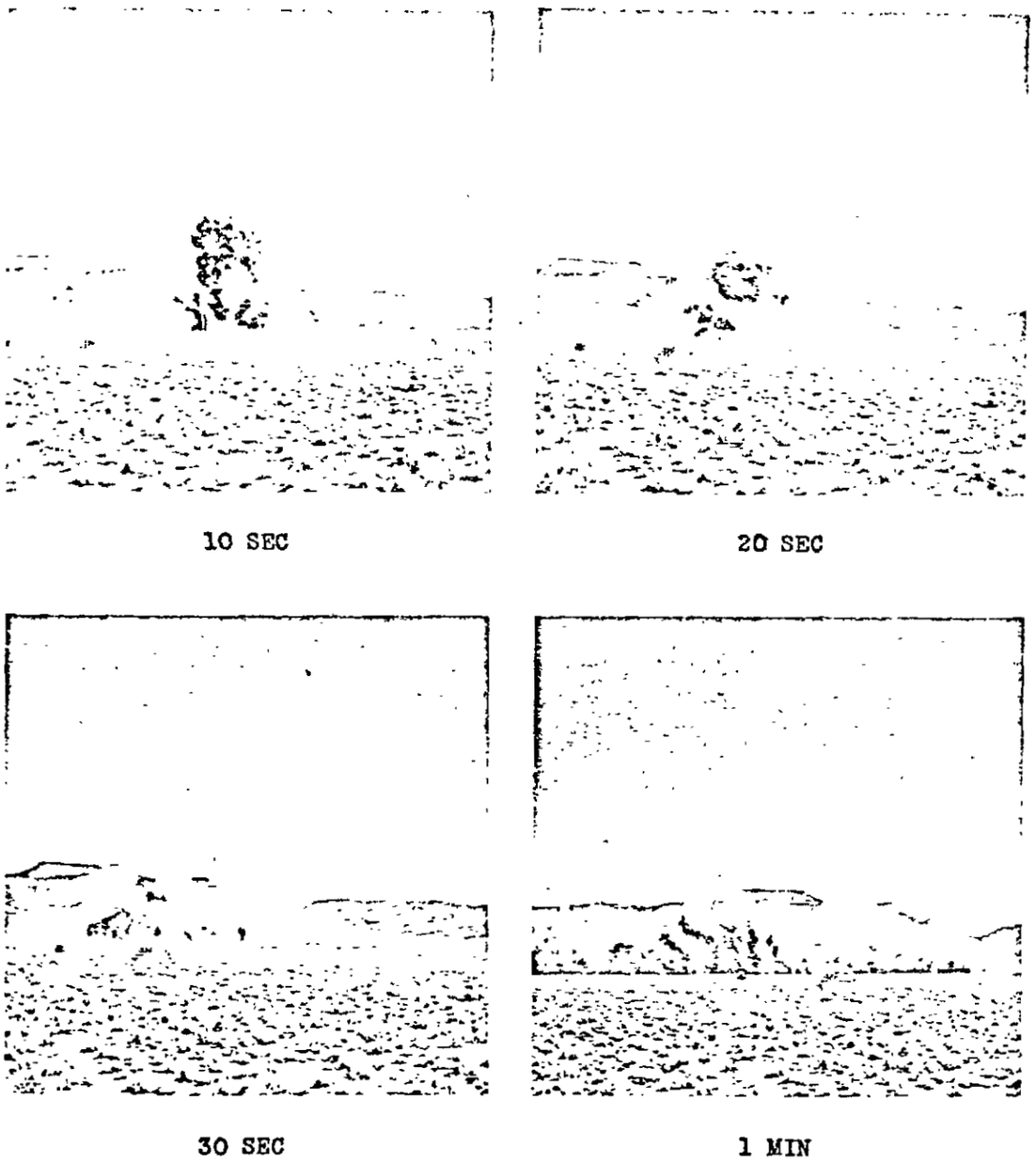

Fig. 4.10 2560 Pounds of High Explosive at 3.7 Times Scaled Depth of Underground Nuclear Shot

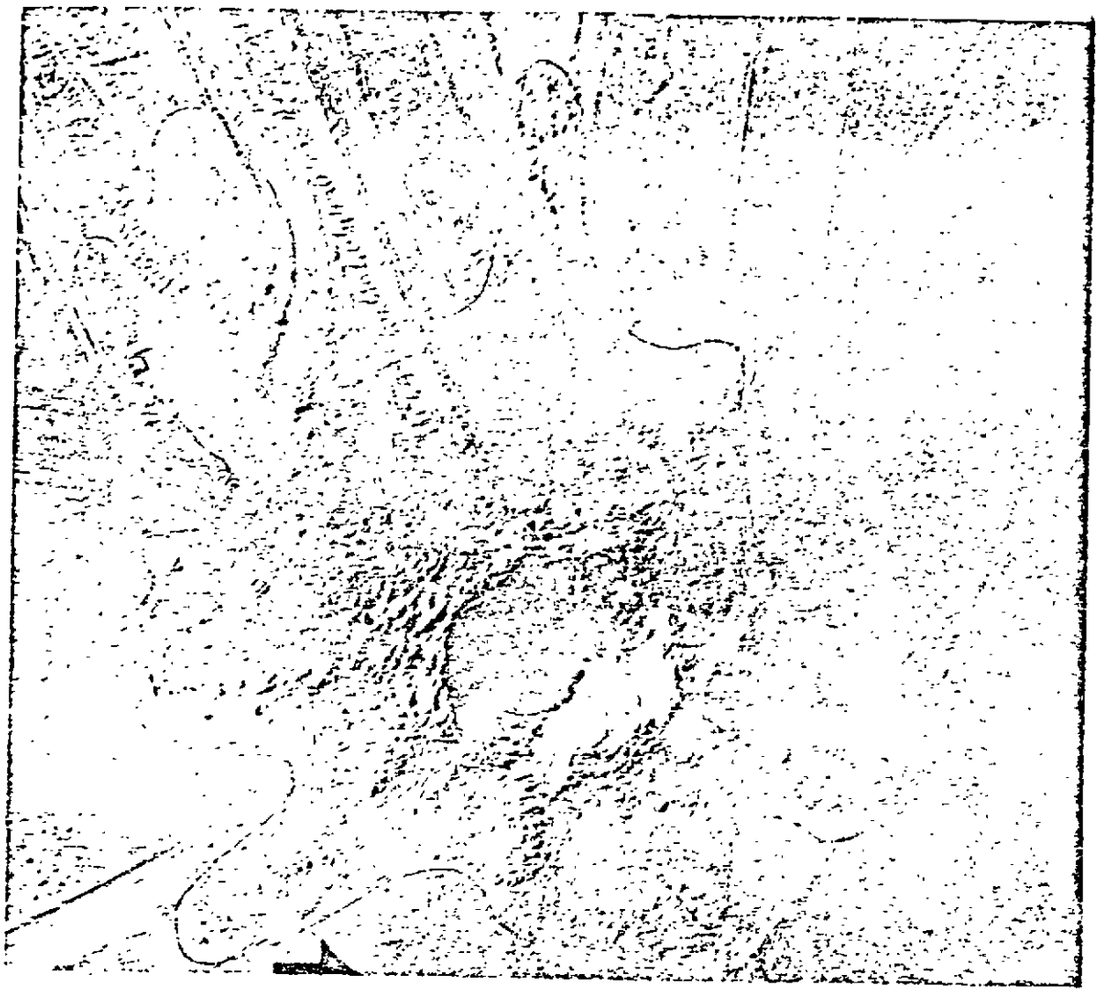

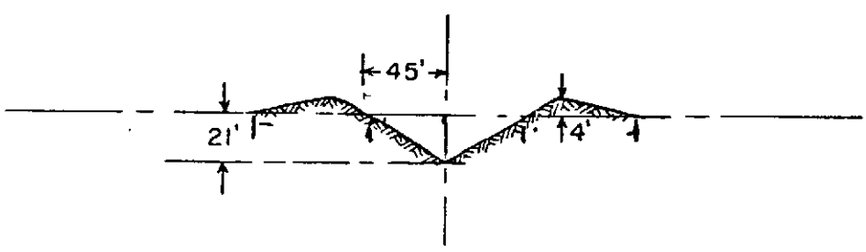

Fig. 4.11 Crater and Lip for the Surface Detonation

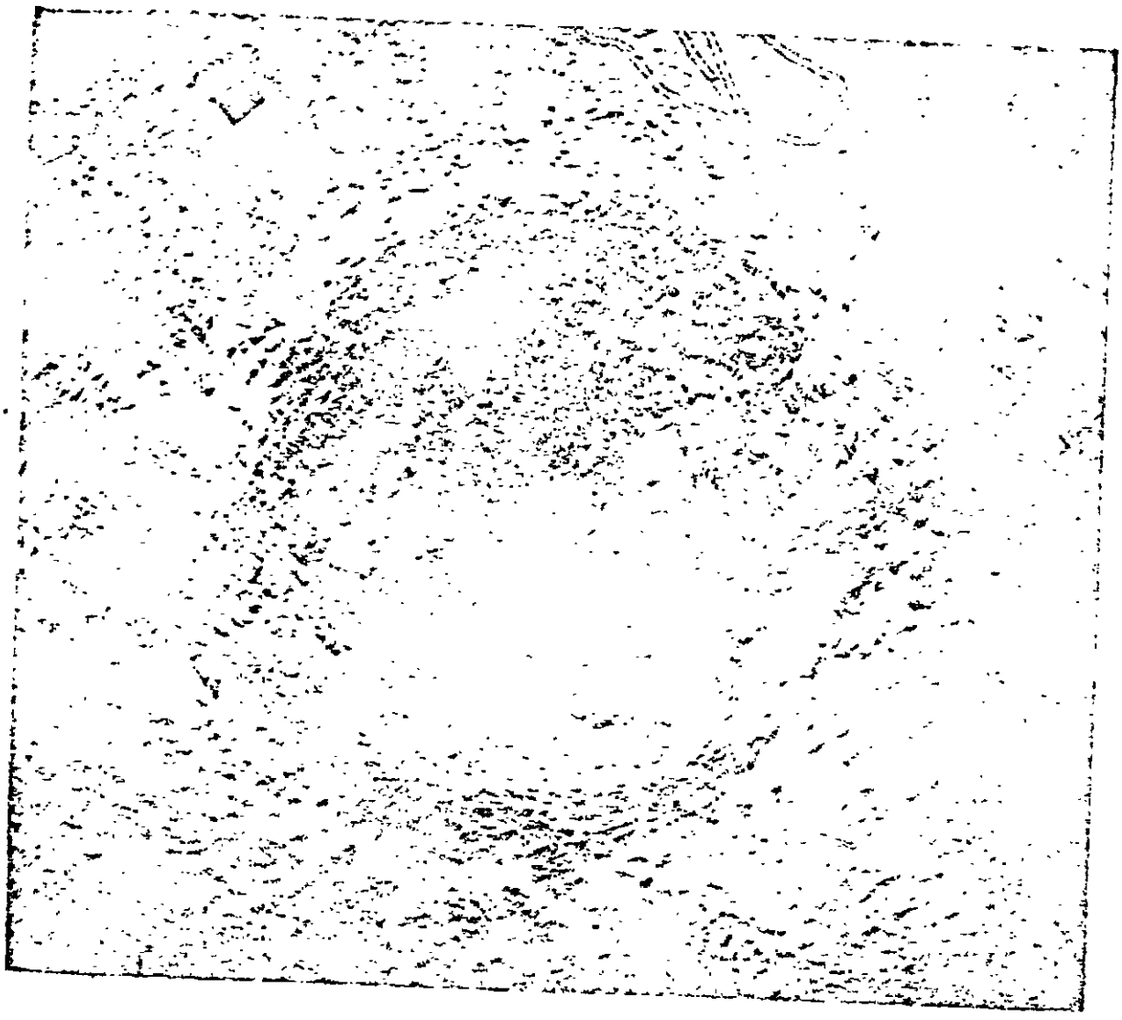

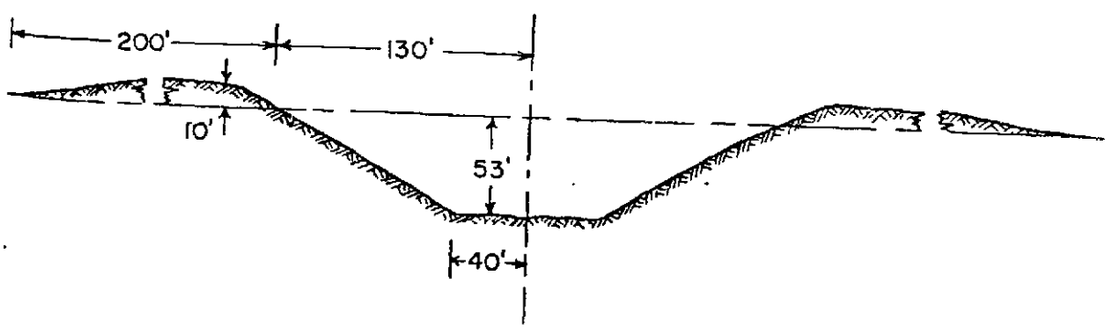

Fig. 4.12 Crater and Lip for the Underground Detonation

CHAPTER 5

AIR BLAST AND GROUND PHENOMENA

5.1 PRESSURE MEASUREMENTS IN THE AIR ABOVE THE BURST

Measurements were made using balloon-suspended gages and rocket trail shock velocity techniques to obtain vertical, air overpressure-distance data. The gage data, however, were not considered reliable and therefore, the curves for pressures in the air for the two nuclear shots are based on shock velocity data. During the surface nuclear shot the primary photographic timing standard for these data failed. This necessitated the use of ground-level gage data on shock-wave arrival times to establish a time scale for the measurements in the air, with the assumption that the shock wave is symmetrical radially along the ground. The surface shot data for the vertical peak pressure distribution are therefore not as reliable as that for the underground shot.

Distribution of peak air overpressure vertically above the two nuclear bursts is shown in Figure 5.1. A striking feature of the graph is that pressures above the underground shot are higher than those above the surface shot. It is also evident that in the case of the underground shot a secondary shock wave overtook and reinforced the initial shock at about 1100 feet in a direction vertically above zero. The cause of the secondary wave is unknown. The existence of a similar secondary shock wave along the ground is not apparent from the measurements taken at ground level.

5.2 PRESSURE MEASUREMENTS ALONG THE GROUND

Peak air overpressure versus distance along the ground for the two nuclear shots is shown in Figures 5.1 and 5.2. Data obtained by rocket trail shock velocity techniques, both along the ground and in the air, are presented together in Figure 5.1 for comparison. It is interesting to note that the shock wave for the underground nuclear shot is not hemispherical but has a greater radius from the explosion center vertically upward than along the ground.

As shown in Figure 5.2 the agreement among the data on peak air pressures at ground level obtained by gages and as calculated from shock velocities using blast switches was found to be good. It is noted that the shock velocity method consistently gave values slightly higher than those measured by gages.

NOL - Shock Velocity
with Shock Trail

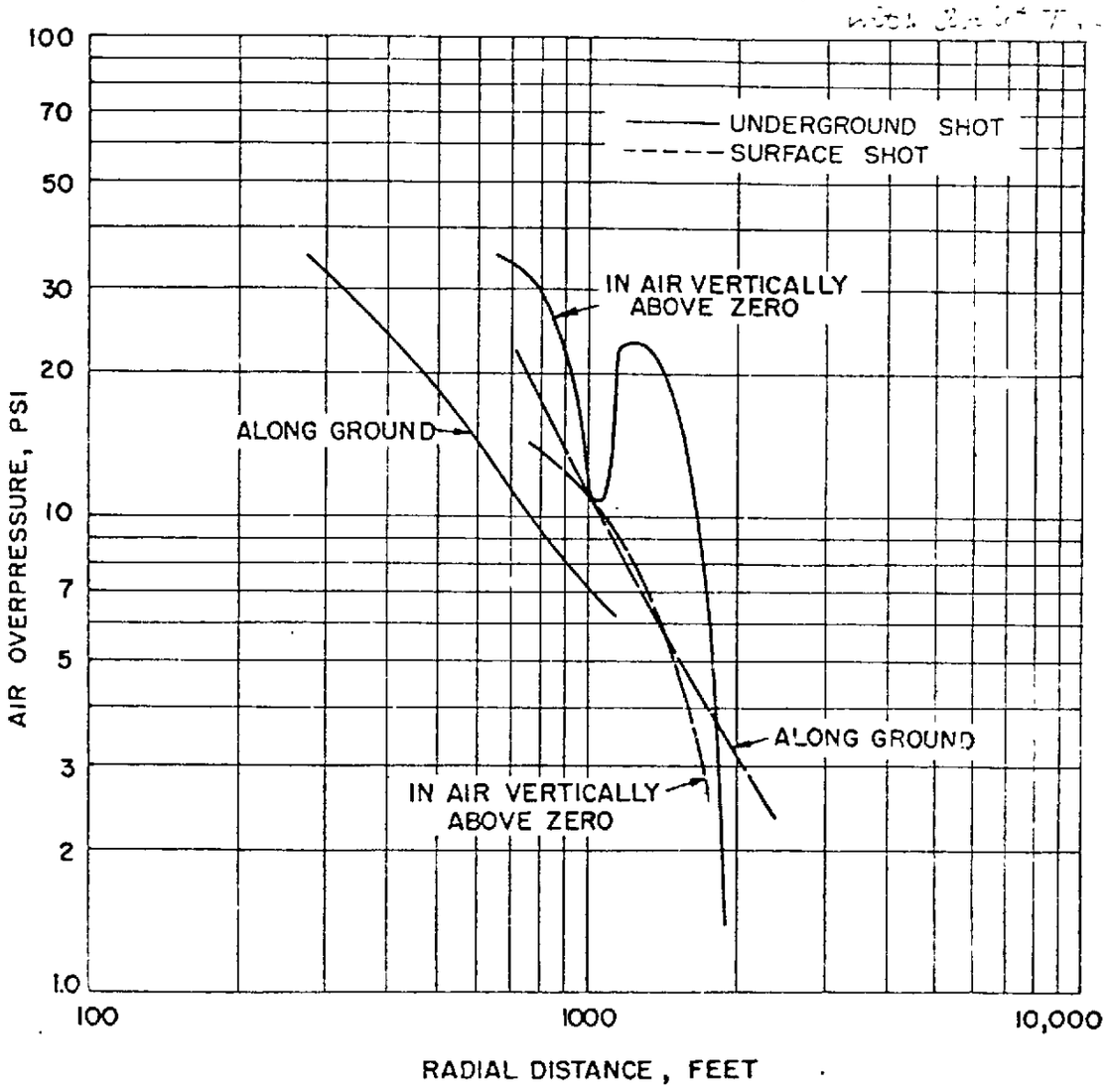

Fig. 5.1 Air Overpressure for Surface and Underground Nuclear Shots from Shock Velocities Measured from Rocket Trails

Data as Measured

SC - Wiancko Gages BRL - Shock Velocity

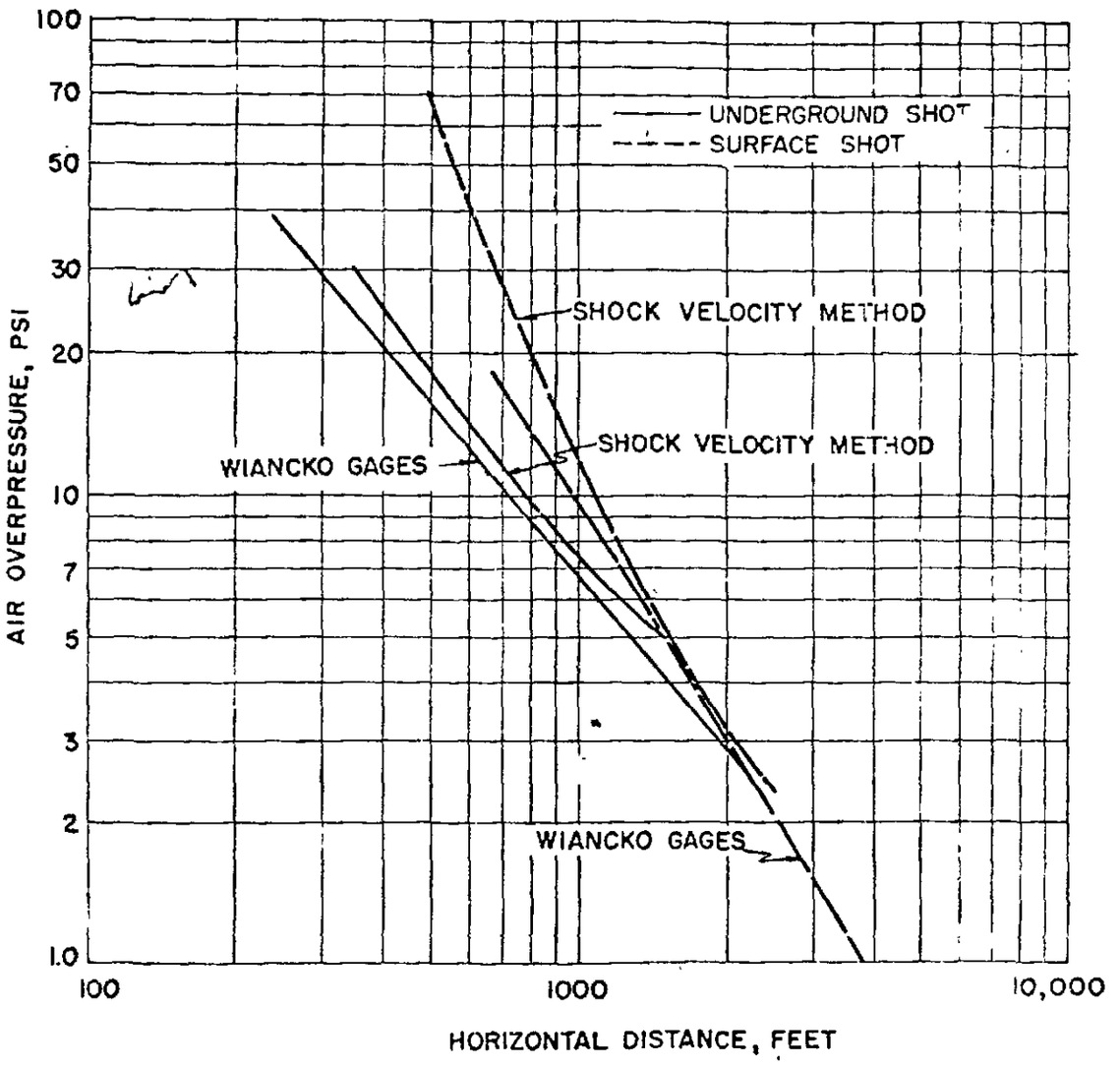

Fig. 5.2 Air Overpressure Along the Ground vs Distance from Zero for Surface and Underground Shots as Measured by Wiancko Gages and as Calculated from Shock Velocities Using Blast Switches

Data as measured for 1.2 KT at NPG

5.3 BLAST EFFICIENCIES

Blast efficiency of an atomic bomb burst is defined as that fraction of the total energy which is in the form of blast energy and is determined by comparison of the charge weight of TNT (W_{TNT}) which will give the same overpressure-distance relationship (for overpressures less than 100 psi) as the total yield of the nuclear weapon (W_A). Blast efficiency has been defined by the equation:

$$\text{Blast Efficiency (in per cent)} = \frac{W_{TNT}}{W_A} \times 100.$$

$\frac{.95}{1.2} \times 100 =$

The peak overpressures along the ground for the surface nuclear shot and the HE-4 data scaled up to 0.95 KT are in good agreement as shown in Figure 5.3. Thus, according to the above definition, the surface nuclear shot exhibited an apparent blast efficiency of about 80 per cent. In contrast, from the results of Operation TUMBLER, the blast efficiency of a nuclear weapon burst in free air was calculated to be about 40 per cent. Thus, the pressure distribution for the 1.2 KT surface nuclear shot might be expected to agree with that for a surface burst of 0.48 KT of TNT, but instead was found to agree with 0.95 KT of TNT. This discrepancy by a factor of two between expected and apparent blast efficiency for the nuclear weapon detonated at the ground surface is attributed to the nature of the air blast overpressures associated with near surface HE detonations[8,9].

Significantly, the peak overpressures along the ground from the GREENHOUSE George shot scaled to 1.2 KT are in agreement with the JANGLE surface shot data for overpressures of 10 psi and less as shown in Figure 5.3. The GREENHOUSE George shot [ ] was fired at a scaled height of burst ($h/W^{1/3}$) of [ ] Thus, scaling of the JANGLE nuclear surface shot to surface burst nuclear weapons of large yield is well verified.

It is also noted from Figure 5.1 that the JANGLE surface shot data and the GREENHOUSE George shot data scaled to 1.2 KT are both in agreement with the TUMBLER free air overpressure data scaled to 2.4 KT. This indicates that the reflective effect of the ground on peak overpressures from nuclear weapons fired on or near the surface of the ground is relatively insensitive to scaled heights of burst up to [ ]

It is possible to compute the TNT equivalent energy release of the underground nuclear charge by comparison with the underground HE shots. Scale factors between the 40,000 pound HE-2 and the nuclear test can be computed for peak pressure, positive phase duration, and positive impulse. These values lead to an equivalent energy yield of about 0.85

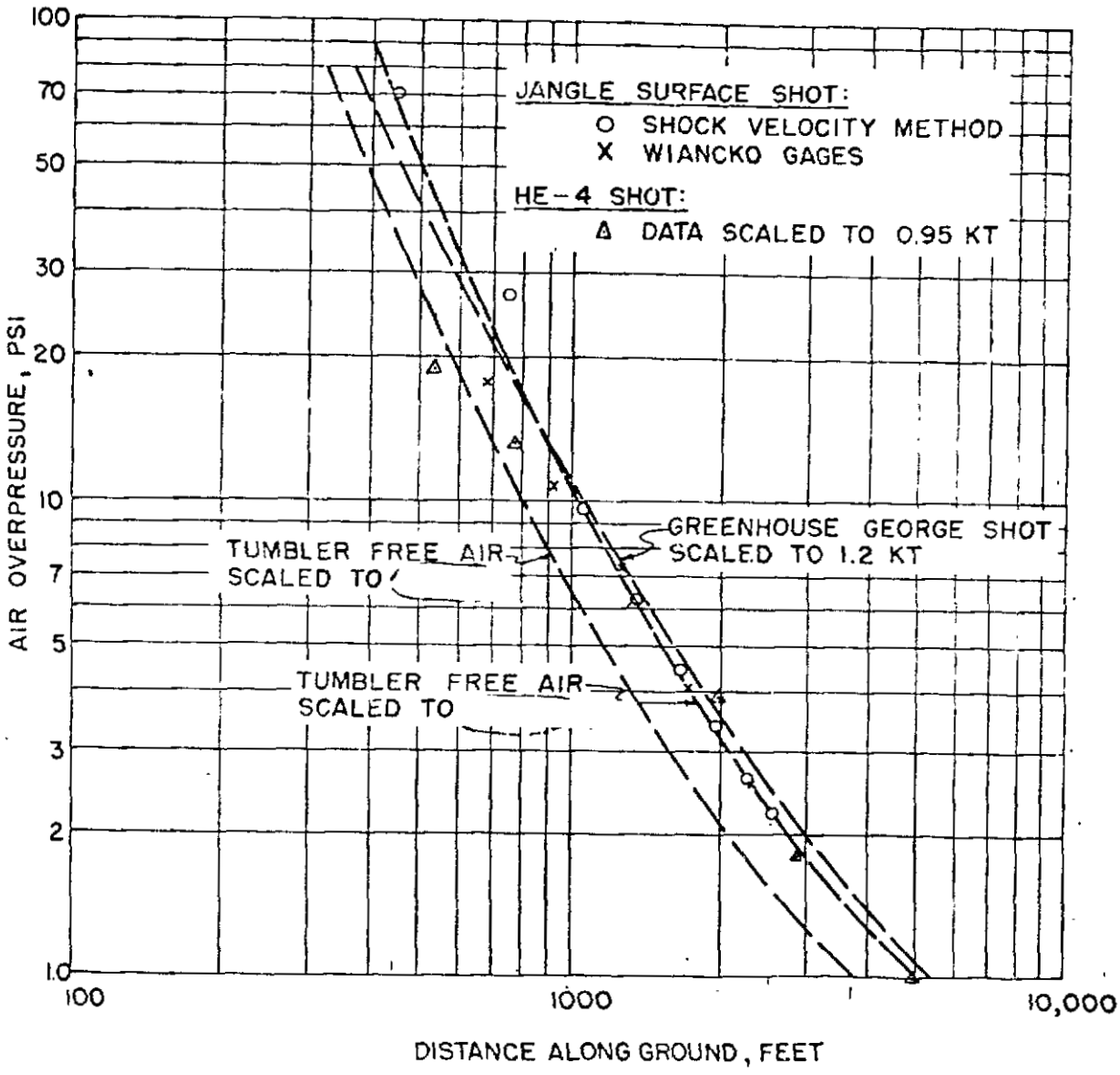

Fig. 5.3 Comparison of Scaled Air Pressures Along the Ground from Surface Shot and in Free Air from Higher Detonations

Tumbler and Greenhouse Data Scaled to Test Conditions

Data as measured for 1.2 KT at NPG

KT for the nuclear charge, as judged by its ability to produce air blast. When the scale factors are based on the 2560 pound HE-1, as well as HE-2, the equivalent "air pressure" yield is closer to 1.0 KT.

5.4 GROUND ACCELERATIONS

On the two JANGLE nuclear shots, as well as the first four HE shots, ground accelerations were measured with Schaevitz and Wiancko accelerometers and these were backed up with Engineering Research Associates, Inc. (ERA) gages. Vertical, horizontal, and transverse accelerations were measured. In general, the ERA gages gave less reliable results than either the Schaevitz or Wiancko gages. Gages were placed along the blast lines with a small number scattered throughout the structures area around the underground zero point. The standard depths were 10, 20 and 30 feet with additional instruments at 3, 5, 17, 34 and 68 feet. Figure 5.4 includes typical acceleration records at several distances. Figure 5.5 shows the variation of ground accelerations with depth in the ground.

Test results in general follow a very complex pattern. Ground accelerations originate from the following sources:

a. Acceleration produced by ground phenomena propagated directly from the point of detonation to the point in question (called primary acceleration).

b. Accelerations produced by ground phenomenon reflected and refracted from underlying rock strata (called secondary acceleration).

c. Acceleration induced in the ground by the passage of the air blast wave directly above the instrument (called primary air blast induced acceleration).

d. Acceleration in the ground produced by the air blast wave by its passage over the ground at positions other than directly above the instrument (called secondary air blast induced acceleration).

The air blast induced effects and the earth effects may be separated with some degree of certainty. The arrival time of the air blast wave agrees well with the time of maximum ground acceleration; therefore, it may be concluded that the maximum ground acceleration was produced by the primary air blast induced acceleration.

The acceleration time curves are very complex, and are made up of many transient pulses and high frequency components. The air blast acceleration frequency varied between 20 and 50 cycles per second for both shots. The primary and secondary acceleration frequency was predominantly in the range of 10 to 14 cycles for the surface shot and in the

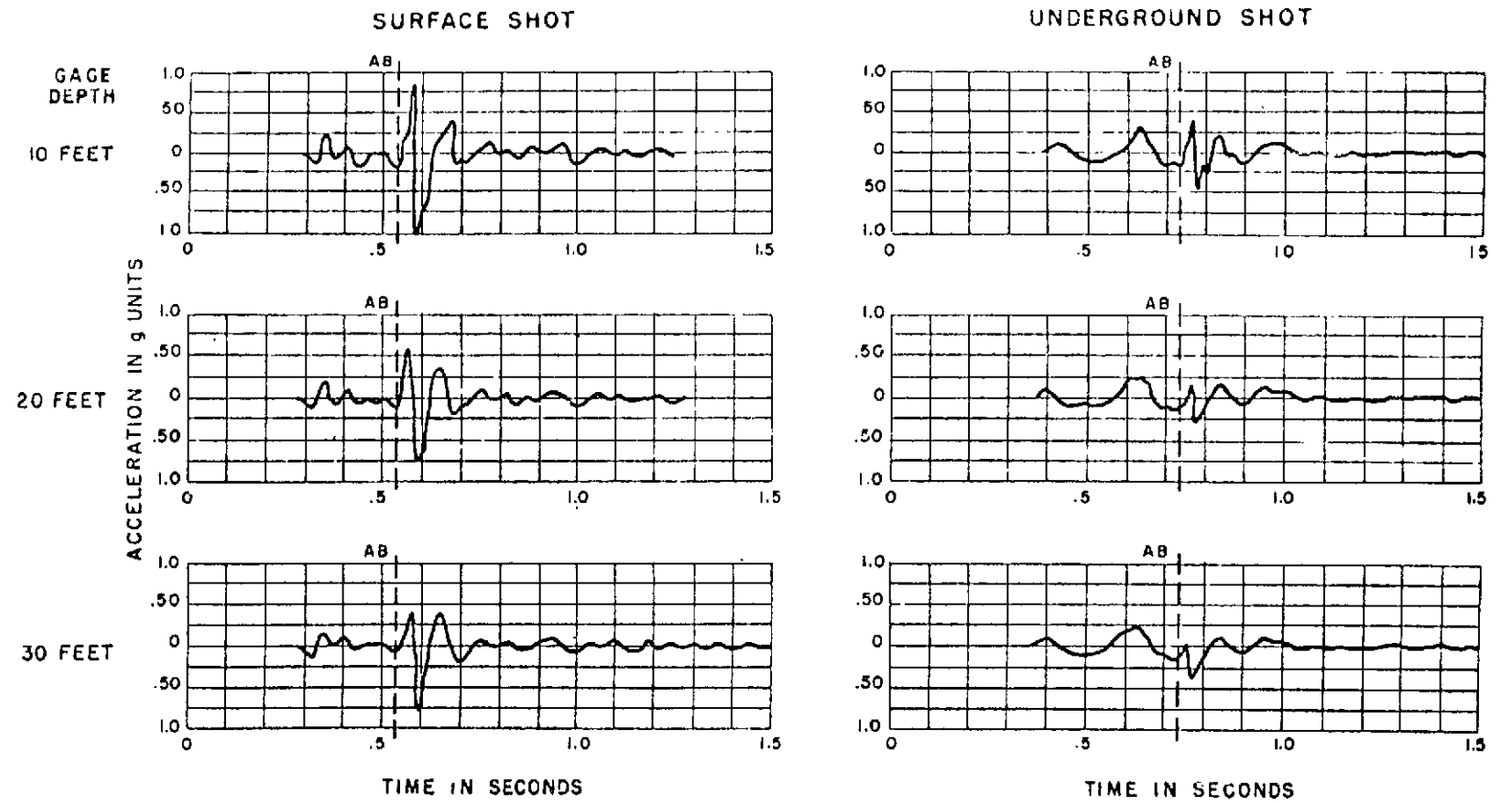

Note: AB Designates Time of Arrival of Air Blast

Fig. 5.4 Accelerometer Records as a Function of Depth. Records are for vertical accelerations at depths of 10, 20, and 30 feet at 1213 feet from zero for the surface and underground shots.

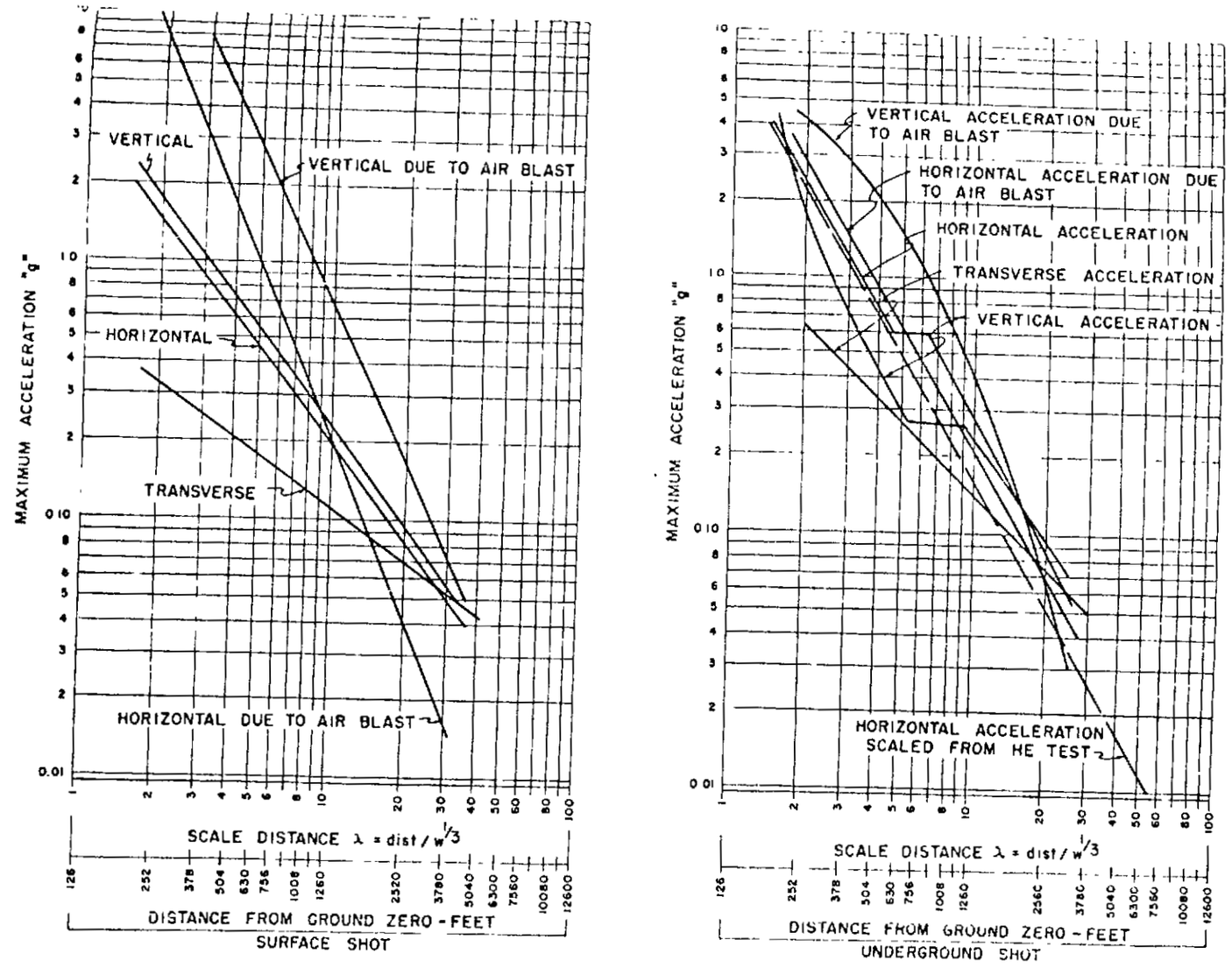

Fig. 5.5 A Comparison of Maximum Accelerations Produced by JANGLE Detonations

range of 3 to 6 cycles for the underground shot. Comparison of the acceleration durations between the JANGLE tests and the Dugway dry clay tests indicate a considerable difference, the Nevada durations being far less for identical HE tests. The pronounced variation of acceleration duration with soil type indicates that earth motion damage criteria would be affected much more by soil type than a consideration of peak acceleration amplitudes alone would indicate.

The surface shot was the more effective in producing high peak values of ground acceleration due to the contribution of air blast. This primary air blast induced acceleration consisted of a single pulse of very short duration and thus carried little impulse as compared to the longer period primary and secondary accelerations which were composed of many cycles. When comparing these latter accelerations, the underground shot was more effective since it produced accelerations with frequencies two or three times lower and magnitudes two or three times larger than the surface shot.

5.5 GROUND PRESSURES

Free ground pressure measurements were made in a pattern similar to that for the ground accelerations. Pressures were measured at the bottom of a fluid column by gages designed to respond to transient hydrostatic pressures. In addition, the ground pressures applied to the buried test structures were measured by means of pressure cells flush-mounted in the exterior building surfaces.

The free ground pressure measurements appear sensitive to a number of parameters other than size of charge, distance from charge, depth of gage and soil type. These include air blast effect transmitted through the ground and through the fluid column, height of the fluid column over the gage, inertia of the fluid column, and matching or acoustic impedance between the earth and the fluid. More important, the hydrostatic pressures measured are scalar quantities although ground pressure is a vector quantity which varies quite markedly with direction of application. Local inhomogeneties in the soil and occlusions of air cause a spread in test data which further obscures the basic trends.

As a result of the variations which were introduced by various parameters as indicated above, there is insufficient data to conclude very much about free ground pressures. No rational pattern has been developed to explain the experimental results; therefore, no extrapolation to operational weapons can be made. No consistent correspondence was found between free ground pressures and ground accelerations nor between free ground pressures and the pressures measured on buried structures. The free ground pressures which have been measured cannot, at present, be put to any use. The chief advantage of retaining the concept of soil pressure is that this is the origin of the propagated

effects.

Ground pressures on the buried test structures were measured in order to determine structural loading, and it is believed that these measurements gave a true indication of the loads applied. For ranges from 500 to 1000 feet, the significant pressure loadings on buried structures were due to air induced ground pressures. Appreciable peak pressures and impulses were observed up to 15-foot depths, the limit of observations. Between 250 and 500 feet it has not been possible to separate air-induced and direct-transmitted ground pressures but the magnitudes and durations of the observed pulses are such that they could be attributed to air-induced effects. A systematic analysis of pressures, as well as accelerations, measured on the test structures is being made as part of the attempt to develop a correlated picture of structural loading by ground shock. This analysis has not progressed sufficiently to allow comment at this time.

It is not possible at this time to translate the results observed in Nevada soil to results in other types of soil. An equally serious matter is the lack of test information regarding the pressure relief which may occur when large deflections are obtained in the structures. This last factor was not observed in the present tests since the test structures were not loaded into the zone of plastic deformation as had been planned.

5.6 PERMANENT DISPLACEMENTS

Permanent displacements, horizontal and vertical, were measured around both zero points. Surveys before and after the shots were made on the location of monuments set flush with the earth surface. It is estimated that the probable error for the horizontal measurements was ± 0.02 feet for each survey with the probable error for vertical control about ± 0.01 feet. Two types of monuments were used. One consisted of ordinary concrete poured into 6-inch diameter holes 3 feet deep. The other type was made of a sawdust-sand-portland cement mixture which had a density of 100 pounds per cubic foot, so as to be about the same density as the surrounding earth. The latter were 6 inches in diameter and 18 inches deep. The light monuments duplicated the heavier along westerly lines from both zero points. The heavy monuments were placed along eight radial lines about each zero. They extended from 217 to 800 feet about the underground zero and from 225 to 800 feet about the surface zero.

In the post-shot surveys, no assymetry was found between the southerly (along the major blast lines), the easterly, and the westerly lines of monuments (along the minor blast lines). Therefore, the post-shot readings were omitted along the other radial lines. No variation in displacements could be noted between the heavy and the light monuments.

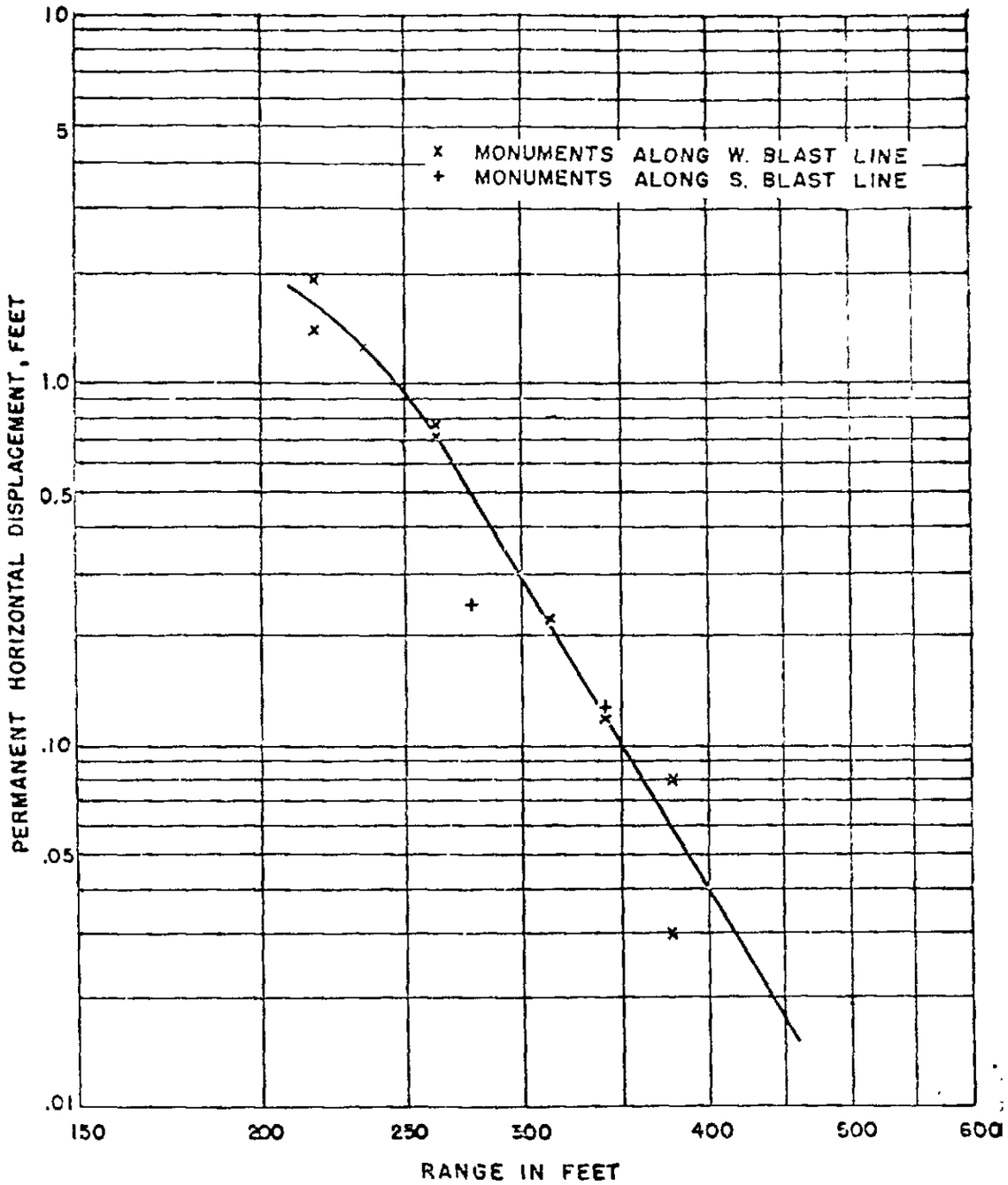

Fig. 5.6 Permanent Horizontal Displacements about the Underground Zero

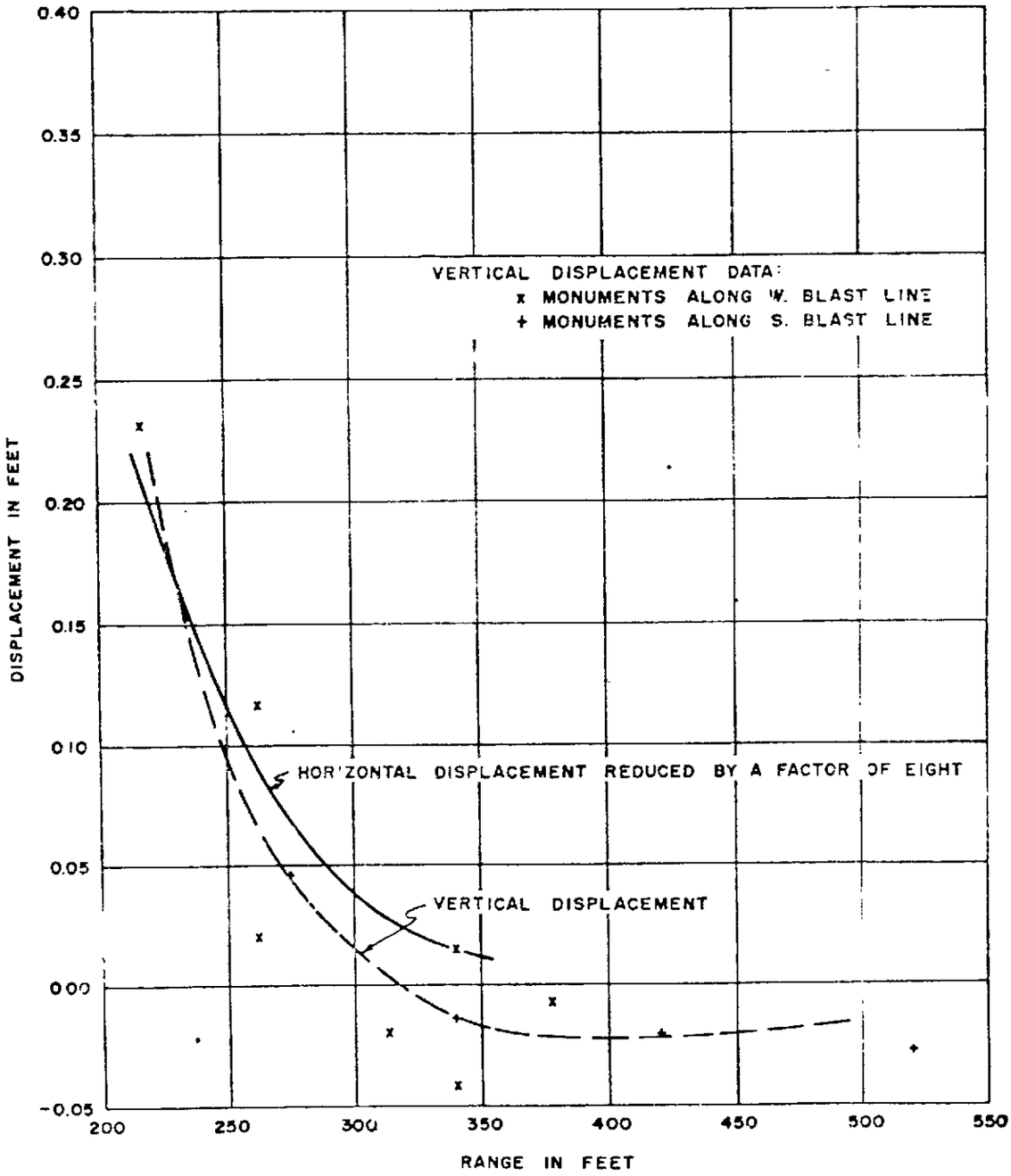

Fig. 5.7 Permanent Vertical Displacements about the Underground Zero

It has been assumed that the monuments gave a true indication of permanent displacements of the ground surface and that displacements were symetrical about each zero.

Figures 5.6 and 5.7 show the observed horizontal and vertical displacements out to a range of 500 feet around the underground zero. It will be noted that this extends well past the point where observed movements are distinguishable from the probable error of the measurements.

Permanent horizontal displacements were all radially outward from zero. They varied in magnitude from 1.8 feet at the 217-foot range down to a negligible amount at about the 400-foot range. Permanent vertical displacements were about one-eighth of the horizontal at respective ranges. They were upward inside of 300 feet and downward between 350 and 500 feet. It would appear that movements upward due to gross displacement of earth near the crater overshadowed a slight subsidence due to some minor consolidation of the soil. As the close-in effect disappeared, the subsidence became apparent at intermediate ranges.

Although extrapolation of observed ground surface displacements to the edge of the underground crater would indicate that about 3 feet of horizontal and ½ foot of vertical displacement occurred, there was no apparent shattering of the natural soil structure on the face of the crater. Raveled surfaces from loose sand and gravel and steeper faces from the better consolidated caliche lenses were clearly differentiated.

No permanent displacements were noted around the surface zero at the inner limit of observations 115 feet from zero. The same apparent integrity of the natural soil structure at the crater face was noted. It should be noted that these observed displacements were far less than would be expected from scaled results of the HE tests at the Dugway Proving Ground 10/.

CHAPTER 6

EFFECTS ON STRUCTURES

6.1 GENERAL

Test structures were located around the underground zero in order to observe the damaging effects of ground shock and air blast and to study structural response to impulsive loading. A list of the test projects and a layout plan for the test structures is included in Appendix E. Measurements were made of the applied loadings, of structural action under these loadings, and of the permanent effects on the test structures. In general, the observed effects on structures agree well with the responses calculated from the observed loadings. Confidence in the methods of calculation is increased accordingly. However, the buried structures were not sufficiently loaded to give deflections into the plastic range and as a result there are still some questionable factors for a determination of their ultimate resistance. More severe handicaps exist in extrapolating the effects of the 1.2 KT bomb detonated in dry, sandy soil in order to evaluate operational weapons detonated in other soils. Such extrapolations require the use of scaling laws along with soil coupling and attenuation factors developed from HE experiments, which failed to predict the results observed in these nuclear tests, particularly with respect to time scaling.

A considerable number of the test structures are not directly representative of standard building types but are targets designed for the study of some particular phase of the complete loading-response pattern. Inferences as to the effect of the test weapon on normal structures cannot be based directly on the observed effects on the test structures but must also take account of their relative resistance compared to normal construction.

6.2 SURFACE STRUCTURES

All of the surface structures received the major portion of their loading from air blast and in no case was the effect of ground acceleration important. This was true for the idealized targets (bare columns supporting massive slabs at ranges from 450 to 875 feet) and for the building replicas (reinforced concrete frames with brick curtain walls at 900 feet and brick chimneys at 750 and 1050 feet). In the case of the idealized targets, the importance of air blast had been realized and an effort made to reduce its effect by streamlining and by presenting as small an area as possible to the blast. Considerable interest has been shown in the high peak values of ground acceleration induced by air blast.

However, it is now apparent that ground acceleration is of negligible importance in determining the extent of structural damage. In the event that greater scaled depths of detonation or other factors should so reduce the relative magnitude of air blast as to make any ground acceleration significant in determining structural damage, it is clear that the air blast induced acceleration will have been similarly reduced in relative magnitude and the primary and secondary accelerations would dominate the picture. This pattern of relative effectiveness is reinforced if consideration is given to the extremely short periods of the air induced acceleration pulses as compared to those directly transmitted.

6.3 BURIED STRUCTURES

The buried test structures were loaded primarily by ground pressures. As was noted in Paragraph 5.5, the significant pressures are attributed to air-blast-induced effects for all but the region immediately surrounding the crater. Although other field conditions might materially alter this picture, the ground pressure pulse which resulted from the air blast had the same relatively slow rise time and long duration as pulses transmitted directly through the earth. As a result, the method of transmission of the ground shock has not been an important factor in the analysis of completely buried structures. Unfortunately, buried cells which were designed to indicate the effect of structural resilience on applied pressure were open at the top and thus received a heavy air pressure loading on the inside at the same time the heavy ground pressure pulse arrived at the outside. Major uncertainties are thus introduced into the results of these tests. The problem of effect on the loading resulting from the motion of the structure or its elements has not been resolved. Such motion has the effect of changing the applied pressure. The degree of change depends upon the relative velocities, at any instant, of the soil particles and the portion of the structure adjacent thereto. This test has given no results from which an estimate of what this effect would be for larger deflections, such as would occur with plastic deformation.

The foregoing discussion of effects on buried construction is concerned solely with the structural shell and not with its contents. It is possible that ground acceleration would be important in determining the damage to relatively fragile contents of a structure strong enough to resist the associated ground pressures.

The limited range of permanent ground displacements noted in Paragraph 5.6 correlates with the lack of damage to structures which would be damaged primarily by displacement. At the underground site these included 14-inch and 18-inch reinforced concrete pavement slabs at 500 feet from ground zero, a continuous 6-inch cast iron water line running from 600 to 1800 feet, 50-foot sections of 15-inch plain concrete pipe covering the same ranges and 6-inch and 12-inch reinforced concrete

pavement slabs at 1200 feet. No evidence of damage or movement was observed for any of these structures.

6.4 SHAFTS

Vertical shafts, made up of nine 5-foot sections of 6-inch pipe, were located at various ranges and with several orientations about both ground zeros to measure variation of permanent displacements as a function of depth. Table 6.1 shows the observed displacements for these shafts around the underground zero. In all cases, the displacement was restricted to the top 5-foot section.

TABLE 6.1

Permanent Displacement of Vertical Shafts
Around Underground Zero

Range (feet)	Orientation	Horizontal (feet)	Vertical (feet)
312.5	West	0.03 (Tangential)	- 0.02
250	South	0.67	+ 0.02
312.5	South	0.83	- 0.05
375	South	0.09	- 0.02
500	South	0.02	- 0.02
312.5	East	0.03	———

Note: + vertical displacement is upward.
Horizontal Displacements are radially out except as noted.

The displacements noted were erratic when compared to the ground surface movements at corresponding ranges. The reasons for this are not clear but it may be due in part to poor consolidation of the backfill between the pipes and the sides of the drill holes. Another possible cause for discrepancies along the line is damage by heavy vehicles which operated in this area between the pre- and post-shot measurements. Similar shafts placed in the same pattern around the surface zero showed no permanent displacements.

6.5 REINFORCED CONCRETE BOX

A massive reinforced concrete box (25' X 25' X 17' high with 5' thick reinforced concrete front and rear walls) was undamaged and was found to have permanent displacement of two or three hundreths of a foot. The box was located 238 feet from the underground zero in a region

where about 0.9 feet horizontal and 0.1 feet vertical movement was observed in the ground surface. The top of the box was 8 feet below normal ground surface. Observations on the vertical shafts, described in the previous section, indicate that permanent ground displacements were essentially surface phenomena. There is no indication that the structure did not move with the earth immediately surrounding it, although the structure's observed permanent displacement was much less than that of the permanent displacement monuments set in the ground surface at this range.

6.6 MISSILES

Sections of reinforced concrete highway strips and vertical walls were placed near the underground atomic burst to provide source material to evaluate the damage potential of missiles produced by underground nuclear explosions. It was shown that little or no military significance should be attached to missiles since high missile density does not extend beyond the area of major damage by air blast. A very low density of missiles was found between 1500 feet and 3000 feet from ground zero. These missiles were originally between 30 and 50 feet from ground zero. Major damage might have accrued in the range 400 feet to 1500 feet from missiles originating 50 to 85 feet from ground zero.

Scaling of missile effect to an operational size weapon detonated under a continuous reinforced concrete runway 18 inches thick reveals that damage by the mechanism of air blast will extend further by a factor of 2 than damage by the mechanism of missiles.

6.7 SUMMARY

Air blast was the significant effect causing damage to surface structures for the 1.2 KT weapon detonated at this shallow depth. It should be noted that the effect of air blast increases in proportion to ground acceleration as the size of the weapon increases.

Earth pressure induced by the passing air blast, rather than pressure transmitted directly through the earth, was the significant effect in determining the maximum loading of shallow buried structures even at relatively short ranges. The region where directly transmitted earth shock was of sufficient strength to damage light underground structures appears to have been limited to an area with a diameter not greater than twice that of the crater.

The effects on the Dugway box and on the soil at the crater surface indicate that very heavy structures would have to be within the crater itself to suffer major damage.

CHAPTER 7

THERMAL RADIATION

7.1 THERMAL RADIATION VS DISTANCE

Figure 7.1 shows a comparison of the observed values of thermal radiation at several distances with the theoretical variation to be expected in extremely clear air. The curve is adjusted in magnitude to fit the data and the scope is determined by theoretical relationships.

7.2 SPECTRUM OF THERMAL RADIATION - SURFACE DETONATION

The spectrum of the thermal radiation from the surface detonation differed from that observed in an air burst in that the major portion of the energy is in the infrared rather than the visible region. The observed spectral distribution at 6000 feet from the burst is shown in Table 7.1. Thermal radiation effects were almost completely absent in the case of the underground detonation.

TABLE 7.1

Spectral Distribution of Thermal Energy at 6000 Feet from the Surface Shot

Wave Length	Total Thermal Energy
Less than 3500 Å	0.0264 cal/cm^2
3500 - 6500 Å	0.0288 cal/cm^2
6500 - 28,500 Å	0.211 cal/cm^2

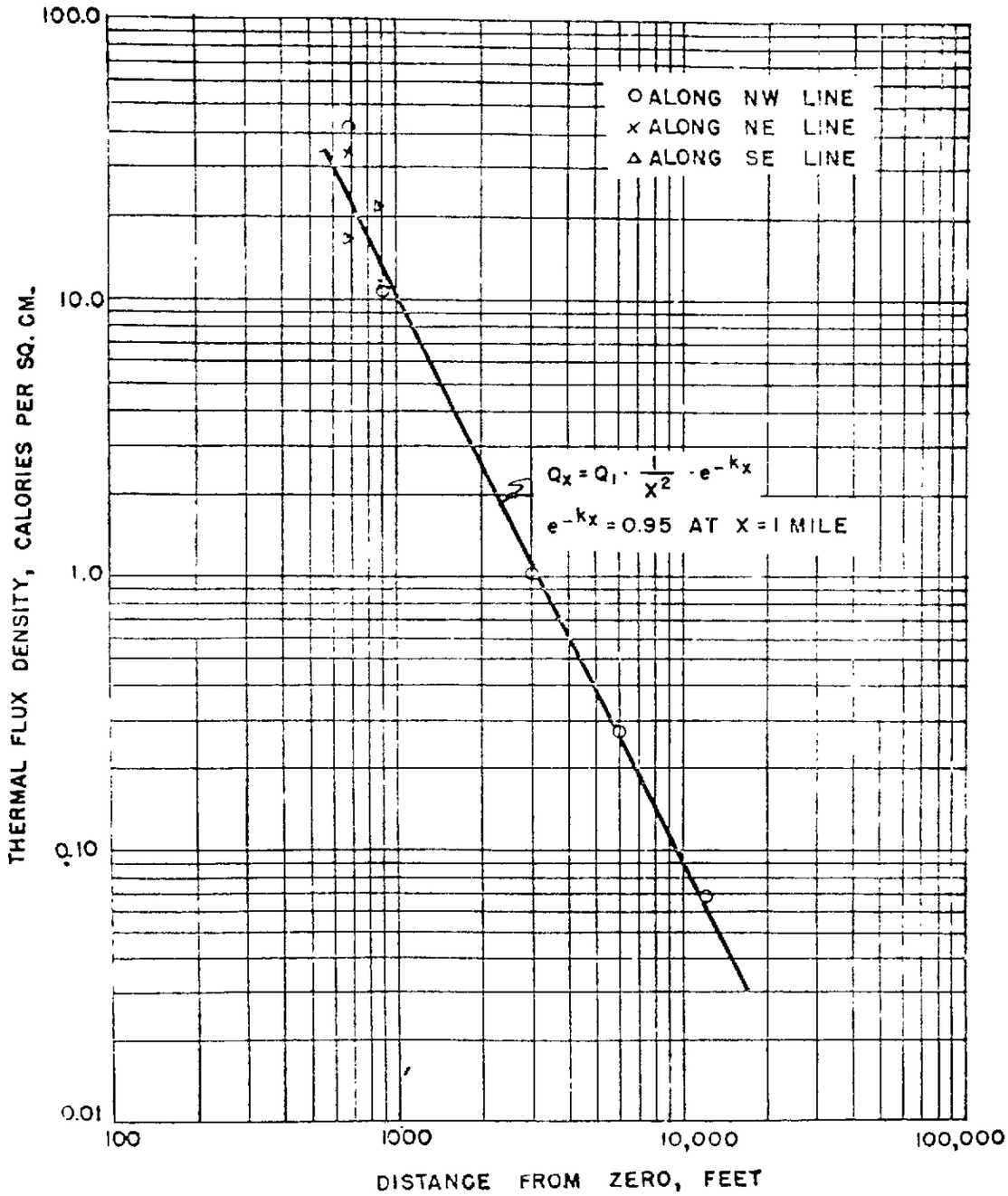

Fig. 7.1 Thermal Energy vs Distance for the Surface Shot

CHAPTER 8

RADIOLOGICAL EFFECTS

8.1 GENERAL

The JANGLE tests demonstrated that surface and underground detonations of atomic weapons are characterized by areas of high residual contamination. The radioactive debris from such detonations is admixed with considerable earth material and forms low clouds with a large proportion of the active materials associated with large particles. The fall-out from the resulting radioactive clouds is largely governed by the size distribution of the particles and the wind. For the JANGLE surface detonation the average wind velocity was about three times that for the underground detonation, based on time of arrival considerations. This resulted in a much longer and narrower downwind streak of contamination for the surface detonation.

8.2 GAMMA RADIATION DOSE RATE VS TIME

Scintillation counter dose rate versus time data were collected for the period from one-tenth second after detonation up to as long as plus 48 hours for both JANGLE shots. Stations were located along six radial lines extending from 2000 feet out to 6000 feet upwind and crosswind and as much as 14,000 feet downwind (see Appendix D).

These scintillation dose-rate measurements were augmented by monitor survey readings with more extensive area coverage (Projects 2.1a and 2.1d). In addition dose-rate versus time data with millisecond time resolution were obtained for BUSTER air bursts at two stations and the JANGLE underground shot at one station (LASL BUSTER/JANGLE Report 10.6). These latter measurements allow correction of the integrated scintillation counter data for the contribution in the first tenth of a second.

Figures 8.1 through 8.4 show dose rate versus time and integrated dose versus time records for one upwind and one downwind line of stations for each of the JANGLE detonations.

Contours of gamma radiation dose rate at one hour after detonation appear in Figure 8.5 for the 1.2 KT surface shot and in Figure 8.6 for the 1.2 KT underground shot. These contours are based on scintillation counter rate measurements, considered reliable to within 25 per cent, augmented with monitor survey data which showed reasonable correlation with the scintillation data.

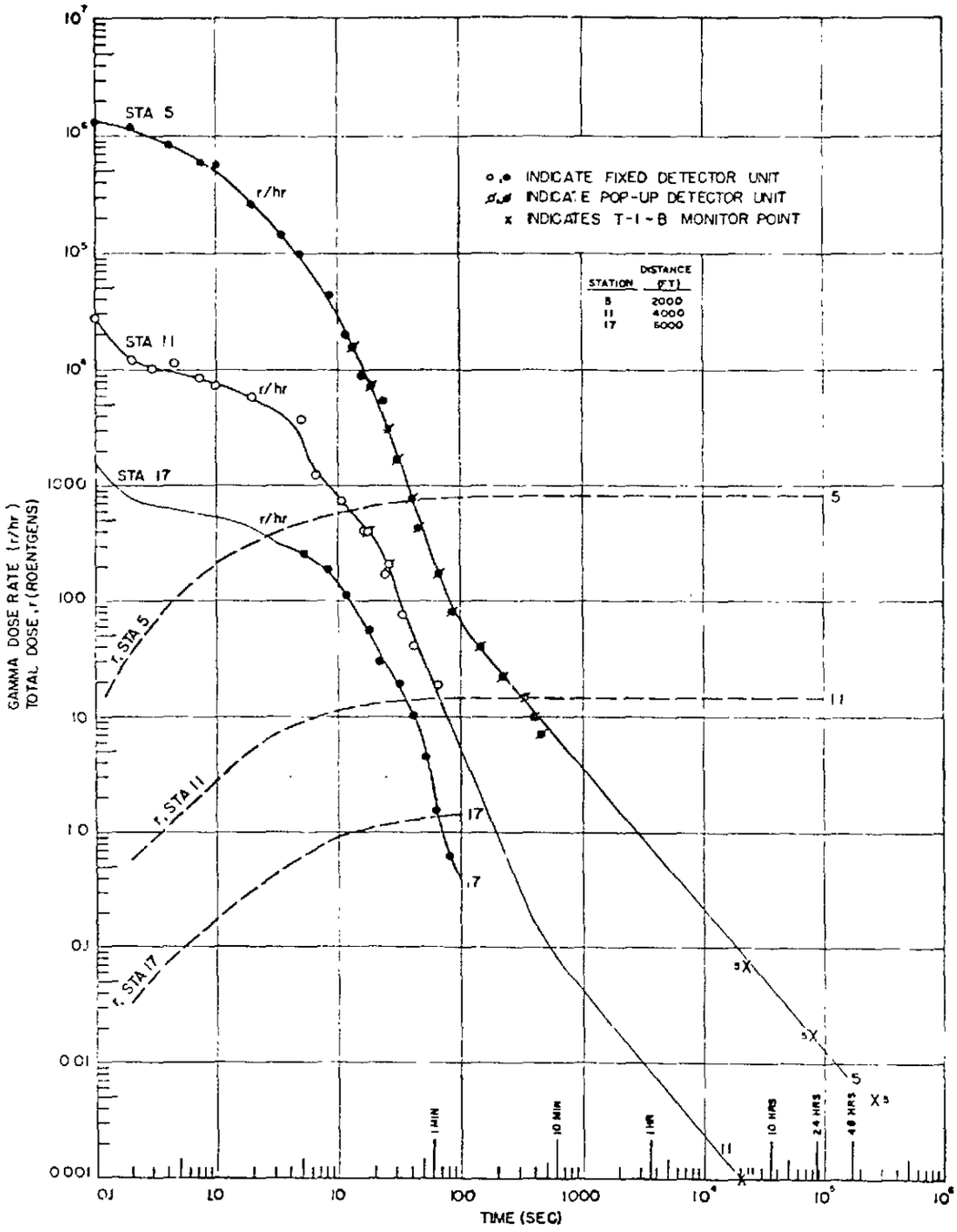

Fig. 8.1 Surface Shot, Dose Rate and Total Dose vs Time, Upwind

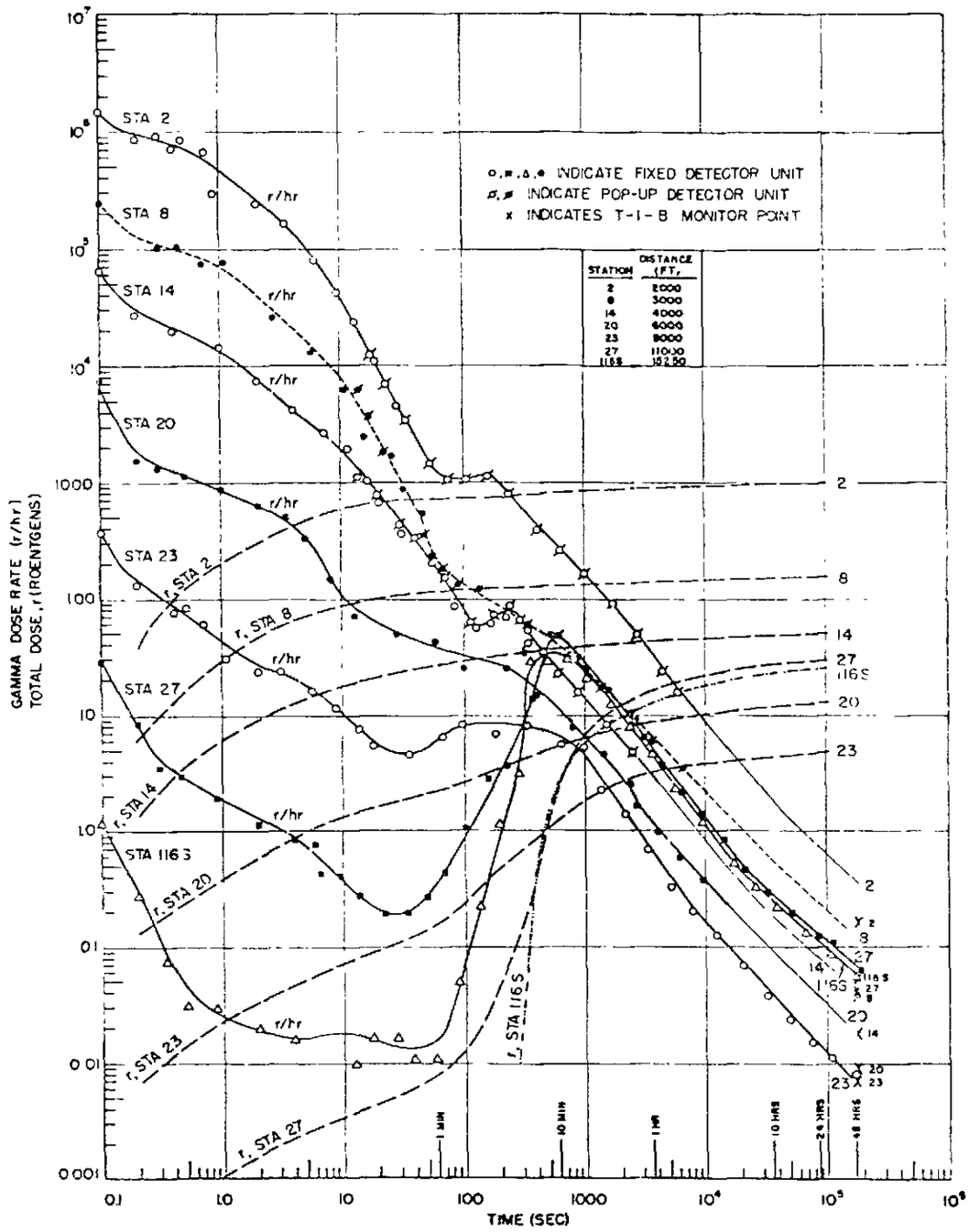

Fig. 8.2 Surface Shot, Dose Rate and Total Dose vs Time, Downwind

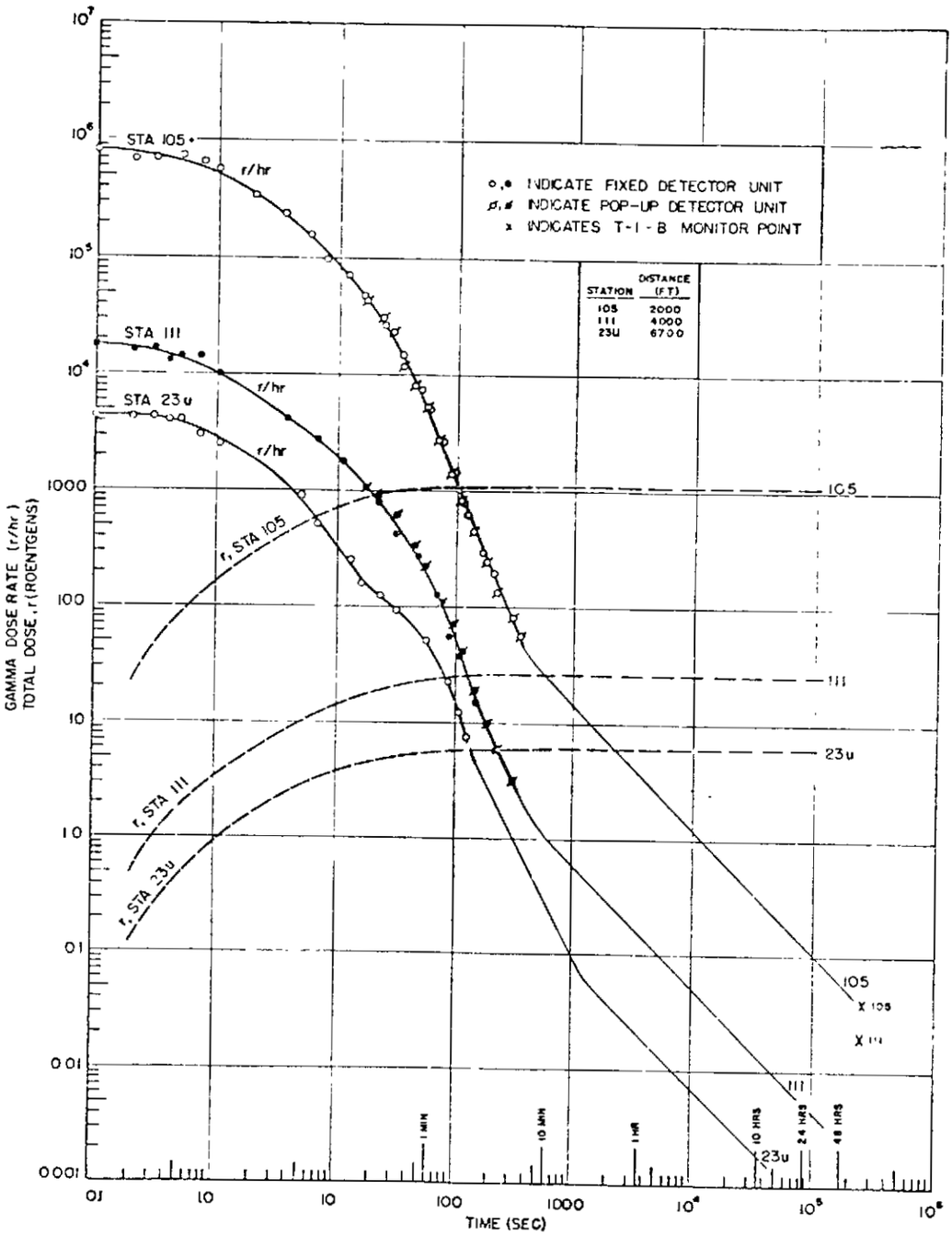

Fig. 8.3 Underground Shot, Dose Rate and Total Dose vs Time, Upwind

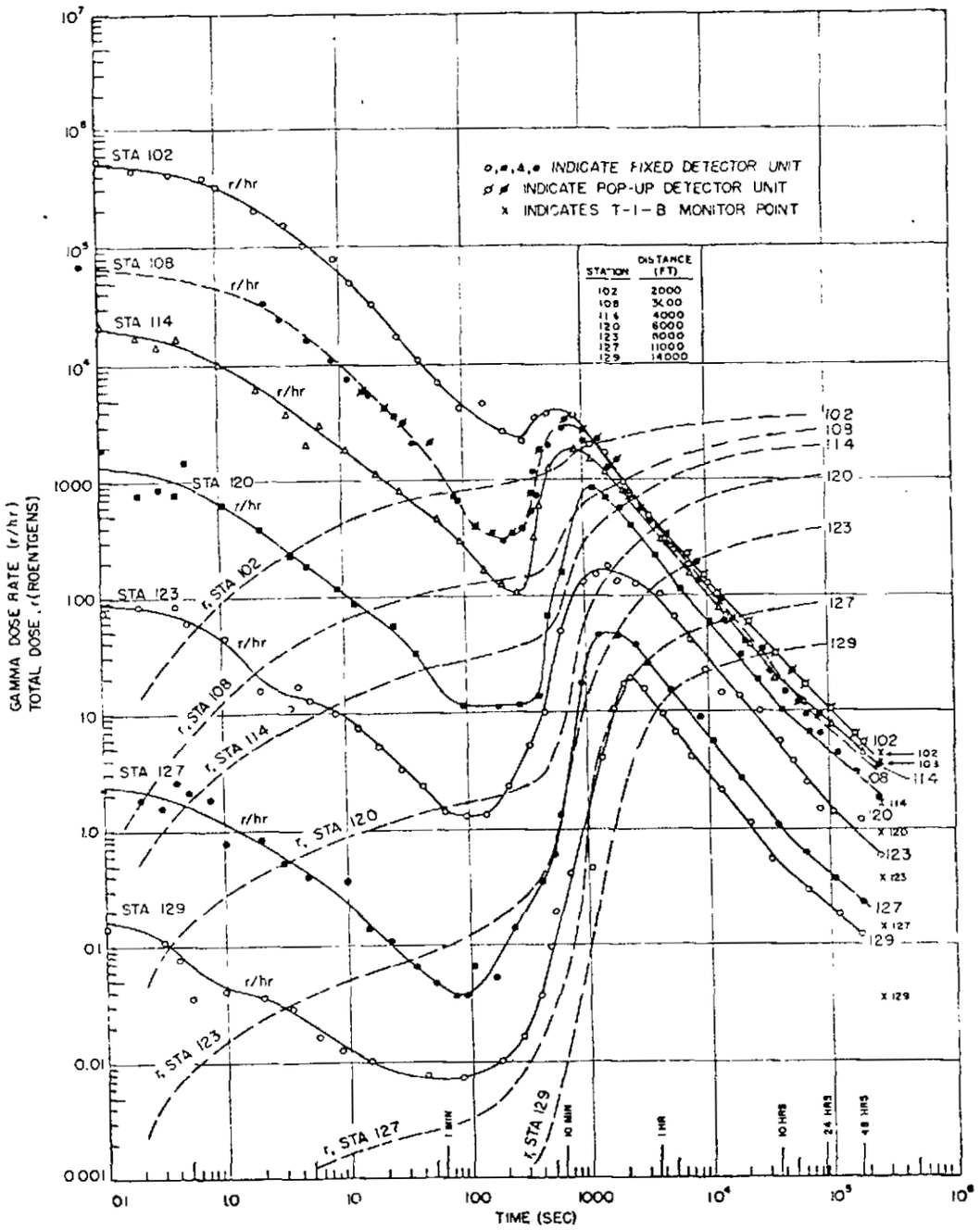

Fig. 8.4 Underground Shot, Dose Rate and Total Dose vs Time, Downwind

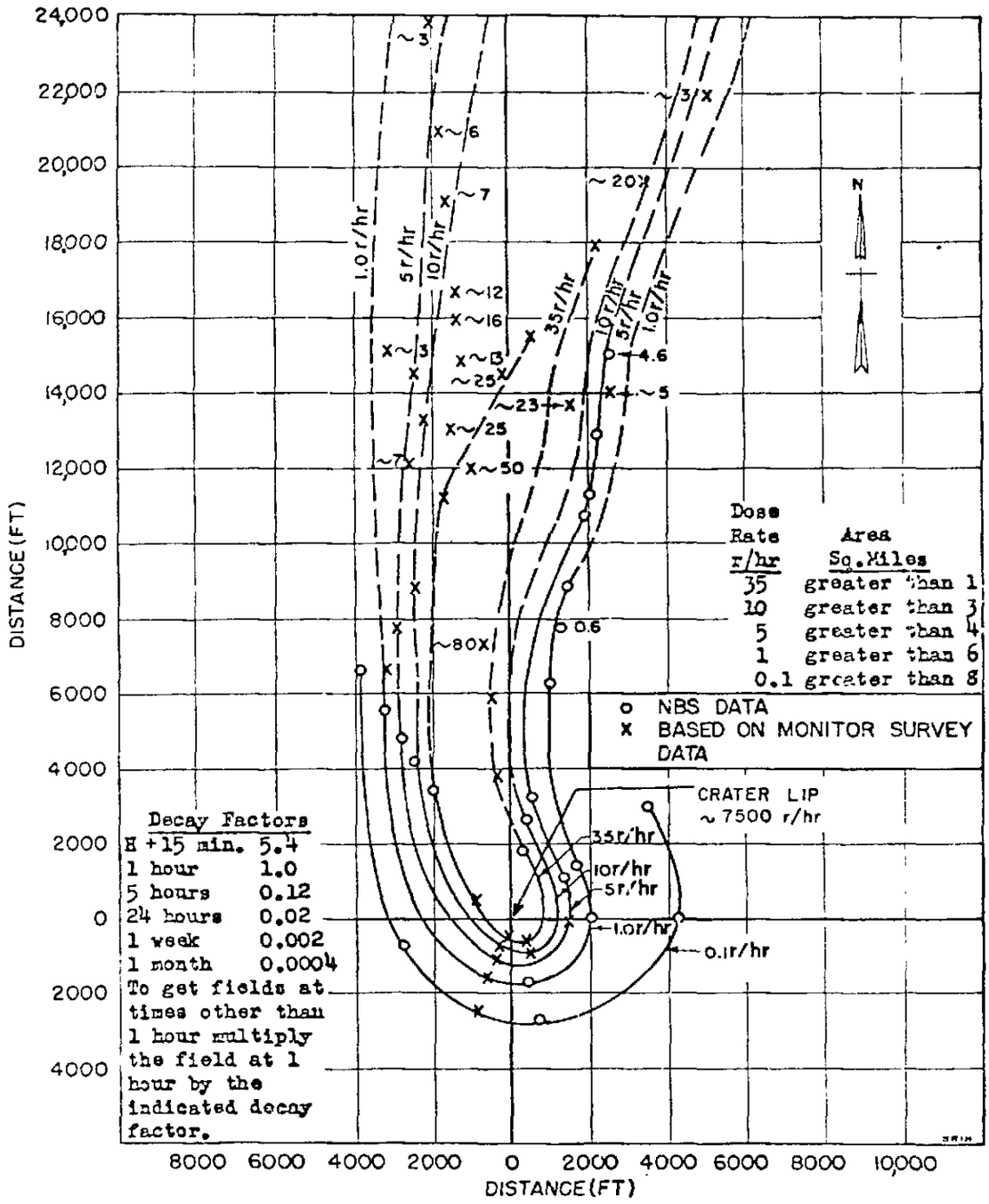

Fig. 8.5 Surface Shot, Gamma Dose Rate Contours at H+1 Hour in Roentgens per Hour (Wind Profile Given in Table B.2)

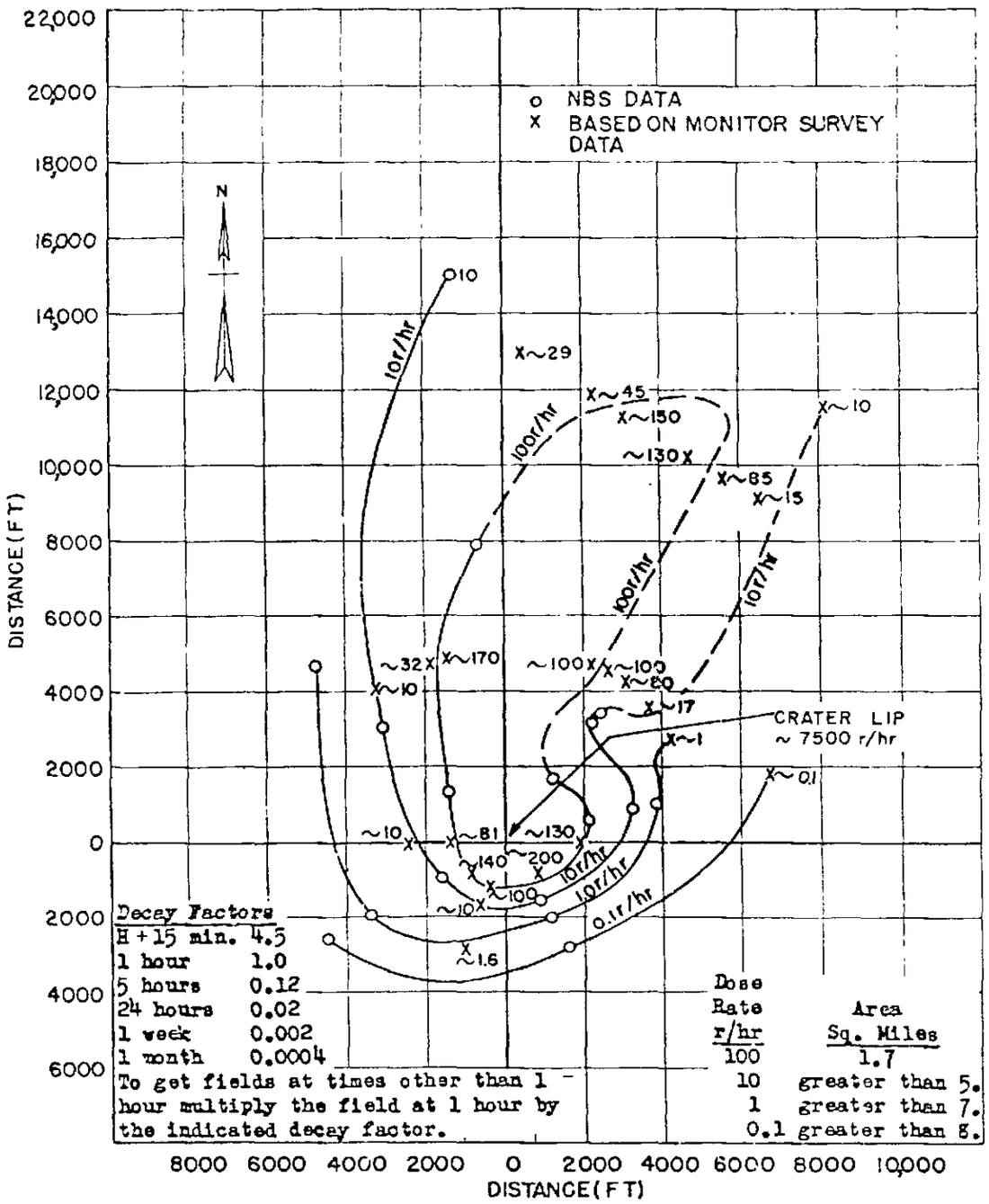

Fig. 8.6 Underground Shot, Gamma Dose Rate Contours at H + 1 Hour in Roentgens per Hour (Wind Profile Given in Table B.2)

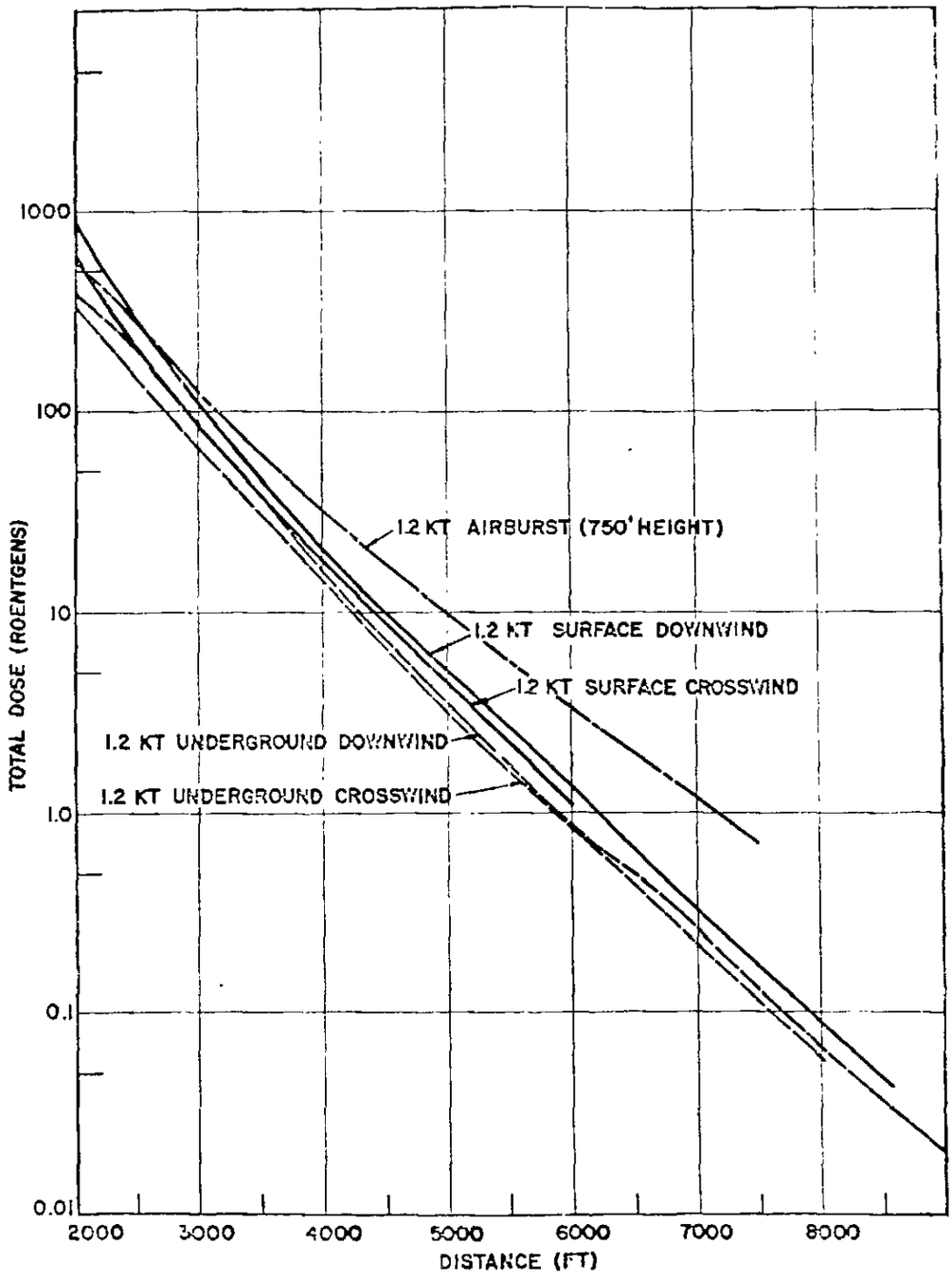

Fig. 8.7 Total Gamma Dose in Roentgens for First 10 Seconds vs Distance from Ground Zero

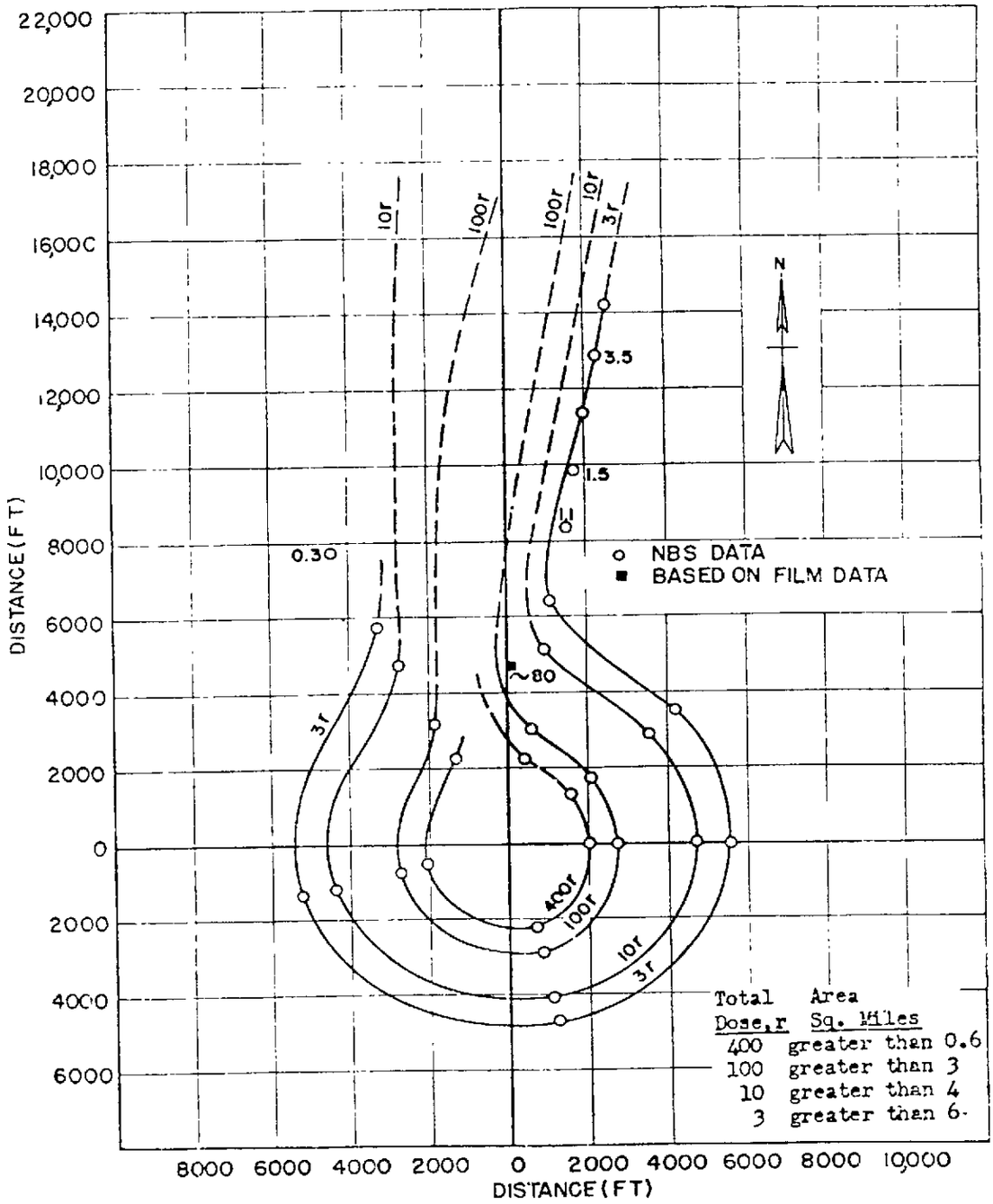

Fig. 5.8 Total Gamma Dose in Roentgens for First 10 Minutes, Surface Shot

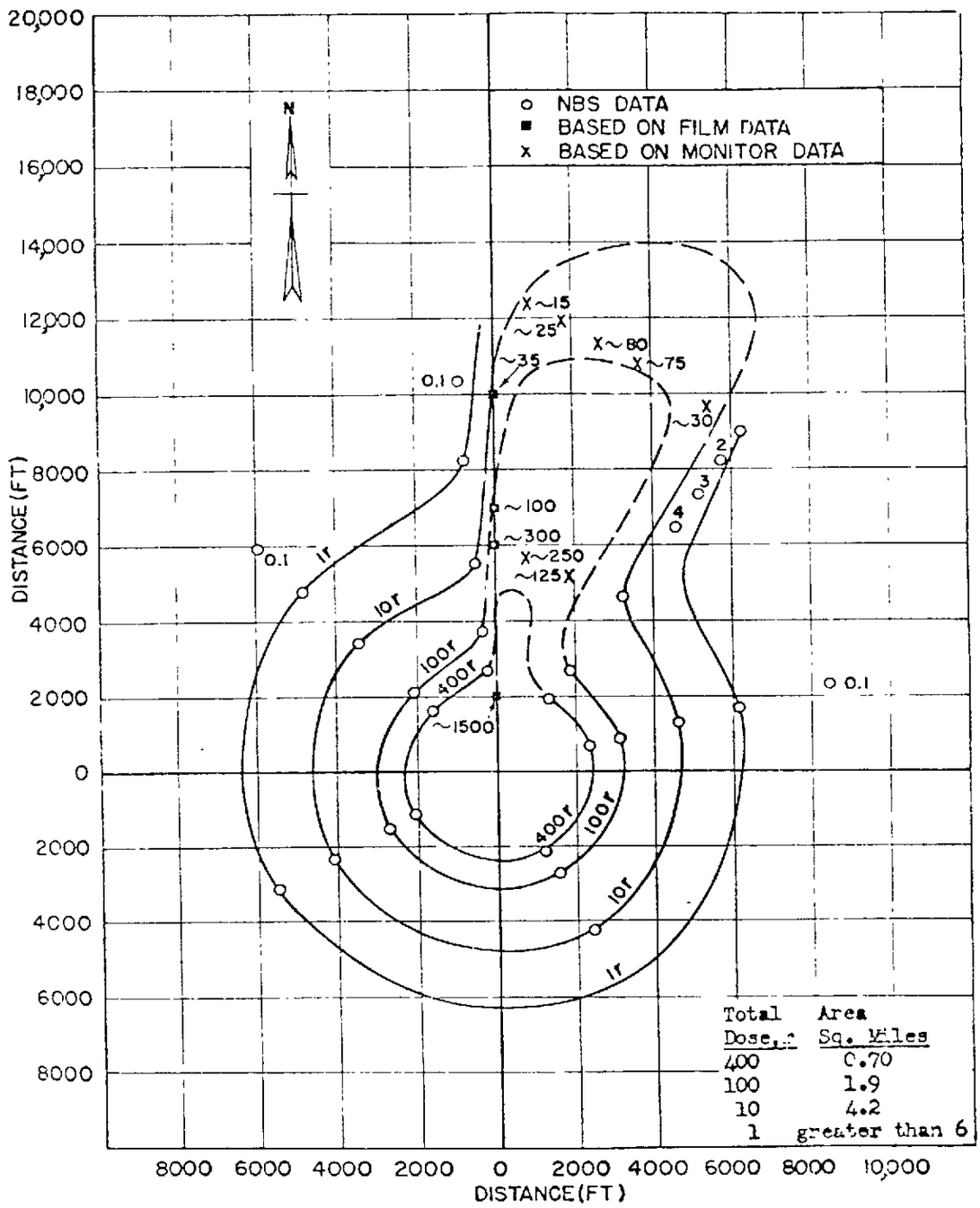

Fig. 8.9 Total Gamma Dose in Roentgens for First 10 Minutes, Underground Shot

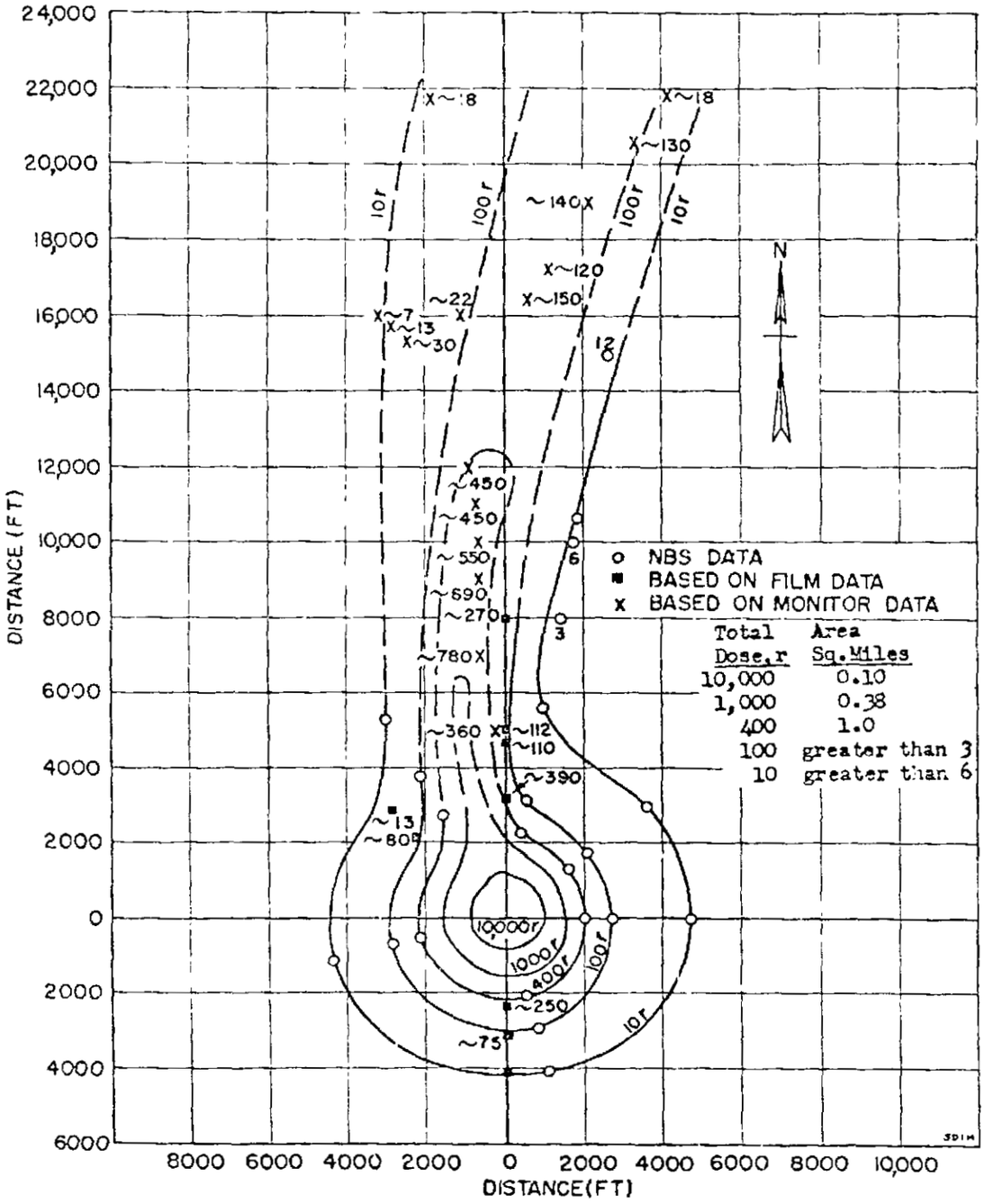

Fig. 8.10 Total Gamma Dose in Roentgens for First Hour, Surface Shot

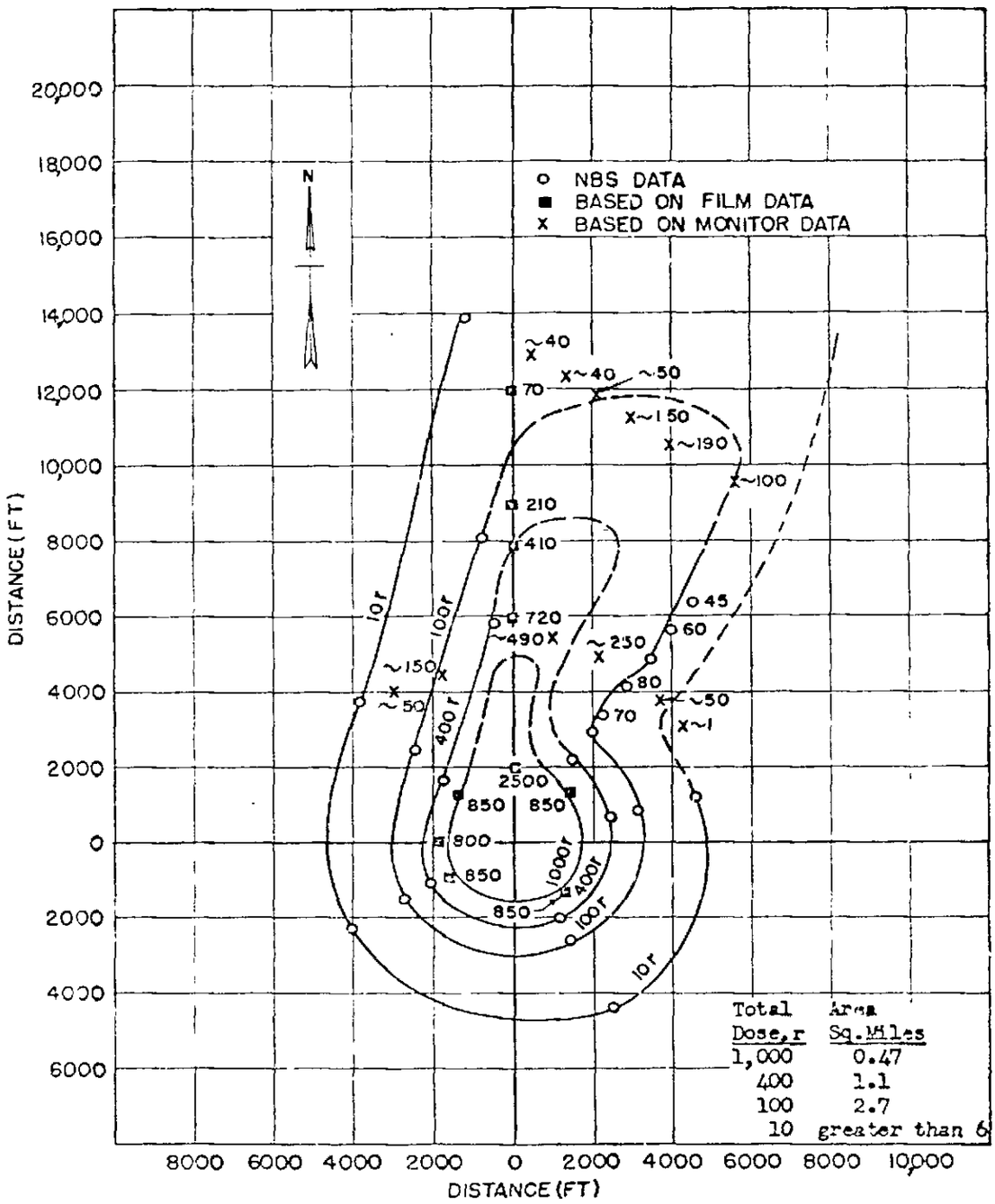

Fig. 8.11 Total Gamma Dose in Roentgens for First Hour, Underground Shot

The normal fission product decay law ($t^{-1.2}$) was found to apply quite reasonably to dose-rate readings except during the period when the neptunium contribution was high relative to total fission product activity. The neptunium contribution was significant for both detonations for the period from 48 hours to two weeks after detonation with a maximum effect at about plus five days. The normal decay law should be applied with caution when correcting monitor data back to two hours or earlier because of time of arrival considerations.

8.3 TOTAL GAMMA RADIATION DOSE MEASUREMENTS

Total gamma radiation dosage data are available from the integration of scintillation counter dose-rate data and from gamma radiation dose film measurements employing the National Bureau of Standards type film dosimeter and holder. The film measurements were taken 3 feet above the ground over a broad pattern extending out to 10 miles downwind. This coverage was augmented by film measurements for calibration and correlation purposes at all particle sampling stations, animal locations, and in foxholes at several distances.

The gamma radiation dosage received in the first 10 seconds versus radial range from ground zero is compared for 1.2 KT air, surface and underground bursts in Figure 8.7. The 10-second dosage for the underground and surface detonations is based on integrated scintillation counter data corrected for the contribution during the first one-tenth of a second. In the first tenth of a second for the underground shot the dose is about 10 per cent of the total received in the first second, while for the surface burst it is probably very nearly that for air bursts or about 50 per cent of the total for the first second (LASL BUSTER/JANGLE Report 10.6).

Gamma radiation dosage contours are presented in Figures 8.8 and 8.9 for the cumulative dosage in the first 10 minutes and in Figures 8.10 and 8.11 for the first hour. These curves were obtained by the integration of scintillation counter dose rate data, augmented by gamma film and monitor data (Project 2.1a).

8.4 RADIOLOGICAL IMPORTANCE OF BASE SURGE

The JANGLE underground shot produced a limited base surge which extended radially upwind about 1700 feet and crosswind as much as 2200 feet. The radiological importance of this marginal base surge is subject to question. Evidence that the contribution of the JANGLE base surge to residual contamination is minor is given in the report of Project 2.0. However, the test results were not sufficiently conclusive to discount the importance of the base surge without further evaluation.

At smaller scaled depths no base surge formation is to be expected.

At greater scaled depths the base surge should increase in importance as an agent for the distribution of contamination. The distribution of contamination for greater scaled depths has not been studied but indications are that mixing and distribution will not be uniform and that a larger portion of the activity will be deposited near the crater.

8.5 GAMMA ENERGY MEASUREMENTS

The effective energy of the gamma radiation in the residual contamination field was investigated by use of sets of energy dependent ion chambers (Project 2.4a). In addition the degraded field spectrum was measured at a number of locations and times of low field intensity by means of a scintillation counter gamma ray spectrometer. Because of technical difficulties, the scintillation spectrometer measurements provided results only for the underground shot and did not provide data on the energy distribution above about 600 kev. The results of these experiments are consistent. They indicate a low effective gamma ray energy with a very high contribution of soft radiation. The principal results are as follows:

a. The effective energy values from the ion chamber measurements varied from 84 to 140 kev for the surface detonation and from 113 to 144 kev for the underground detonation. These results apply only to points of relatively low gamma field intensity for periods after the first several hours.

b. In general the effective energy value decreased with distance from the crater and decreased with time over the first several days. The decrease with distance is attributable to a larger proportionate contribution of scattered radiation at the more distant points where the concentration of local contamination is lower. The decrease with time may be in part attributable to the growth of neptunium contribution (see Paragraph 8.8).

Figure 8.12 gives the energy distribution of the degraded gamma radiation at two points of low field intensity for the underground shot. The location of stations indicated on the figure are identified in Figure D.2. The high proportion of soft radiation is significant since there is a wide divergence in the energy response of most radiation measuring instruments for these low energies.

8.6 BETA RADIATION MEASUREMENTS

Beta film measurements were carried out to determine the beta-ray energies and the ratio of beta to gamma-ray ionization resulting from the residual contamination following underground and surface atomic detonations (Project 2.4a). The principal results of these measure-

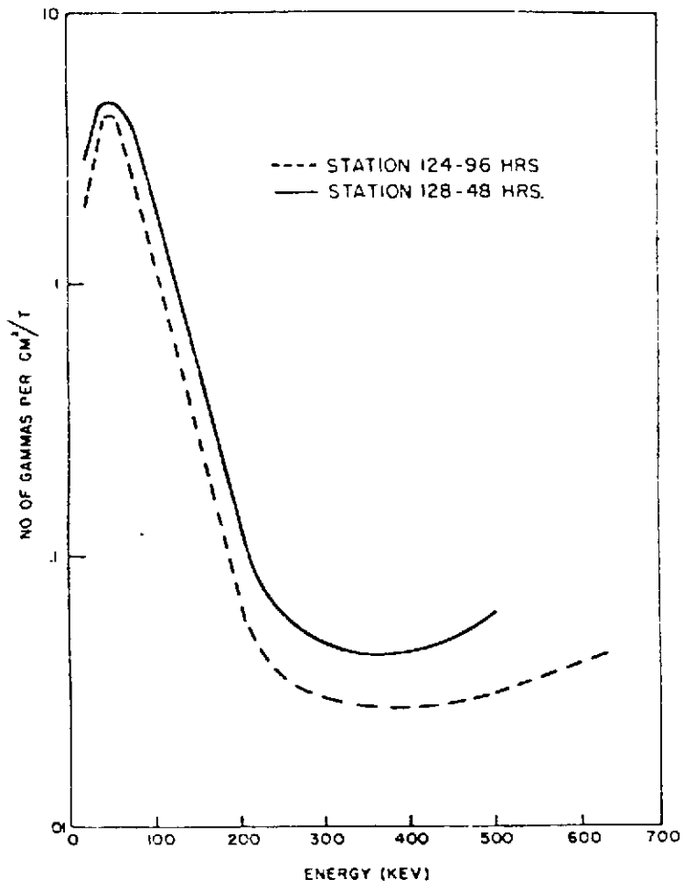

Fig. 8.12 Gamma Flux vs Energy, Low and Intermediate Energy Regions, Underground Shot

ments are summarized as follows:

a. The equivalent maximum energy of beta rays of residual contamination resulting from the surface detonation was 1.7 Mev or less averaged over a period of 24 hours following the detonation.

b. The equivalent maximum energy of beta rays of residual contamination resulting from the underground detonation was 2.0 Mev or less averaged over a period of 70 hours following the detonation.

c. Ratios of beta to gamma ionization as measured by photographic film packets ranged from 2 to 100 depending upon the location of the packets with reference to the residual contamination area. The highest

figure was obtained at a distance of 1.5 inches above the contaminated surface. The rapid decrease in the beta-gamma ionization ratio as the distance is increased indicates that clothing will afford substantial protection and that beta radiation is a potential hazard only for contamination in direct contact with the skin.

8.7 PARTICLE STUDIES

Fall-out and near ground dust clouds were sampled extensively with a variety of collectors over a broad pattern extending downwind a distance of 10 miles. Scattered measurements of fall-out and dust concentrations were made at greater distances. These collections were examined to determine particle size distribution as a function of distance, the size and activity distribution of radioactive particles, and the concentration of radioactive particles in dust clouds. Numerous studies were carried out to determine the physical and chemical nature of individual radioactive particles.

Voluminous data have been compiled and are presented in the reports of Projects 2.5a-1, 2.5a-2, and 2.5a-3. These data are at present in an incomplete state of correlation and evaluation. There are numerous inconsistencies in the data that result from the limitations of the collection instruments and of the techniques employed in the analysis of size distributions for the wide range of particle sizes involved. In addition there are insufficient data to establish the rate of fall-out with time and the per cent of total radioactivity that was carried by the smaller size fractions which largely remained airborne. These factors, together with the evidence of very incomplete mixing of radioactive and inert debris, seriously limit the reliable determination of the gross size distribution of the radioactive particulates.

8.7.1 Principal Results and Conclusions from Particle Studies

The specific activity of fall-out from both JANGLE detonations increased with distance downwind, testifying to the incomplete mixing of radioactive products with gross crater debris and indicating association of active material with the upper cloud. Although the specific activity increased with distance, the total activity at a given station decreased with distance.

The bulk of the activity of the fall-out material in areas of significant residual contamination resulting from the surface shot was associated with large particles. For the underground shot a substantial portion of the activity was associated with particles under 75 microns. The fraction of total activity carried by particles in the smaller size range increased with radial distance within the base surge area and increased more slowly in the downwind direction beyond the surge limit. The per cent of total station activity associated with

particles under 75 microns diameter at stations along the downwind line is presented in Figures 8.13 and 8.14.

The per cent of total activity carried in each of three arbitrary size ranges, averaged over 10 fall-out collections made within 3 miles downwind of the point of detonation, is presented in Table 8.2.

TABLE 8.2

Activity vs Particle Size
Downwind

Size of Fraction (μ)	Surface Shot Per cent of Total Fall-out Activity	Underground Shot Per cent of Total Fall-out Activity
0 - 2	0 - 1	0.5 - 1
2 - 20	0 - 6	2 - 5
> 20	93 - 100	94 - 96

Studies of time of arrival of fall-out indicate that the heavy initial fall-out at the more distant stations even for the underground detonation originates from material carried in the higher levels of greater wind speed with subsequent lighter depositions of material carried by the lower winds.

The highest sampled concentrations of radioactive materials in the near ground dust clouds appear to be about 10^{-3} and 10^{-1} microcuries of beta activity per cubic centimeter of air for the surface and underground detonations respectively. These concentrations were measured at downwind distances of about 2000 to 4000 feet. The concentrations fell off rapidly crosswind and at greater distances downwind. The values of concentrations given above apply to an exposure averaged over the approximate period from arrival to departure of the cloud and with the beta activity corrected to the average time of exposure. Thus for the underground shot, the concentration of 10^{-1} microcuries per cubic centimeter is an average for 10 minutes exposure with the beta activity corrected to about 8 minutes after detonation.

It is of interest to note that inhalation by animals located in areas receiving the highest dust concentrations from the underground shot did not result in retention of physiologically significant amounts of activity. See Paragraph 8.9. The fraction of the total activity carried by particles in size range of 0.5 to 8 microns diameter, while not well established by the data, was certainly low. The particles in this size range are considered to determine the inhalation hazard.

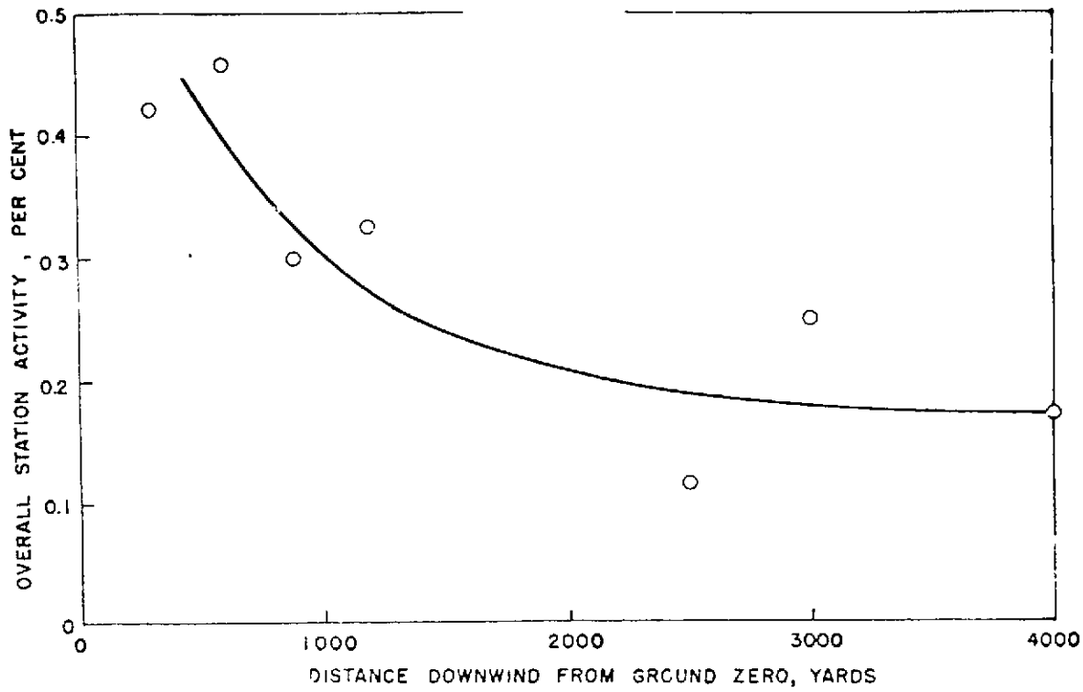

Fig. 8.13 Per Cent of Total Station Activity Found in Particles of Less Than 75 Microns Diameter vs Distance Downwind, Surface Shot

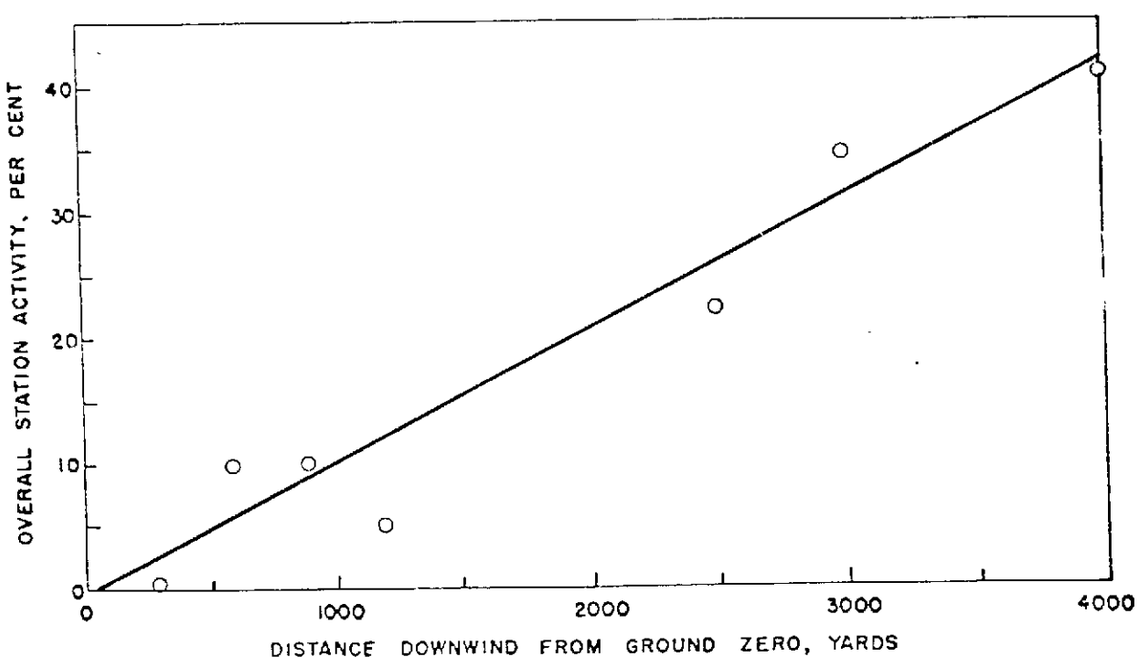

Fig. 8.14 Per Cent of Total Station Activity Found in Particles of Less Than 75 Microns Diameter vs Distance Downwind, Underground Shot

8.8 NATURE OF RESIDUAL CONTAMINATION

Radiochemical analyses and decay and absorption measurements were made for a wide variety of samples of residual contamination. Core samples from the crater lips were taken to determine the depth distribution of radioactive materials. Surface samples from the crater lips and fall-out samples were examined to assess variations in the relative abundance of fission products and in the occurrence of neutron induced activities with distance. The more significant results of these studies are the following:

a. Neptunium-239 was found to be the only isotope other than fission products that contributed significantly to residual contamination. During the period between 15 and 300 hours the beta activity of neptunium was greater than that of the fission products. At the time of its highest relative contribution, about five days after detonation, the neptunium activity was about three times the total fission product activity. Since the neptunium is produced by neutron capture [redacted] core uranium-238, the ratio of neptunium to total fission products is determined by the ratio of uranium-238 captures to total fissions and will vary for different weapons. A negligible amount of neptunium relative to total fission products will result from the detonation of a [redacted] weapon.

b. The total contribution of neutron induced activity in the soil material was found to be no more than a few per cent of the total fission product activity. The amount of neutron induced soil activity relative to fission product activity is highest at the crater lips. It may be appreciable in this location during the first day or two due to the contribution from sodium-24, potassium-42 and manganese-56. Neutron induced soil activity should be small for surface and subsurface detonations in most soils for all weapons except those in which the ratio of escape neutrons to total fissions is markedly increased over the ratio for the JANGLE weapon.

c. The beta and gamma radiation decay rates for both JANGLE detonations show departure from the normal fission product decay rate, particularly during the first two weeks when the neptunium contribution is significant. The beta activity of soil samples from the surface burst can be represented by an equation describing only the decay of fission products and neptunium (see Figure 8.15). The same representation did not give good agreement with the observed decay for the underground shot samples, indicating perhaps a larger contribution of induced soil activities, more extensive fractionation of fission products, or both.

d. Most of the radioactivity at the crater lips for both craters was concentrated on the surface with a rapid fall off of specific activity with depth. At a depth of one inch the activity was less than

five per cent of the surface activity and some of the subsurface activity may be due to unavoidable contamination arising from the method of core sampling.

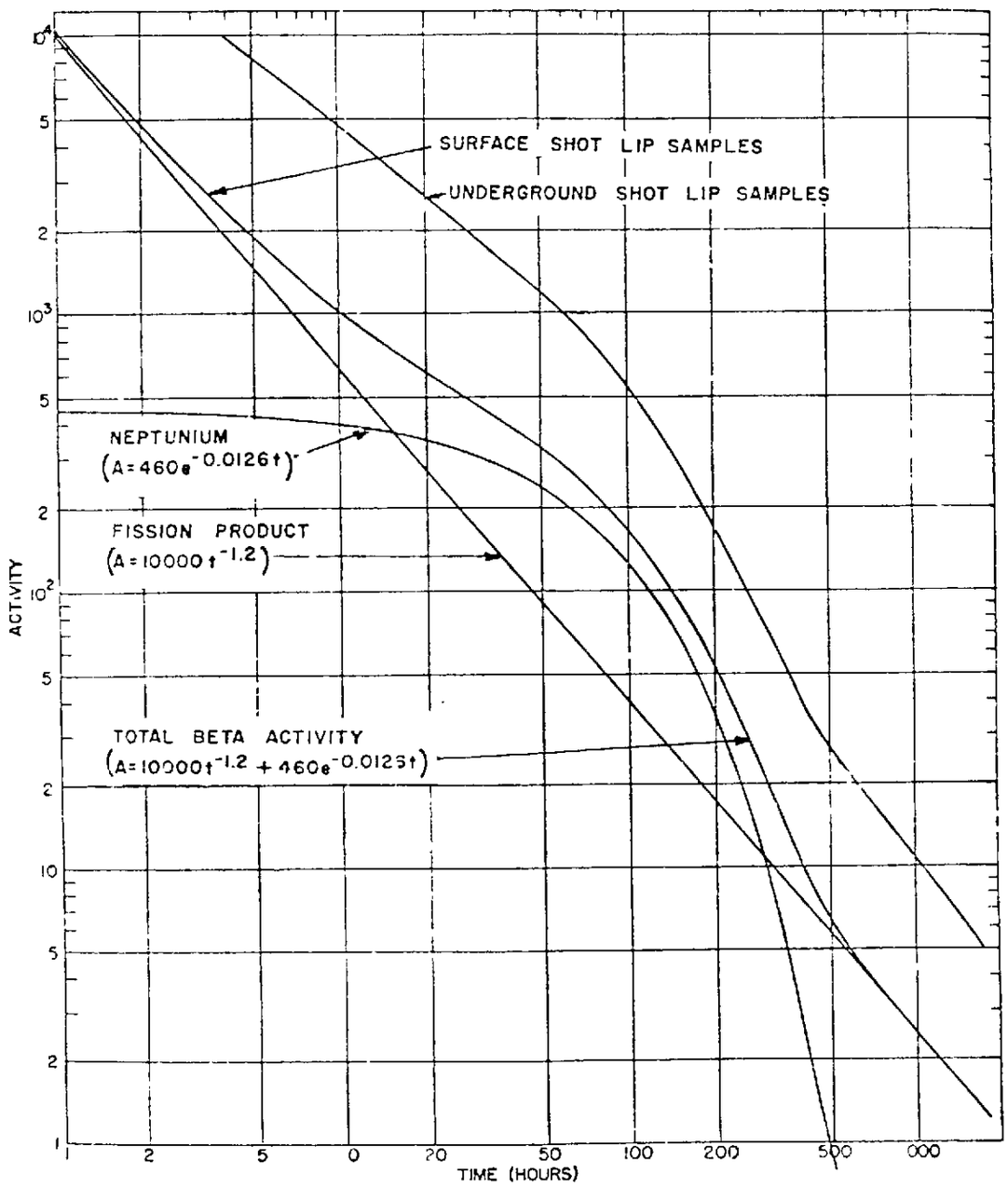

Fig. 8.15 Beta Activity vs Time, Crater Lip Samples

e. The degree of fractionation of fission products from the JANGLE detonations was shown to be quite great and dependent on the place and method of sampling. Strontium-89 and barium-140, whose relative concentration increased with distance and with time of collection, were found to fractionate more than other fission products.

f. Experiments on effect of weathering and leaching of residual contamination on the ground with water, detergents, and chemical agents indicated very little transport of contamination by such methods.

8.9 INHALATION STUDIES

Dogs and sheep were exposed on the ground surface and in foxholes at distances of 2500 to 8000 feet in the predicted downwind direction from each shot. The purpose of the exposure was to allow the assessment of hazards due to inhalation of radioactive dusts associated with these detonations and to compare internal and external radiation dosages.

The animals exposed during the underground detonation overlapped the center of concentration of downwind dusts and fall-out in the range of exposure distances. Those exposed during the surface detonation were crosswind with a consequently low exposure of active materials.

Exposed animals were sacrificed in groups on a time schedule from H + 10 hours to D + 70 days. Lung tissue, soft tissues, bone, urine, and gut contents were ashed and assayed for radioactivity. Radioautographs of tissue sections were made.

Total body activity for animals exposed in the underground test ranged from 2 to 31 microcuries corrected to time of sacrifice. For lung tissue, integrated dosage due to beta emission ranged between 0.2 and 9.0 rep. Radioautographs of lung tissues indicated the presence of a few alpha emitting particles. Bone analyses indicated some uptake of Ba^{140} and Sr^{90}.

The amounts of activity taken up by the combined action of inhalation and ingestion are not considered to be physiologically significant even for animals receiving cumulative external gamma radiation dosages up to several thousand roentgens.

Consideration of increases in concentration and exposure period for larger detonations under conditions comparable to the JANGLE tests indicates total radioactivity uptake should increase approximately as the cube root of the yield with little change in the relative internal to external dosage ratios.

It is clear that no inhalation hazard of military significance independent of an external hazard of more serious consequence exists for personnel in the open or even for those with moderate shielding in

vehicles or foxholes.

The internal dose, independent of the external gamma radiation hazard, appears to be insufficient to produce tissue damage over a short period of time. However, the possibility of long term biological effects due to inhalation is not ruled out although there is no positive evidence that such long term hazards exist.

These conclusions should be applied with caution to conditions varying widely from those of the JANGLE tests since concentrations of active particles in the size range of 0.5 to 8 microns, which determine the inhalation problem, may be altered considerably for other soils, depths of detonation, and meteorological conditions.

8.10 GAMMA DEPTH-DOSE MEASUREMENTS

Gamma radiation depth-dose measurements in approximately unit density material were made at positions upwind of both the surface and underground points of detonation, using the same techniques employed at the GREENHOUSE and BUSTER tests (Project 2.4b).

The results apply only to initial gamma radiation independent of appreciable contribution from residual contamination. They indicate no significant difference in the variation of initial gamma radiation dose with depth for the JANGLE detonations from that for air bursts.

8.11 SAMPLING TECHNIQUES

Remote-controlled weasels were successfully employed for early sampling of particulate materials in areas of high gamma radiation intensity. In addition the use of retrievable missiles for such sampling was tested with success.

The use of remote-controlled vehicles has the advantage of range of operation. Further, such vehicles can be equipped for core sampling and a variety of other mechanical functions. The experience gained in the techniques of remote control, including the television monitoring system that was successfully employed in this test, should contribute to the application of these techniques in other fields of interest.

Within their limited range, the use of retrievable missiles is indicated as a far more economical method for the remote collection of surface samples. It should be no problem to scale up the missile size for appreciable increase in range. Larger missiles of this type should be adequate to meet most requirements for remote surface sampling in connection with further atomic tests.

CHAPTER 9

TESTS OF SERVICE EQUIPMENT AND OPERATIONS

9.1 INTRODUCTION

At Operation JANGLE the field suitability of equipment and techniques developed to minimize the restrictions and hazards associated with widespread residual radioactive contamination was evaluated. Operation JANGLE was the second operation during which atomic bombs were detonated in such a way as to produce areas of high intensity radioactive contamination sufficiently large to be of significance to military operations.

The first such detonation was Bikini Baker where ships and equipment suffered serious mechanical damage in an area of only three quarters of a square mile while ships well beyond this area, particularly in a downwind direction, incurred extensive residual radioactive contamination. As a result of Bikini Baker considerable military research and development effort was devoted to providing techniques and equipment to alleviate residual radioactive contamination hazards. This effort led to the development of radiac equipment built to military specifications, development of radioactive decontamination procedures, and the application of individual and collective protective equipment. Those portions of the test program of Operation JANGLE which were concerned with the field evaluation of these developments and with tests to determine capabilities of standard service equipment in areas of serious residual radioactive contamination are briefly summarized in this section.

9.2 EVALUATION OF MILITARY RADIAC EQUIPMENT

Four types of portable radiac survey instruments were field tested by actual usage in area survey, health monitoring, and decontamination work. All instruments required considerable preparation and maintenance work and the majority were heavy and large. None of these instruments were capable of indicating more than 50 r/hr although, even under the conservative tolerances specified for these tests, limited operations were conducted in areas of several hundred roentgens per hour intensity.

Two types of portable radiac survey instruments (AN/PDR-18 and AN/PDR-32) received limited informative testing for engineering and technical guidance. Radiac Set AN/PDR-32 was the most satisfactory of all the instruments from the standpoint of size, weight, and maximum range (500 r/hr), however, its ruggedness and reliability as a military survey instrument were not established.

A developmental model of an automatic unit for processing wet-type, radiation dosage film was operated and evaluated during these tests. The unit was found to be unsatisfactory since it could not maintain uniform photographic development when operating for periods of time longer than 20 minutes. During this operation one man developed by hand more film per hour than the automatic unit can process at its theoretical maximum speed of 600 badges per hour. It was decided during this test that the loading, developing, washing, and drying times were not the most significant factors in the overall rate of film handling and processing. The more time-consuming operations were those involving the removal of the film from the packets, reading the film on the densitometer, recording of results and various other handling details.

Laboratory models of portable air monitoring equipment, designed to determine the air loading of radioactive particles, were operated in the contaminated area to determine feasibility of portable monitors and to obtain information for future development. Paragraph 8.9 indicates that radioactive airborne dust is not a hazard in military field operations.

9.3 AERIAL RADIOLOGICAL SURVEY TECHNIQUES

Airborne radiac equipments (AN/ADR-4, Type F-1, and AN/ADR-1) have been developed by the Navy and Air Force for use in the rapid survey of areas of radioactive contamination on the ground (Projects 2.1c-1 and 2.1c-2). The equipment was designed to measure the gamma dose-rate at altitude and introduces a correction for altitude to determine ground intensity. It was considered that this information, when correlated with the airplane's course, ground speed and a point of orientation, would permit the construction of dose-rate contour maps of the ground contamination.

Experience in the JANGLE tests indicates that the operational difficulties and evaluation problems involved in the rapid aerial survey of contaminated areas, resulting from surface and underground atomic detonations, lend doubt to the reliability of such techniques and to their utility in military operations. The principal difficulties involved are the following:

a. Pockets of airborne debris remain over areas of irregular terrain for considerable periods after the cloud has passed downwind. There is no way of discriminating between airborne debris and ground contamination, particularly since the distribution of airborne activity varies in concentration and extent with altitude. The presence of airborne debris will result in excessively high survey readings.

b. Maintaining reliable records of ground and course speed for low-level flight over irregular terrain with a high speed aircraft is a

difficult problem.

c. The steep gradient of gamma radiation intensity with distance from ground zero for surface and underground bursts results in high readings due to the contribution of highly scattered radiation. This renders unreliable the evaluation of ground intensities except for points of peak intensity.

Another rapid radiological survey of ground zero and the adjacent highly contaminated ground area was performed in low-flying aircraft instrumented with standard radiac set AN/PDR-T1B and automatic recording equipment (Project 6.1). The location of ground zero and the area of highest fall-out intensity were approximately determined by this survey.

The survey equipments are useful for the location of contaminated areas and establishing the extent of such areas. However, it is subject to question that aerial survey techniques can, in the face of the problems involved, provide dose-rate contour maps of ground contamination sufficiently reliable and early to assist ground operations. It appears that the military application of these techniques should be carefully reviewed.

9.4 PROTECTION AND DECONTAMINATION OF LAND TARGETS AND VEHICLES

Operation JANGLE provided the first opportunity to field test procedures for decontaminating components of a typical land target complex. It also provided basic information upon which the need for and the feasibility of decontaminating objects subjected to contamination by a surface or underground atomic bomb detonation may be evaluated. The results are largely limited to conditions where the contamination is distributed in a dry state. Some of the data are at variance with Bikini Baker where the contamination was distributed in a wet state.

It was found that only horizontal and near horizontal exposed surfaces retained contamination to a significant extent. Only gross changes in surface roughness were found important to the retention of contamination, and these were insignificant in comparison with the effect of surface orientation. The results of the tests of decontamination procedures are summarized in Table 9.1.

It was found feasible to reduce the general radiation intensity in a contaminated land target complex by a factor of 5 to 10 by decontamination procedures using standard construction equipment. However, the effort required to accomplish this is so extensive that radioactive decay will compare favorably with decontamination in reducing radiation levels under most operational situations.

TABLE 9.1

Decontamination Effectiveness

Material or Object	Reduction Average (%)	Most Suitable Method	Approximate Rate of Accomplishment
Open Land	88	Scraping plus peripheral plowing	Scraping: ½ acre/equip. hr; plowing: 3 acres/equip. hr
Asphalt	90	High pressure hosing	1800 sq ft/equip. hr
Buildings	80	High pressure hosing	1200 sq ft/equip. hr
Roof Panels	90	High pressure hosing with detergent	600 sq ft/equip. hr
Painted Surfaces	90	High pressure hosing with scrubbing	1200 sq ft/equip. hr
Vehicles	80	Vacuuming inside, high pressure hosing with detergent outside	½ hr for Med. Tank
Wood	98	Surface removal	1200 sq ft/equip. hr

TABLE 9.2

Vehicle Shielding

Vehicle	Reduction (%)*
M-24 Tank Inside	90
M-24 Tank on Fenders	60
M-26 Tank Inside	95
M-26 Tank on Fenders	60
T18E1 Personnel Carrier	90
2½ Ton Truck	50
3/4 Ton Truck	70
¼ Ton Truck	50

* These reductions do not apply at early times particularly in areas of highest gamma intensity, when the higher effective gamma energies are envolved and consequently shielding factors will be considerably lower.

Military vehicles and tanks afforded considerable shielding to occupants while operating in a contaminated area. Average percentage reductions measured in low intensity areas after one day are shown in Table 9.2.

Vehicles operated in the most highly contaminated areas became radioactively contaminated to a degree significant only under AEC working tolerances. When the ground was wet following a rain, this condition was aggravated. However, under no circumstances would this contamination be of importance to a military operation.

9.5 MILITARY INDIVIDUAL AND COLLECTIVE PROTECTION DEVICES AND CLOTHING

Chemical Corps protective clothing, Class I (impregnated) and Class III (non-impregnated), was evaluated for contaminability and ease of decontamination by inert exposure to the direct fall-out and by exposure on personnel working in contaminated areas. Impregnated clothing picked up more contamination than non-impregnated and was more difficult to decontaminate. However, none of the clothing retained contamination in excess of the acceptable AEC tolerance for continuous retention and use without decontamination. All clothing effectively prevented contamination of the portions of the body it covered.

Collective protectors for tanks, E26, were tested for suitability both during the period of fall-out and during operations in highly contaminated areas. Although they were found to provide complete protection from the inhalation of radioactive materials, Paragraphs 8.9 and 9.6 indicate that there is no need for this protection.

Individual protective mask, M9A1, was evaluated for protection against inhalation of radioactive materials. No measurable activity was found to have penetrated the masks worn in the contaminated area produced by the surface burst. Again in Paragraph 8.9 it is indicated that no military requirement for this protection exists.

9.6 EVALUATION OF POTENTIAL RESPIRATORY HAZARDS ASSOCIATED WITH TANK OPERATIONS IN A RADIOACTIVELY CONTAMINATED AREA

Several tanks and an armored personnel carrier were operated through contaminated areas (as high as 50 r/hr). The dust introduced into the vehicles by this operation was measured for gross radioactive content. These measurements established the fact that no military hazard to personnel in the vehicles is to be expected under the most favorable conditions for the creation of a radioactive dust hazard.

Although this project concluded that there may be a potential long term hazard, the continued lack of positive evidence to this effect casts severe doubt that this hazard does exist.

9.7 CONSIDERATION OF RADIOACTIVE CONTAMINATION IN MAJOR OVERHAUL OF AIRCRAFT TURBO-JET ENGINES

Two Allison J-33-A-35 engines from two piloted Air Force T-33A aircraft which had been flown through a radioactive cloud on Operation BUSTER were processed through routine major overhaul. No airborne radioactive contaminant hazard existed during engine removal operations three or four days after contamination. Disassembly was started 36 days after exposure for one of the engines and 92 days for the other. It was found that special precautions were required to meet standard AEC industrial safety requirements but no great difficulty was experienced in complying with these requirements.

9.8 CLOTHING DECONTAMINATION AND EVALUATION OF LAUNDRY METHODS

Standard and special U. S. Army Quartermaster Corps laundering methods and standard laundry equipment were evaluated for field decontamination of clothing and selected fabrics. No clothing worn by personnel became contaminated to a significant degree during this operation. Therefore, this project was carried out with clothing deliberately contaminated with radioactive material from the fall-out area.

The project evaluated the standard and several special laundering formulae, various types of clothing materials, and monitoring instruments (Project 6.7). The significant result of this project is the indication that clothing contamination resulting from work in areas contaminated by atomic bomb detonations will not produce even minor injury to personnel. This conclusion is based on consideration of the data on saturation values of deliberate clothing contamination reduced to one hour after detonation. The resultant exposure to personnel would be less than that required to produce even slight skin irritation (comparable to mild sunburn). Other conditions, such as muddy terrain and much higher specific activity, could increase the amount of contamination received by clothing, but an increase in level of several orders of magnitude would be required to produce injury. In these cases it is certain that routine standards of cleanliness would effectively prevent injury from this cause.

9.9 EVALUATION OF U.S. ARMY FIELD WATER SUPPLY EQUIPMENT AND OPERATIONS

U. S. Army, 3000 gallon, rubber coated, nylon fabric, water tanks filled with drinking water were found to be undamaged within 500 yards from the nuclear surface detonation.

On the occasion of this test, the water in the tanks did not become contaminated nor was neutron induced activity produced. It was calculated, however, that water in open tanks would have been contami-

nated to a level above the acceptable risk level 1/ for 10 days use as a result of fall-out if the tanks had been located in the heavy fall-out area. This area would roughly correspond to the area showing 100 r/hr or greater at one hour.

Drinking water which was deliberately contaminated to a significant level by adding radioactive crater lip debris was processed through an Army 150 GPM Diatomite Water Purification Set. This equipment removed 84.5 per cent of the dissolved or suspended radioactive matter from the drinking water.

CHAPTER 10

INDIRECT BOMB DAMAGE ASSESSMENT

10.1 GENERAL

Operational and experimental data were obtained on radar returns from atomic bursts using airborne radar equipment carried in bomb delivery type aircraft. This technique is being developed as an all-weather method of determining yield and location of ground zero.

10.2 METHOD

The method involves motion picture photography of the PPI sector scan presentation of radar returns. Both X-band radar (AN/APS-23) and Ku-band radar (AN/APS-43) were utilized on this operation. The developed film showing the reflective effects is analyzed for the required data from which ground zero can be determined. From this and from estimates of yield the area of damage can be estimated.

10.3 UNDERGROUND DETONATION

The underground burst was detected with both the X-band and the Ku-band radars. It appeared as a bright spot on the PPI that persisted for 1 minute and 12 seconds before dissipating. This return differed radically from that of an air burst, the latter first appearing as a horseshoe-shaped return which expands and gradually dissipates.

10.4 SURFACE DETONATION

Due to equipment failures no returns were recorded from the surface burst. Since air bursts have been detected, it is probable that reflective effects from the surface burst would have been obtained had the equipment been operative.

10.5 CONCLUSION

It was determined that the center of the bright spot obtained as a radar return from an underground nuclear detonation is the location of ground zero. It was not possible to determine yield from the reflective effects obtained by this method and the phenomena which produces these effects have not been firmly established.

The radar return obtained with the Ku-band radar was more clearly defined than that obtained with the X-band radar. The duration of return was approximately the same for both.

CHAPTER 11

LONG-RANGE DETECTION

11.1 RADIOCHEMICAL ANALYSES

Samples of airborne bomb debris from the surface shot were collected after transport over distances of 1700 and 14,000 statute miles and were identified by radiochemical analysis. Good agreement existed at those distances between the locations of the debris and its path as determined by meteorological trajectories. The debris from the underground shot was sampled and identified after 800 miles of travel, but meteorological trajectory error, combined with small cloud dimensions, resulted in failure to sample the cloud at 1700 miles. Debris could not be identified from collections at 14,000 miles probably because of the high background resulting from other atomic explosions.

The significant result of the radiochemical analysis is that fission product ratios vary widely with altitude and range of sample collection, and depart radically from the values given by the established fission yield curves. This was determined from samples collected on the ground and at low and high altitudes from the initial cloud, and from air samples collected at distances up to 1700 miles. This effect has not been observed previously in the U. S. tests on towers or air drops. It indicates the necessity to study all possible methods of examining the debris from surface and underground explosions in order to determine the relation between the fissionable materials, tamper elements, and products of neutron reactions in tamper and core.

11.2 ACOUSTIC DETECTION

Significant signals were detected by all acoustic stations located within 1800 miles of the detonation point for both JANGLE tests. The underground explosion was detected at a range of 2300 miles.

Signal levels measured at long range were roughly equivalent to those recorded for air bursts during Operation BUSTER. It thus appears that the acoustic detection technique is just as effective for surface and shallow underground bursts as for air bursts.

The marked directional effect in propagation favoring transmission to the east verified expectations for winter propagation conditions.

11.3 SEISMIC DETECTION

Seismic test facilities were located in Wyoming, Oklahoma, Alabama,

and Alaska. Installations in Wyoming and Oklahoma, at 670 and 1000 miles respectively, were in an area classified as a close-in seismic shadow. Although detection in this area was presumed to be more difficult than at greater ranges beyond the shadow, the Wyoming installation proved to be superior to all the others. The surface shot was detected at this latter location with an instrumental gain of 400,000 yielding a signature with a signal/noise ratio of 1 : 1 and the underground burst was detected with a signal/noise ratio of 2 : 1. The seismic energy from these two shots was found to be about equivalent to that from Baker shot, Operation BUSTER.

The significant results from this test included (1) the observation for the first time at long range of an anomalously strong signature corresponding to a velocity of 3.2 km/sec; (2) evidence that geological considerations leading to quiet installations may be overriding in selecting future seismic sites; and (3) information which will permit narrowing the band width from 10 octaves to 3 octaves with resultant greater sensitivity. Non-detection of the low yield shots beyond the Wyoming installation is believed due partly to the use of equipment with a gain of less than 100,000 at the remote stations and partly to the absorption of a large amount of energy (possibly as high as 90 per cent) in the valley alluvium surrounding the detonation point.

CHAPTER 12

EXTRAPOLATION OF TEST RESULTS TO OPERATIONAL CONDITIONS

12.1 INTRODUCTION

In extrapolating the observed effects of the test weapons at the test site to estimate the probable effect of operational sized weapons on potential operational targets, it is necessary to consider the influence of many variations between the conditions of the test and other very common conditions. One of these variations is the difference in size of the weapons. This requires scaling, a purely mathematical process during which other variables are considered to be constant. Scaling has uncertainties which are, however, very much less than those to be expected from variations in conditions at the point of delivery.

12.2 INFLUENCE OF SOIL

The target soil along with the velocity and attitude at impact determine the penetration of the weapon. Figure 2.1 shows the variation in expected penetration due to soil type and impact velocity. In turn, the depth at which detonation occurs is one of the important factors in determing the fraction of available energy which is coupled into the ground. High explosive experiments have shown that the soil characteristics influence directly the coupling of energy into the ground. A third effect of the soil is its influence on the attenuation of ground shock phenomena with distance. It is important to note that all these effects are additive. That is, a soil type which allows deeper penetration also gives better coupling of energy into the ground and a lower attenuation to ground transmitted phenomena.

The underground shot at the Nevada Test Site indicated that for surface structures air blast would be the damaging mechanism. However, small charge HE experiments show that air blast decreases rapidly as depth of burial increases[8]. Comparison of Dugway and Nevada HE data for identical charge depth but different soil shows a reduction of peak overpressure by a factor of two at the Dugway dry clay site. If delivery were effected under conditions which would favor deeper penetration (i.e., plastic clay) both of the above factors would be operating to give a major reduction in radii for specific peak overpressures. Damage to surface structures by air blast would be correspondingly reduced.

Damage to structures from ground-transmitted phenomena would be enhanced by the delivery of the to achieve maximum penetration, i.e., in plastic clay at maximum striking velocity. Structural damage at Dugway was experienced as a result of ground-transmitted phenomena.

The Dugway soil is not the most favorable for ground transmission of shock, but is thought to be intermediate between the most favorable and that at the Nevada Test Site. It is therefore expected that the radius of structure damage due to ground transmitted phenomena would be increased under more favorable conditions.

Due to serious differences in the ambient field phenomena between the HE data from Dugway and JANGLE and between the JANGLE HE series and the nuclear shots, a quantitative expression of the above factors does not appear warranted at this time. In addition to the discrepancies existing in the ambient field phenomena, major questions as to the structural loading and the effect upon it of structural response remain unanswered. If, however, it is assumed that the differences in ambient field phenomena are due solely to variation in coupling of energy into the ground by nuclear detonations as compared to high explosive detonations, rough estimates can be made.

The crater due to the underground nuclear shot scaled according to laws derived from HE experiments and the crater due to the surface nuclear shot can be correlated with HE data by applying a rational correction factor. (See Paragraph 12.4.1.) Accordingly, the crater sizes expected in various soils are shown in Table 2.1.

At greater depths of penetration the base surge will assume greater importance in the spread of radioactivity with a resultant increase in the dosages and contamination level within the base surge area. The optimum condition for base surge formation is indicated from HE studies to be at a scaled depth of about $\lambda_c = 1.0$ (300 to 400 ft for the MK-8).

The type of soil and its moisture content will influence base surge formation. The base surge radial growth curves presented for Dugway HE tests indicate that dry sand is the most favorable, wet clay the least favorable, and dry clay intermediate in effectiveness for base surge formation. Thus a base surge produced by an explosion in dry sand is larger and grows faster than the surge produced in clay soils.

Particle size distribution may be markedly affected by soil type. One would expect a clay soil to have a smaller particle size on the average and result in a greater spread of contamination than would be found for sand.

In the above an essentially homogeneous soil medium has been considered. Lack of detailed knowledge of the geology underlying the target area would render the picture indeterminate for ground-transmitted phenomena.

Although data to support this conclusion are very meager, it does not appear that soil changes would have a major influence on the effects

to be expected from a surface detonated weapon.

12.3 INFLUENCE OF METEOROLOGY

The wind profile up to the height of the upper cloud will affect the pattern and extent of areas of significant residual contamination resulting from surface and underground atomic detonations. Although the active particles are initially associated with the fireball and its cloud outgrowth, the fall-out process begins at an early time during the rise and expansion of the cloud. At all times thereafter the active particles form an extended source continuous from the upper cloud to the ground. The rate of fall-out from the cloud and base surge if produced and consequently the trajectory of falling particles are not well established. However, certain general conclusions with regard to the influence of wind on the distribution of residual contamination can be made.

12.3.1 Effect of Wind Velocity on the Distribution of Residual Contamination

The wind will exert little influence on the distribution and intensity of residual contamination in the vicinity of ground zero and immediately downwind where the contamination is primarily associated with very large particles which fall rapidly.

The effective wind velocity influencing the distribution of fall-out is approximately the average velocity of winds from the ground to the height of the upper cloud. The time of fall and consequently the downwind displacement of particles in a given wind increases with decreasing particle size.

The downwind increment of area of significant early dosage is roughly proportional to the effective wind velocity. Although the concentration of residual contamination at a given point downwind varies inversely as the wind velocity, its time of arrival at that point also varies inversely with wind velocity. These effects compensate to give approximately the same integrated dose.

The period of arrival of fall-out at a given point downwind is governed by the wind profile. For winds of constant velocity at all levels up to the upper cloud, the period of arrival is equal to the cloud diameter divided by the wind velocity. Where the wind velocity varies with height, the period of arrival increases with distance. This increase in period at any distance is roughly proportional to the range of wind velocities involved.

Decay considerations indicate active material of earliest arrival makes the greater contribution to total dosage. At intermediate

to long distances downwind this earlier fall-out material is that which spent a proportionally longer period in the regions of higher wind velocity. Thus, for wind profiles involving a wide range of velocities, the effective wind velocity shifts toward the higher values, particularly at increasing distances.

The effect of wind velocity on areas receiving an integrated gamma dose in excess of 400 roentgens and on areas receiving significant residual contamination are presented in Table 12.1 for an 83 KT surface and a MK-8 underground detonation. The winds chosen for each are zero wind, the JANGLE effective winds, and twice the JANGLE effective winds.

12.3.2 Effect of Wind Shear

A shear in winds at any level up to the cloud height affects the distribution and extent of significant residual contamination in a complicated manner. Because the per cent of the total activity which is left in the trail of the cloud within a given fraction of its height of rise is not known, the effect of wind shear is not subject to quantitative evaluation. However, it can be expected that at all downwind points a wind shear will smear out the contamination pattern in a crosswind direction. This would result in broadening the area of significant contamination at short distances downwind and in reducing the downwind extent of contamination of any given intensity level.

12.3.3 Effect of Rain

Rain will have an influence on the spread of radioactive contamination from both types of shots. The radiation doses and contamination levels may be greatly increased and the overall areas affected reduced.

Rain would probably have an effect on the air blast expected from either type detonation. Estimates range from no reduction in air blast to 50 per cent reduction in the peak overpressure at a given distance.

Thermal radiation will be affected by atmospheric clarity in the same manner as for an air burst.

12.3.4 Effect of Delivery Technique

The method of delivery of the [ ] will determine its velocity and attitude on impact. These govern the depth of penetration expected in a given soil as shown in Figure 2.1. Lesser penetration will decrease the size of the crater and other underground effects and increase the air blast effects.

TABLE 12.1

12.4 SCALING

Estimates of effects from the penetrating weapon and the KT weapon on the ground surface, presented in Part I, were made by scaling the effects of the two 1.2 KT test explosions with the aid of the HE tests at Nevada, Dugway, Arco and elsewhere. It is strictly true that no model law can be fulfilled in detail unless the medium itself is identical in scale. In particular, if any inhomogeneities such as stratification, are present different tests even at the same site can not be scaled one to another. The depths of burial of most prospective targets are such that their scaled depths ($d/W^{1/3}$) are much smaller when considered in connection with nuclear weapons than is the case in connection with HE weapons. These shallow scaled depths are in a region where previous experience with HE has shown a wide spread in values from nominally identical explosions. The methods and relationships used in scaling the various effects, together with their reliability, are discussed below.

12.4.1 Craters

Crater scaling appears to be reliable and consistent with HE results for nuclear detonations at a scaled depth greater than $\lambda_c = 0.13$. Crater scaling for surface nuclear detonations appears to be similarly reliable when proper account is taken of the much poorer coupling of energy into the ground which occurs for a nuclear detonation. This difference is developed in the report of Project 1.9-2, which is summarized in this section.

The work of C. W. Lampson[3] on HE craters has given an expirical relationship for the size of the crater produced by an underground charge expressed as

$$R = 1.3\ CEk^{1/12}\ W^{1/3}$$

where

R = Crater radius in feet
C = Depth factor
E = Explosive factor
k = Soil constant
W = Charge weight in pounds

The soil constant for the Nevada site was found to be about 8000 based on an average soil density of 1.6 and an average seismic velocity of 3000. The depth factor is a function of the scaled depth and the variation is reported in References 3 and 4. The explosive factor E is unity for HE, and less than unity for nuclear shots in consideration of the difference between total yield and mechanical yield of the nuclear bomb. The crater radii of the underground HE shots calculated by the above relationship are found to be in good agreement with those observed as shown in Table 12.2. If the crater radius from the underground nuclear detonation is calculated using the equivalent mechanical energy of the weapon as 0.7 it is found to be within 7 per cent of the observed value.

TABLE 12.2

Crater Radii Calculations from Lampson's Relationship

	W	$W^{1/3}$	λ_c	C	E	$k^{1/12}$	Radius (Feet) Calc'd	Observed
HE-1	2560	13.68	-0.15	.43	1	2.11	16	18
HE-2	40000	34.2	-0.15	.43	1	2.11	41	38
U	1.2KT	134	-0.13	.42	$(0.7)^{1/3}$	2.11	139	130
HE-4	2560	13.68	0.15	.14	1	2.11	5	7
S	1.2KT	134	0.03	.26	$(0.07)^{1/3}$	2.11	43	45

In the case of the surface nuclear detonation, the observed crater radius is about half that calculated from the Lampson relationships for HE: 45 feet versus 86. Clearly, there is better ground coupling for a surface detonated HE charge than occurs for a nuclear weapon detonated under similar conditions. The Project 1.9-2 report indicates that only about 2 per cent of the mechanical energy will be coupled into the ground for a surface nuclear detonation, based on calculations of the rate of energy transfer into the earth and into the air during the very early phases prior to breakaway. Lampson's work with HE indicates that 20 per cent of the energy will be coupled into the ground for a surface HE charge. This difference can be adequately represented by using a figure of $(0.1 \times 0.7)^{1/3}$ for the explosive factor, E, in Lampson's equation for crater radius from surface detonations, as compared to $E = (0.7)^{1/3}$ for scaled depths of detonation $\lambda c \leq 0.13$. The transition in the zone between has not been established.

Estimates for crater radii for the [ ] penetrating weapon and the [ ] weapon on the ground surface presented in Part I were calculated from Lampson's equation using soil constants and depth factors reported in Reference 3 and presented in Table 12.3.

TABLE 12.3

The crater radius for the 35-foot depth in sand presented above is high since the appropriate E factor will lie somewhere between $(0.7)^{1/3}$ and $(0.07)^{1/3}$.

It should be pointed out that an extensive high explosive program was required by Lampson to develop the empirical relationship. This relationship contains a number of uncertainties; for example, the accuracy of the soil constant k is no better than ± 25 per cent. In addition, there is considerable scatter in the data obtained from

identical shots fired under the same environmental conditions.

Crater depths and consequently the volumes are more indeterminate than are crater radii. The crater volumes for the operational weapons presented in Part I are estimated on the basis of the following reduced equation for the volume of a cone with a radius to depth ratio of 2:

$$V \text{ (cubic yards)} = 0.02 \text{ (R feet)}^3$$

12.4.2 Air Blast Overpressure

Air pressure measurements for the surface nuclear test when compared to the surface HE shot (HE-4) indicate a difference in the distance attenuation factor. On the other hand, it was found that the nuclear curve and a well verified small-charge free-air curve[5] had equal slopes at the 20 psi level ($\lambda = 6$) and for 7 psi and less ($\lambda = 10$). This latter agreement may be a possible basis for scaling the air pressure from larger charges by use of the conventional explosion $W^{1/3}$ model law.

In the case of the underground nuclear test, comparison can be made with the air blast from Shots HE-1 and HE-2. Except for close-in values ($\lambda = 6$ or less, P = 10 psi) good agreement is reached and scaling on the basis of the $W^{1/3}$ law of the air blast for larger charges at the Nevada site is probably justified. There is a marked difference between the air blast obtained for Shot HE-3 (Project 1(9)-1) in Nevada and Dugway high explosive tests for presumably identical shots at a scaled depth $\lambda c = 0.5$. This difference between tests at different sites is greater than that between the HE-nuclear results at the same site. This means that the scaling by the $W^{1/3}$ law of the air blast from underground nuclear bursts for other than the Nevada site is subject to some uncertainty.

12.4.3 Ground Accelerations

Earth accelerations and the difficulties of scaling require an investigation of wave forms and distance attenuation factors. In the case of the underground shot the distance attenuation factor for the first peak of earth-transmitted horizontal acceleration is distinctly different from that observed on Shots HE-1 and HE-2. The curve for attenuation with distance of the earth-transmitted vertical acceleration has a step which indicates a subsurface layer of higher seismic velocity beneath the JANGLE site. The HE-nuclear attenuation factors appear to be the same for the vertical accelerations, but this attenuation curve step introduces uncertainty at larger distances.

Examination of the accelerometer wave forms for the earth-transmitted effects indicates that the duration of the smoothed first pulse does not follow the conventional $W^{1/3}$ model law. Deviations from

the $W^{1/3}$ law are probably due to inhomogeneities in the medium.

In addition to the earth-transmitted acceleration there was an air-blast induced effect. This effect can be calculated for the higher yield weapons but it is not considered of sufficient importance to do so.

For a more detailed discussion of ground accelerations reference is made to reports from Project 1.1, 1(9)a and 1(9)-1.

12.4.4 Ground Pressures

Poor correlation is found to exist between the free ground pressure-reduced distance relations obtained for the nuclear shots and the high explosive tests and as a result scaling becomes virtually impossible. The previously accepted relationships for scaling free ground pressures3/ are found to be inapplicable. This previous work was based on gages buried at depths of approximately 3/2 $W^{1/3}$. The phenomena measured at JANGLE were relatively near the surface of the ground with gages primarily in the region 1/10 $W^{1/3}$ with a few gages as deep as 1/2 $W^{1/3}$, and Lampson has previously reported that this is an indeterminate region as far as true ground propagation is concerned.

An attempt is being made to correlate earth pressures applied to the test structures in order to determine some logical pattern for the earth pressure phenomena. This study has not progressed far enough to allow comment at this time.

12.4.5 Thermal Radiation

On the basis of previous air burst experience it is known that the thermal energy emitted by an atomic bomb which reaches a specific distance is approximately proportional to the yield of the bomb. Therefore, it is assumed that the thermal effect at a given distance from surface detonated weapons can be scaled in the same manner from the results of the surface shot. The scaling relationship, including the correction for atmospheric attenuation, is thus:

$$Q_2 = Q_1 \frac{W_2}{W_1} e^{(k_1 - k_2)d}$$

where Q is the thermal energy in cal/cm^2 received at any given distance d in feet, W is the energy release of the weapon and k is the appropriate atmospheric attenuation coefficient expressed in reciprocal feet. The atmospheric attenuation coefficient, k, is about 3.92 divided by the visibility in feet. For the conditions of the JANGLE surface detonation $k = 9.72 \times 10^{-6}$ ft.$^{-1}$. The thermal energy as a function of distance for

the JANGLE surface detonation is presented in Figure 7.1.

12.4.6 Radiological Effects

The methods and assumptions involved in scaling the radiological effects observed for the JANGLE detonations to estimates for weapons of larger yield are presented in the report of Project 2.0. The predictions based on this scaling are very sensitive to variations from the JANGLE conditions. The scaling of the JANGLE results involved the assumption of the absence of directional wind shear and of the same particle size distribution. For the smaller particle size distribution which may be expected with clay soils a larger fraction of the active debris will remain airborne for a longer period of time. A shear in wind direction will smear out the pattern of contamination crosswind at all distances. Both effects increase the area over which the contamination is deposited and will result in much smaller high dose rate areas. High winds will have similar effect. The predictions for the [redacted] KT surface detonation with an estimated cloud height of about 20,000 feet will be much more sensitive to these effects than the [redacted] with an estimated cloud height of 10,000 feet for a 50-foot depth of burst. Thus, the resultant areas of significant residual contamination may be considerably smaller than those estimated for many operational situations, particularly in the case of a large surface burst.

Lack of information on the initial vertical distribution of radioactive debris, and on the influence of soil type on the particle size distribution, limits the extrapolation of radiological effects to highly idealized conditions. A discussion of the methods of the scaling process follows:

12.4.6.1 Dose-rate Scaling

The JANGLE residual contamination one hour dose-rate contours were extrapolated empirically to give the new one hour contours for operational weapons as follows: First a family of ellipses was fitted to the JANGLE contours with ground zero as a common focus and a major axis directed downwind. A new family of ellipses was drawn for each operational weapon by scaling up the crosswind dimension by $W^{1/4}$ (since the cloud diameter scales as $W^{1/4}$) and taking an interfocal distance directly proportional to the average wind speed. A new dose-rate value is then assigned to each ellipse such that the area dose-rate products integrate to give the same fractions of the total activity as that for the corresponding JANGLE contour. The details of the method are presented in the report of Project 2.0.

12.4.6.2 Total Dose Scaling

The total gamma radiation dose received in periods

up to 10 seconds at a given radial distance from ground zero is scaled directly with yield from the integrated dose rate versus distance data of Project 2.1a for both JANGLE detonations. The principal source of this initial gamma dose is the fission product radiation from the fireball and cloud. The effect of wind and the contribution of fall-out can be neglected for periods up to 10 seconds. The more rapid decrease of initial dose with range from the point of detonation for those bursts as compared with air bursts is accounted for by the loss of a large fraction of the scattered radiation due to the proximity of the earth.

The total gamma radiation dose received in periods longer than 10 seconds requires the integration of the dose rate from time of arrival of fall-out to the end of the period considered and addition of this to the 10-second dose. The time of arrival was taken from the Project 2.1a gamma dose-rate records which indicate an effective wind of 5 miles per hour for the JANGLE underground burst and 15 miles per hour for the surface burst. The time of arrival goes approximately inversely as the effective wind velocity. The normal $t^{-1.2}$ decay law was used for the dose-rate integration.

12.4.7 Reliability of Scaling Radiological Effects

The predicted areas of significant radiological effect for surface and underground detonations, scaled by the methods described in Project 2.0 report and summarized above, have greatest reliability for wind conditions approximating those of the JANGLE test. The reliability varies with the time period or area considered as follows:

Predicted total dose values should be correct well within a factor of two in areas where most of the cumulative gamma radiation dose come from initial or cloud radiation.

The 10-second total dose areas should be correct to within 20 per cent because of the fairly good precision with which the initial radiation can be calculated.

The accuracy of the 10-minute dose curves is in doubt by as much as 50 per cent in areas because insufficient data on early fall-out behavior are available as a basis for scaling.

Prediction of fall-out is less reliable since in general one will find hot spots in relatively cool areas and cool spots in areas of high activity levels. Thus, although the expected variation of the average intensity along a predicted dose-rate contour does not exceed a factor of 3, the dose rate at specific points along such contours may well be one hundred-fold higher or lower than the average value.

The dose-rate scaling method used appears to be a reasonable one but some assumptions made in its application are open to question. In the process of fitting ellipses to the JANGLE surface shot data the contours were somewhat broadened. In the normalization process the fraction of total activity falling out in one hour for operational weapons was taken as equal to that for the JANGLE detonations. For greater cloud heights the one hour fall-out should involve a smaller fraction. In addition it was assumed that essentially all the activity came down in one hour for both JANGLE detonations. It appears from the surface shot data that a considerable fraction did not fall out in the first hour.

Complete evaluation of the dose-rate scaling problem has not been carried out. Some revision in shape and reduction in area contaminated to a given dose-rate level is indicated, particularly for estimates for surface atomic detonations. However, it is considered that such modifications will fall within the limits of stated reliability for conditions of detonation approximating those of the JANGLE test.

Areas within contours, whether for dose rate or total dose, are much less sensitive to irregularities in the explosive and distribution process than the dose rates at a point, partly because of the steep gradient of the contours and partly because the concept of an area within a contour involves an averaging process. Predicted values for areas resulting from detonations carried out under conditions not too far different than at JANGLE should be correct well within a factor of 2.

It must be emphasized that the reliability of scaled estimates is reduced as the conditions of detonation become appreciably different than those for the JANGLE test. Because the initial vertical distribution of radioactive debris is not known, no reliable estimates can be made for irregular wind profiles involving high wind velocities or involving a shear in wind direction below cloud height. Furthermore, the influence of soil type on radioactive particle size distribution and consequently on the fall-out pattern has not been evaluated.

CHAPTER 13

CONCLUSIONS AND RECOMMENDATIONS

13.1 CONCLUSIONS

It was demonstrated that some of the scaling relationships developed from studies of conventional high explosive detonations are applicable to nuclear detonations. In general, correlation has not been established for phenomena which involve energy transmission through the soil. An important limitation to scaling from previous HE results is that the scaled depths for measurements ($d/w^{1/3}$) which are of interest in the study of nuclear weapons are much less than those involved in the HE tests on which are based the empirical formulae for predicting explosive effects as functions of distance.

Craters resulting from underground and surface nuclear detonations can be calculated from the empirical relationships developed for craters from HE detonations when rational corrections are made for the smaller fractions of total energy which are coupled into the ground in the case of the nuclear detonations.

Air blast overpressures along the ground from nuclear explosions of a given yield are essentially the same over the range of scaled heights of burst ($h/w^{1/3}$) from zero to 0.25 ft/lbs$^{1/3}$. For surface detonations, there is a significant difference in air blast overpressures along the ground from nuclear explosions as compared to those from equivalent HE explosions. For underground detonations, air blast overpressures along the ground from nuclear and equivalent HE explosions were found to be in reasonably good agreement.

Ground transmitted phenomena of the nuclear detonations - earth accelerations, earth pressures and displacements - did not agree with scaled results of HE detonations. The degree to which these discrepancies may be attributed to soil effects or the degree to which they may be attributed to surface phenomena have not been resolved at this time. It has been noted that the soil properties do not scale and that the zone of interest for the nuclear detonations (shallow scaled depths) is one where HE experiments indicated a wide spread in results.

Surface and underground nuclear detonations produce extensive areas of high radioactive contamination. Fissionable material economy consideration indicates the surface nuclear detonation to be potentially the more important radiological weapon. Unfortunately, reliable prediction of areas of residual contamination and consequently areas of lethal dosage can be made only for highly idealized conditions.

The capabilities and limitations were established for some of the techniques and equipment developed for military operations in which atomic weapons are used. Consideration of the JANGLE test results and of the problems inherent in military operations indicates that a number of these techniques and equipment are not in fact required.

13.2 RECOMMENDATIONS

Knowledge in the field of military effects of surface and underground atomic explosions should be extended in the areas listed below. A large part of the effort can be accomplished by further evaluation of published test data and by the continuation and extension of existing HE test programs.

1. Identification and evaluation of the parameters which have significant effect on the development and attenuation of ground shock and air blast from surface and underground atomic explosions.

2. Correlation of ground shock, cratering, and air blast phenomena between HE and nuclear explosions on the surface and underground.

3. Predictions of loading of buried structures on the basis of free medium phenomena.

4. The interaction between buried structures and immediately adjacent earth layers under conditions where large structural deflections occur.

5. Cratering effects from nuclear detonations at small scaled distances from the ground surface, either underground or in the air.

6. Determination of the initial vertical distribution of radioactive bomb debris.

7. Determination of the mechanisms involved in the initial distribution and subsequent fall-out of radioactive bomb debris.

8. Determination of the influence of soil type and depth of burial on the particle size distribution of radioactive bomb debris.

In the event that additional nuclear tests are required for these studies, particular care should be taken to ensure that sufficient time for necessary preparatory work is provided to give reasonable assurance of a successful test.

In addition, a critical review should be made of the techniques and equipment developed for radiological defense in the light of need as well as performance. This review should stress tolerance levels considered significant for military operations.

REFERENCES

1/ Report of the 10 and 11 April 1950 Meeting of the AFSWP Special Sites Panel, 8 June 1950. Top Secret Control Symbol C-987-F/SWP

2/ Capabilities of Atomic Weapons, TM23-200, OPNAV-P-36-00100, AFOAT 385.2, 10 July 1951, with Supplement 1, 8 February 1952

3/ Lampson, C. W., Final Report on Effects of Underground Explosions, NDRC Report No. A-479, 20 February 1946

4/ The Effects of Atomic Weapons, June 1950, U. S. Government Printing Office

5/ NAVORD Report Rem 3, Project Elsie Final Report, 1 April 1952

6/ Behavior of Truss Bridges Under Blast from an Atomic Bomb, Phase II-General Study of Truss Bridges, Massachusetts Institute of Technology, July 1951

7/ Handbook of Atomic Weapons for Medical Officers NAVMED P-1330, FM 8-11, AFM 160-11

8/ NAVORD Report 1863, The Behavior of the Shock Wave in Air from Small HE Charges

9/ NAVORD 2123, Experimental Shock Wave Reflection Studies

10/ Underground Explosion Test Program, Final Report, Vol. I - Soil, Engineering Research Associates, Inc., 30 August 1952

APPENDIX A

JANGLE REPORT VOLUMES

A.1 GENERAL

The titles of the reports for Operation JANGLE are listed below. Reports of related projects are bound as volumes. Each volume and each project report bears a WT number for reference purposes.

BLAST AND SHOCK MEASUREMENTS I
WT-366

Project	Title	Agency	Project Officer
1.1 (WT-388)	Ground Acceleration Measurement	Naval Ordnance Laboratory	W. E. Morris
1.2a-1 (WT-323)	Peak Air Blast Pressures Along the Ground from Shock Velocity Measurements	Ballistic Research Laboratory	E. E. Minor
1.2a-2 (WT-385)	Transient Ground Mechanical Effects from HE and Nuclear Explosions	Ballistic Research Laboratory	E. E. Minor

BLAST AND SHOCK MEASUREMENTS II
WT-367

1.2b (WT-364)	Close-in Ground Measurements	Armed Forces Special Weapons Project	W. F. Gannon CHEELE, USN
1.3a (WT-324)	Free Air Shock Arrival Times	Brookhaven Nat'l Laboratory	J.B.H. Kuper
1.3b (WT-389)	Free Air Peak Pressure Measurements	Naval Ordnance Laboratory	J.F. Moulton, Jr.
1.3c (WT325)	The Measurement of Free Air Atomic Blast Pressures	Cambridge Research Center	J. O. Fann Maj. USAF
1.4 (WT-306)	Air Pressure vs Time	Sandia Corp.	W. J. Howard

BLAST AND SHOCK MEASUREMENTS III
WT-368

Project	Title	Agency	Project Officer
1.5a (WT-382)	Transient Ground Displacement Measurement	Naval Ordnance Laboratory	W. E. Morris
1.5b (WT-326)	Detection of Time of Arrival of First Earth Motion	David Taylor Model Basin	G. W. Cook
1.6 (WT-353)	Earth Displacements (Shear Shafts)	Office of the Chief of Engineers	H.J. Sundstrom
1.7 (WT-357)	Ground Acceleration (Shock Pins)	Office of the Chief of Engineers	H.J. Sundstrom
1(9)a (WT-380)	Ground Acceleration, Ground and Air Pressures for Underground Test	Stanford Research Institute	E. B. Doll
1(9)b (WT-390)	Base Surge Analysis for Nuclear Tests	Naval Ordnance Laboratory	W. E. Morris

UNDERGROUND EXPLOSION THEORY
WT-369

1.9 (WT-358)	Theoretical Studies of the Shock Wave	Office of Naval Research	J. W. Smith
1.9-1 (WT-328)	Application of the Kirkwood-Brinkley Method to the Theory of Underground Explosions	RAND Corp	J. J. Gilvarry
1.9-2 (WT-378)	Notes on Surface and Underground Explosions	Armed Forces Special Weapons Project	D. T. Griggs
1.9-3 (WT-350)	Predictions for the Underground Shot	Stanford Research Institute	E. B. Doll

HIGH EXPLOSIVE TESTS
WT-365

Project	Title	Agency	Project Officer
1(9)-1 (WT-377)	Scaled HE Tests	Stanford Research Institute	E. B. Doll
1(9)-2 (WT-349)	Composition of Clouds Formed by TNT	Stanford Research Institute	E. B. Doll
1(9)-3 (WT-410)	Tests and Observations on Craters and Base Surges	Armed Forces Special Weapons Project	D.C. Campbell CDR, USN
1(9)-4 (WT-339)	Base Surge Analysis for HE Tests	Naval Ordnance Laboratory	W. E. Morris

GEOLOGIC, HYDROLOGIC AND THERMAL FEATURES OF THE SITES
WT-343

1(8)a (WT-343)	Geologic, Hydrologic and Thermal Features of the Sites	U. S. Geological Survey	A. M. Piper

SEISMIC REFRACTION SURVEY
WT-327

1(8)a-1 (WT-327)	Seismic Refraction Survey	United Geophysical Company	B. O. Perkins

AIR WEATHER SERVICE PARTICIPATION IN OPERATION JANGLE
WT-361

1(8)b (WT-361)	Air Weather Service Participation in Operation JANGLE	Air Weather Service	E. H. Karstens LtCol, USAF

SCALING OF RADIOLOGICAL EFFECTS
WT-391

2.0 (WT-391)	Scaling of Radiological Effects	Technical Operations, Inc.	M. G. Schorr and E. S. Gilfillan

GAMMA RADIATION MEASUREMENTS
WT-370

Project	Title	Agency	Project Officer
2.1a (WT-329)	Gamma Radiation as a Function of Time and Distance	National Bureau of Standards	L. Costrell
2.1b (WT-392)	Gamma Radiation as a Function of Time with Droppable Telemeters	Bureau of Aeronautics	J. H. Terry CDR, USN
2.1c-1 (WT-330)	Aerial Survey of Distant Contaminated Terrain	AFOAT-1	W. D. Urry
2.1c-2 (WT-351)	Aerial Survey of Local Contaminated Terrain	Bureau of Aeronautics	J. H. Terry CDR, USN
2.1d (WT-380)	Monitor Survey of Ground Contamination	Armed Forces Special Weapons Project	J. Johnson CDR, USN
2.3-1 (WT-331)	Total Gamma Radiation Dosage	Evans Signal Laboratory	M. B. Forbes LtCol, USA
2.3-2 (WT-393)	Foxhole Shielding of Gamma Radiation	Engineer Research and Development Laboratory	T. J. Walsh

BIOLOGICAL HAZARDS
WT-372

2.4a (WT-345)	Beta-Ray and Gamma-Ray Energy of Residual Contamination	Naval Research and Development Laboratory	E. Tochilin
2.4b (WT-332)	Gamma Depth Dose Measurement in Unit Density Material	National Medical Research Institute	F. W. Chambers CDR, USN
2.4c (WT-348)	Gamma Ray Spectrum of Residual Contamination	Brookhaven National Laboratory	J.B.H. Kuper
2.7 (WT-396)	Biological Injury from Particle Inhalation	National Institutes of Health	F. Smith

PARTICLE STUDIES
WT-371

Project	Title	Agency	Project Officer
2.5a-1 (WT-394)	Airborne Particle Studies	Army Chemical Center	C. Robbins LtCol, USA
2.5c-2 (WT-395)	Fall-out Particle Studies	Naval Research and Development Laboratory	I. J. Poppoff
2.5a-3 (WT-333)	Radiochemical Studies of Large Particles	Army Medical Center	R. Maxwell Col, USA
2.8 (WT-335)	Analysis of Test Site and Fall-out Material	U. S. Dept. of Agriculture	L. T. Alexander

RADIOCHEMICAL MEASUREMENTS AND SAMPLING TECHNIQUES
WT-373

2.6a (WT-334)	Remotely Controlled Sampling Techniques	Evans Signal Laboratory	M. B. Forbes LtCol, USA
2.6c-1 (WT-386)	Nature and Distribution of Residual Contamination I	National Institutes of Health	C. Maxwell
2.6c-2 (WT-397)	Nature and Distribution of Residual Contamination II	Naval Research and Development Laboratory	N. E. Ballou
2.6c-3 (WT-363)	Retrievable Missiles for Remote Ground Sampling	National Institutes of Health	C. Maxwell

NAVY STRUCTURES TEST
WT-404

3.1 (WT-404)	Navy Structures Test	Bureau of Yards and Docks	C. B. Hazzard LCDR, USN

ARMY STRUCTURES TEST
WT-387

3.2 (WT-387)	Army Structures Test	Office of Chief of Engineers and Mass. Institute of Technology	T. C. Stark

AIR FORCE STRUCTURES TEST
WT-405

Project	Title	Agency	Project Officer
3.3 (WT-405)	Air Force Structures Test	Air Materiel Command and Armour Research Institute	R.R. Labourveau CAPT, USAF

ENGINEER SOIL MECHANICS TESTS
WT-336

3.29 (WT-336)	Engineer Soil Mechanics Tests	Naval Civil Engineer Research and Evaluation Laboratory	F. E. Lovance

STRUCTURE INSTRUMENTATION
WT-406

3.28 (WT-406)	Structure Instrumentation	Sandia Corp	H.E. Lenander

TECHNICAL PHOTOGRAPHY
WT-374

4.1 (WT-354)	Aerial Technical Photography Operations	Air Research and Development Command	F. M. Crawford Maj, USAF
4.1a-1 (WT-398)	Ground Technical Photography Material Operations	Sandia Corp	H. C. Barr
4.1a-2 (WT-345)	Photographic Analysis	Sandia Corp	H. C. Barr

CRATERING AND MISSILE PHENOMENA
WT-375

4.2 (WT-399)	Cratering Effects of Underground-Surface Detonated Atomic Bombs and Influence of Soil Characteristics on Crater	Naval Civil Engineer Research and Evaluation Laboratory	F. E. Lowance
4.5 (WT-338)	Characteristics of Missiles from Underground Nuclear Explosions	Stanford Research Institute	R. B. Vaile

EVALUATION OF MILITARY RADIAC EQUIPMENT
WT-337

Project	Title	Agency	Project Officer
6.1 (WT-337)	Evaluation of Military Radiac Equipment	Evans Signal Laboratory	M. B. Forbes LtCol, USA

PROTECTION AND DECONTAMINATION OF LAND TARGETS AND VEHICLES
WT-400

6.2 (WT-400)	Protection and Decontamination of Land Targets and Vehicles	Naval Research and Development Laboratory and Army Chemical Center	W. E. Strope and S. R. Sinnreich

TESTS OF SERVICE EQUIPMENT AND OPERATION
WT-376

6.3-1 (WT-401)	Evaluation of Military Individual and Collective Protection Devices and Clothing	Army Chemical Center	J.R.Hendrickson
6.3-2 (WT-402)	Evaluation of Potential Respiratory Hazards associated with Vehicular Operations in a Radioactively Contaminated Area	Army Chemical Center	E. H. Enquist
6.7 (WT-347)	Clothing Decontamination and Evaluation of Laundry Methods	Office of the Quartermaster General	A. H. Parthum Maj, USA
6.8 (WT-340)	Evaluation of U. S. Army Field Water Supply Equipment and Operations	Engineer Research and Development Laboratory	D.C. Lindsten

CONSIDERATION OF RADIOACTIVE CONTAMINATION IN THE MAJOR OVERHAUL OF AIRCRAFT TURBO-JET ENGINES
WT-403

6.6 (WT-403)	Consideration of Radioactive Contamination in the Major Overhaul of Aircraft Turbo-jet Engines	Naval Research and Development Laboratory	H. A. Myers Maj, USAF

ACCOMPLISHING OPERATIONAL TESTS OF TECHNIQUES FOR INDIRECT BOMB DAMAGE ASSESSMENT
WT-344

Project	Title	Agency	Project Officer
6.4 JANGLE (6.5BUSTER) (WT-344)	Accomplishing Operational Tests of Techniques for Indirect Bomb Damage Assessment	Wright Air Development Center	F. E. James

RADIOCHEMICAL, CHEMICAL AND PHYSICAL ANALYSIS OF BUSTER AND JANGLE BOMB DEBRIS
WT-320

7.3 JANGLE (7.1BUSTER)	Radiochemical, Chemical and Physical Analysis of BUSTER and JANGLE Bomb Debris	AFOAT-1	P. Wignall LtCol, USAF

SEISMIC WAVES FROM A-BOMBS DETONATED OVER A LAND MASS
WT-321

7.3 JANGLE (7.5BUSTER) (WT-321)	Seismic Waves from A-Bombs Detonated over a Land Mass	AFOAT-1	P. Wignall LtCol, USAF

AIRBORNE LOW-FREQUENCY SOUND FROM ATOMIC EXPLOSIONS DURING OPERATION BUSTER/JANGLE
WT-322

7.3 JANGLE (7.6 BUSTER) (WT-322)	Airborne Low-Frequency Sound from Atomic Explosions During Operation BUSTER/JANGLE	AFOAT-1	P. Wignall

APPENDIX B

CONDITIONS FOR NUCLEAR TESTS

B.1 GENERAL

The times, weapon description, meteorological data and other information on test conditions are given in Tables B.1 and B.2.

Yucca Flat, the site of the detonations, is an alluvial fill in a basin-range valley. There is no apparent stratification but rather the mass is heterogeneous containing pockets or lenses of caliche, coarse grained, and extremely fine sand. The particles are very angular thus interlocking to a high degree. This condition augmented by cementation produces a coherent mass. The area is extremely dry and the soil very porous. No water table has been found in the flat, although one hole drilled to a depth of over 1500 feet showed a slight trace of water at the bottom. This type of soil is characterized by a high attenuation to the transmission of ground phenomena. Tables B.3 and B.4 give a consolidation of the various soil characteristics.

TABLE B.1

Nuclear Detonations

	Surface Shot	Underground Shot
Date	19 Nov 1951	29 Nov 1951
Time (PST)	0900	1200
Yield	1.2 ± 0.1 KT	1.2 ± 0.1 KT
Weapon		
Fissionable Material		
Position of Center of Gravity		17' underground in shaft with 12' earth cover
Elevation of Ground Zero (above MSL)	4213.0 feet	4299.0 feet

TABLE B.2

Meteorological Conditions

	Surface Shot	Underground Shot
Atmospheric Pressure	871.5 mb	872.0 mb
Temperature	1.0°C/33.8°F	14.5°C/58.0°F
Relative Humidity	47 per cent	35 per cent
Winds		
Surface	190° - 2 knots	180° - 2 knots
6000 feet MSL	170 - 13	150 - 5
8000	180 - 26	210 - 15
10,000	200 - 32	230 - 21
12,000	200 - 37	240 - 24
14,000	210 - 40	200 - 25
Cloud Cover		
10,000 feet MSL	1/8 altocumulus	- - - - -
16,000	4/8 altocumulus	- - - - -
29,000	- - - -	1/8 cirrus
31,000	7/8 cirro-stratus	- - - - -
Ground Temperature		
3 foot depth	13.1°C/55.7°F	10.7°C/51.2°F
5	16.3°C/61.2°F	14.4°C/58.0°F
10	17.9°C/64.2°F	17.4°C/63.1°F
20	16.3°C/61.5°F	16.1°C/61.0°F

TABLE B.3

Subsoil Characteristics at Zero Points

Surface Zero (Depth in feet)		Underground Zero (Depth in feet)	
Sand and gravel, lightly cemented	0-275	Sand and gravel	0-76
Boulders, limestone	275-278	Gravel, cemented	76-128
Gravel, lightly cemented	278-300	Boulders	128-130
Sand and gravel, lightly cemented	300-340	Sand and gravel	130-135
Sand, not cemented	340-365	Gravel, cemented	135-160
Boulders	365-369	Sand and gravel	160-175
Sand	369-370	Sand and gravel, cemented	175-210
Gravel, cemented, medium hard	370-405	Sand and gravel	210-240
Gravel, cemented	405-449	Gravel, cemented	240-415
Sand, cemented	449-502	Sand and gravel, cemented	415-465
		Sand, cemented	465-500

TABLE B.4

Density and Seismic Velocities at Zero Points

Field Density of Valley Fill (Including retained moisture)			
Surface Zero		Underground Zero	
Range in Depth (feet)	Range in Density	Range in Depth (feet)	Range of Density
0.5 - 16.0	Maximum 1.81 Minimum 1.37 Average 1.59	0.5 - 15.8	Maximum 1.76 Minimum 1.30 Average 1.59

Caliche layers may have a density as high as 2.05

TABLE B.4 (Cont'd)

Seismic Velocity as a Function of Depth		Apparent Seismic Velocity at the Surface as a Function of Distance	
Depth (feet)	Velocity (feet/sec)	Distance (feet)	Apparent Velocity (feet/sec)
0	2620	0 - 600	4400
100	3070		
200	3490	600 - 800	3900
300	3690		
500	4100	800 - 1600	3500
600	4300		

APPENDIX C

BASIC PHYSICAL MEASUREMENTS

C.1 GENERAL

A summary of the basic physical measurements taken at Operation JANGLE is given in Table C.1. A detailed listing of these measurements is given in Table C.2.

TABLE C.1

Summary of Basic Physical Measurements

Measurement	Surface Nuclear Shot		Underground Nuclear Shot	
	Range(ft.)	Bearing	Range(ft.)	Bearing
Ground acceleration by horizontal, transverse and vertical accelerometers	275 - 3000	S20°W	200 - 3000 262 - 3080	S20°W N70°W
Ground acceleration by shock pin stations	562.5-1875 625 - 1250 625 - 1250	S20°W N70°W S70°E	562.5-1875 625 - 1250 625 - 1250	S20°W N70°W S70°E
Hydrostatic earth pressure	275 - 3000	S20°W	200 - 3000 217 - 3080	S20°W N70°W
First earth motion arrival time	——	——	5 - 542	S20°W
Shear shaft stations	250 - 1000 312.5-750 312.5-750	S20°W N70°W S70°E	250 - 1000 312.5-750 312.5-750	S20°W N70°W S55°E
Transient displacement fiducial markers	——	——	275 - 1890	S20°W
Peak air pressure (velocity method)	300 - 2700	S20°W	300 - 1500	S20°W
Air blast as a function of time	500 - 4200 3100 3100 3100 3100	S20°W N15°E E N45°S N20°N	500 - 3100 314 - 3080 1250 1250 1250	S20°W N70°W N28°W N20°S N39°N

TABLE C.2

TABLE C.2

Basic Physical Measurements

Scaled Radius, λ (1)	Radial Distance, Ft. (2)	Measurement (3)	Gage Depth Ft. (4)	Gage Type (5)
Underground Nuclear Shot:				
.033	5	q	17	BS
.061	7.8	q	17	BS
.076	9.6	q	17	BS
.093	11.8	q	17	BS
.115	14.6	q	17	BS
.138	17.5	q	17	BS
.180	21.5	q	17	BS
.206	26.0	q	17	BS
.250	31.5	q	17	BS
.309	39.0	q	17	BS
.396	50	q	17	BS
.420	53	q	17	BS
.452	57	q	17	BS
.492	62	q	17	BS
.539	68	q	17	BS
.595	75	q	17	BS
.654	83	q	17	BS
.738	93	q	17	BS
.793	100	q	5	PS
.889	102	q	17	BS
.888	112	q	17	BS
.976	123	q	17	BS
.992	125	q	5	PS
1.07	135	q	17	BS
1.17	148	q	17	BS
1.19	150	q	5	PS
1.28	162	q	17	BS
1.40	177	q	17	BS
1.41	178	q	5	PS
1.53	193	q	5	BS
1.59	200	X, X', Y, Y'	10	S
1.59	200	P	10	WP
1.69	213	q	17	BS
1.72	217	q	5	PS
1.72	217	P	10, 17, 34	W
1.88	237	q	17	BS
1.89	238	X, Y	10	ERA+
1.98	250	Q (1)	0–45	--
2.07	262	q	5	PS
2.08	262	P	10	W
2.08	262	X, Y	5	WA
2.10	265	q	17	BS
2.18	275	P	10, 20, 30	WP
2.18	275	X, X', Y, Y'	10	S
2.18	275	P	10*	WA
2.18	275	X, Y	10	ERA
2.35	297	q	17	BS
2.38	300	b	4	GE
2.40	312.5	Q(1, 2, 4)	0 – 45	
2.49	314	q	5	PS
2.49	314	3	1.166*	WP
2.49	314	P	10	W
2.49	314	X, Y	5	WA
2.5	314	3	4*	WP
2.64	333	q	17	BS
2.70	340	X, Y	10	ERA
2.70	340	X, X', Y, Y	10	S
2.70	340	X, Y, Y'	20	S
2.70	340	X, X', Y, Y'	30	S
2.70	340	P	10	WP
2.70	340	P	10*	WA
2.70	340	X	10	WA
2.74	345	X, Y	10	ERA+
2.97	375	Q(1, 2, 4)	0 – 45	
3.0	378	q	5	PS
3.0	378	X, Y	5	WA
3.0	378	P	10	W
3.0	378	X, P, Y	17, 34, 68	W, WA
3.34	420	X, X' Y, Y'	10	S
3.34	420	P	10	WP
3.34	420	P	10*	WA
3.34	420	X, Y	10*	ERA
3.57	450	b	4*	GE
3.62	456	q	5	PS
3.62	456	X, Y	5	WA
3.62	456	P	10	W
3.96	500	3	4*	WP
3.96	500	Q(1, 2, 4)	0 – 45	
4.13	520	X, X', Y, Y'	10	S
4.13	520	P	10	WP
4.13	520	P	10*	WA
4.13	520	X	10	WA
4.13	520	X, Y	10	ERA

TABLE C.2 (Cont'd)

Scaled Radius, λ	Radial Distance, Ft.	Measurement	Gage Depth Ft.	Gage Type
4.15	525	X, Y	10	ERA+
4.30	542	q	5	PS
4.3	542	X, P, Y	5	W, WA
4.3	542	3	1.166*	WP
4.46	562.5	S(1)	2	
4.76	600	b	4*	GE
4.85	610	X, Y	10	ERA+
4.96	625	Q(1), S(2,3)	0–45, 2	
5.09	642	P	10, 20, 30	WP
5.09	642	P'	30	WP
5.09	642	X, X', Y, Y'	10	S
5.09	642	X, X', Y, Y'	20	S
5.09	642	X, X' Y	30	S
5.09	642	P	10*	WA
5.09	642	X	10	WA
5.09	642	X, Y	10	ERA
5.2	655	X, Y	5	WA
5.2	655	P	10	W
5.4	680	3	4*	WP
5.73	723	b, 3	400*, 600*	BJ, WP
5.75	725	X, Y	10	ERA+
5.95	750	b	4*	GE
5.95	750	Q(1,2,4), S(1,2,3)	0–45, 2	
6.00	755	X, Y	10	ERA+
6.25	788	X, Y	5	WA
6.25	788	P	10	W
6.30	794	X, Y	10	ERA
6.30	794	X, X', Y, Y'	10	S
6.30	794	P	10	WP
6.30	794	P	10*	WA
6.30	794	X	10	WA
6.70	845	X, Y	10	ERA
6.94	875	S(1)	2	
6.96	880	X, Y	10	ERA+
7.14	900	b	4*	GE
7.3	920	3	4*	WP
7.5	945	X, Y	5	WA
7.5	945	P	10	W
7.5	945	3	3.33*	WP
7.80	982	X, X', Y, Y'	10	S
7.80	982	P	10	WP
7.80	982	P	10*	WA
7.80	982	X, Y	10	ERA
7.93	1000	Q(1), S(1,2,3)	0–45, 2	
7.97	1005	X, Y	10	ERA+
8.15	1025	P	10	W
8.15	1025	X, P, Y	17, 34, 68	W, WA
8.33	1050	b	4*	GE
8.35	1055	X, Y	10	ERA+
9.52	1200	b	4*	GE
9.63	1200	X, X', Y	10	S
9.63	1200	X, Y, Y'	20	S
9.63	1200	X, X', Y, Y'	30	S
9.63	1213	P	10, 20, 30	WP
9.63	1213	P'	20	WP
9.63	1213	P	10*	WA
9.63	1213	X	10	WA
9.63	1213	X, Y	10	ERA
9.75	1230	X, Y	[illegible]	WA
9.75	1230	P	10	W
9.92	1250	3	4*	WP
9.92	1250	3	0	In(4)
9.92	1250	S(1,2,3)	2	
10.7	1350	b	4*	GE
11.7	1480	X, Y	5	WA
11.7	1480	P	10	W
11.7	1480	3	3.33*	WP
11.9	1500	X, X', Y, Y'	10	S
11.9	1500	P	10	WP
11.9	1500	b	4*	GE
11.9	1500	S(1)	2	
11.9	1500	P	10*	WA
11.9	1500	X, Y	10	ERA
13.5	1700	3	4*	WP
13.5	1700	X	0	In(5)
14.8	1875	S(1)	2	
15.0	1890	X, Y, Y'	10	S
15.0	1890	X, X', Y, Y'	20	S
15.0	1890	X, X', Y	30	S
15.0	1890	P	10, 20, 30	WP
15.0	1890	P'	30	WP
15.0	1890	P	10*	WA
15.0	1890	X	10	WA
15.0	1890	X, Y	10	ERA
16.9	2130	X, Y	5	WA
16.9	2130	P	10	W
16.9	2130	3	4	WP

TABLE C.2 (Cont'd)

TABLE C.2 (Cont'd)

Scaled Radius, λ	Radial Distance, Ft.	Measurement	Gage Depth Ft.	Gage Type
18.2	2300	X	4*	WP
18.5	2331	X,X',Y,Y'	10	S
18.5	2339	X, Y	10	
18.8	2351	P	10	ERA
23.6	3000	X,X',Y,Y	10	WP
23.8	3000	P	10	S
23.8	3000	X, Y	10	WP
24.4	3080	X, Y	5	ERA
24.4	3080	P	10	WA
24.4	3080	X	3.33*	X
24.6	3100	X	4*	WP
Surface Nuclear Shot:				
1.98	250	Q(1)	0-45	
2.18	275	P	10	
2.18	275	X,X',Y,Y'	10	WP
2.18	275	X,Y	10	S
2.18	300	X	4	ERA
2.40	312.5	Q(1,2,3)	0-45	GE
2.70	340	X,Y	10	
2.70	340	X,X',X,Y	10	ERA
2.70	340	X,Y,Y'	20	S
2.70	340	X,X',Y,Y'	30	S
2.70	340	P	10,20,30	WP
2.70	340	P'	20	WP
2.97	375	Q(1,2,3)	0-45	
3.34	420	X,X',Y,Y'	10	S
3.34	420	P	10	WP
3.34	420	X,Y	10*	ERA
3.96	500	X	4*	WP
3.96	500	Q(1,2,3)	0-45	
4.13	520	X,X',Y,Y'	10	S
4.13	520	P	10	WP
4.13	520	X,Y	10	ERA
4.46	562.5	S(1)	2	
4.76	600	X	4*	GE
4.96	625	Q(1),S(2,3)	0-45,2	
5.09	642	P	10,20,30	WP
5.09	642	P'	30	WP
5.09	642	X,X',Y,Y'	10	S
5.09	642	X,X',Y,Y'	20	S
5.09	642	X,X',Y	30	S
5.09	642	X,Y	10	ERA
5.4	680	X	4*	WP
5.95	750	Q(1,2,3),S(1,2,3)	0-45,2	
6.30	794	X,Y	10	ERA
6.30	794	X,X',Y,Y'	10	S
6.30	794	P	10	WP
6.70	845	X,X	400*,600*	AV, PS
6.94	875	S(1)	0-45, 2	
7.14	900	X	4*	GE
7.3	920	X	4*	WP
7.40	932	X,X',Y,Y'	10	S
7.40	932	P	10	WP
7.40	932	X,Y	10	ERA
7.53	1000	Q(1),S(1,2,3)	2	
5.52	1200	X	4*	GE
5.63	1200	X,X',Y,Y	10	S
9.63	1200	X,Y,Y'	20	S
9.63	1200	X,X',Y,Y'	30	S
9.63	1223	P	10,20,30	WP
9.63	1223	P'	20	WP
9.63	1223	X,Y	10	ERA
9.92	1250	X	4*	WP
9.92	1250	S(1,2,3,)	2	
11.5	1500	X,X',Y,Y'	10	S
11.9	1500	P	10	WP
11.5	1500	X	4*	GE
11.9	1500	S(1)	2	
11.9	1500	X,Y	10	ERA
13.5	1700	X	4*	WP
14.2	1800	X	4*	GE
14.8	1875	S(1)	2	
15.0	1890	X,X,Y,Y'	10	S
15.0	1890	X,X',Y,Y'	20	S
15.0	1890	X,X',Y	30	S
15.0	1890	P	10, 20, 30	WP
15.0	1890	P'	30	WP
15.0	1890	X,Y	10	ERA
16.6	2100	X	4*	GE
18.2	2300	X	4*	WP
18.5	2331	X,X',Y,Y'	10	S
18.5	2379	X,Y	10	ERA
18.8	2381	P	10	WP
19.0	2400	X	4*	GE
21.4	2700	X	4*	GE
23.8	3000	X,X',Y,Y	10	S

TABLE C.2 (Cont'd)

Scaled Radius, λ	Radial Distance, Ft.	Measurement	Gage Depth Ft.	Gage Type
23.8	3000	P	10	WP
23.8	3000	X,Y	10	ERA
24.6	3100	X	10	
24.6	3100	X	4*	WP
KE-1:				
2.01	37.56	X	4*	GE
2.06	28.4	X,Y	5	WA
2.49	34	X	1.166*	WP
2.49	34	X,P,Y	5	X, WA
2.49	34.22	X,Y	1.5	ERA
3.0	41	X,Y	5	WA
3.0	41.52	X,Y	1.5	ERA
3.62	49.5	X,Y	5	WA
4.30	58.8	X,P,Y	5	X, WA
4.30	58.8	X	1.666*	WP
4.3	58.98	X, Y	1.5	ERA
5.2	71.1	X,Y	5	WA
5.54	75.84	X	4*	GE
6.25	85.5	X,Y	5	WA
6.25	85.78	X,Y	1.5	ERA
7.5	102.5	X	1.166*	WP
7.5	103.3	X,Y	1.5	ERA
8.0	109.57	X	4*	GE
9.0	123	X,Y	5	WA
10.2	139.64	X	4*	GE
10.8	148	X,Y	5	WA
10.8	148.44	X,Y	1.5	ERA
12.4	169.57	X	4*	GE
13.0	178	X,Y	5	WA
13.0	178	X	1.166*	WP
14.6	199.57	X	4*	GE
15.9	217	X,Y	5	WA
18.6	262.28	X	1.5	ERA
19.2	262	X,Y	5	WA
23	314	X,Y	5	WA
23	314	X	1.166*	WP
27.6	378	X,Y	5	WA
27.6	378.34	X,Y	1.5	ERA
39.6	542	X,Y	5	WA
39.6	542	X	1.166*	WP
57.5	788	X,Y	5	WA
75	1025	X,Y	5	WA
75	1025	X	1.166	WP
108	1480	X,Y	5	WA
KE-2:				
1.72	58.8	P	5	X
2.06	71.1	X,P,Y	5	X, WA
2.49	85.5	Q	5	PS
2.49	85.5	X,Y,Y,Y'	5	X
2.49	85.5	X	1.166*	WP
2.49	85.5	X,P,Y	5	X, WA
2.49	85.5	P	5	WP
2.49	85.5	X,Y	5	ERA
2.89	99.18	X	4*	GE
3.0	102.5	X,X',Y	5	S
3.0	102.5	Q	5	PS
3.0	102.5	X,P,Y	5	X, WA
3.0	102.5	P	5	WP
3.0	102.5	X,Y	5	ERA
3.6	123	X,Y,Y'	5	S
3.6	123	P	5	WP
3.6	123	P'	5	WP
3.62	123	X,Y	5	WA
3.62	123	X,Y	5	ERA
4.30	148	X,P,Y	5	X, WA
4.30	148	X	1.166*	WP
4.37	149.4	X	4*	GE
5.22	178	X,X',Y,Y'	5	S
5.2	178	P	5	WP
5.2	178	X,Y	5	WA
5.7	178	Q	5	PS
5.2	178	X,Y	5	ERA
5.56	190.23	X	4*	GE
6.35	217	X,P,Y	5	X, WA
6.35	217	X	1.166*	WP
6.58	225.15	X	4*	GE
7.46	255.38	X	4*,	GE
7.5	262	X,X',Y	5	S
7.5	102.5	X,Y	5	WA
7.66	262	P	5	WP
7.66	262	P'	5	WP
7.66	262	X,Y	5	WA
7.66	262	X,Y	5	ERA
8.33	285.16	X	4*	GE

TABLE C.2 (Cont'd)

Scaled Radius, λ	Radial Distance, Ft.	Measurement	Gage Depth Ft.	Gage Type
9.2	314	H,V	5	WA
9.21	315.2	b	Lo	GZ
10.0	344.87	b	Lo	GZ
10.9	374.86	b	Lo	GZ
11.0	375	P	5	WP
11.0	376	H,V	5	H
11.0	378	H,P,V	5	H, WA
11.0	378	B	1.166*	WP
11.0	378	H,V	5	IRA
14.9	512	P	5	WP
15.0	512	B	1.166*	WP
15.0	542	H,V	5	IRA
15.9	542	H,H',V	5	H
23	788	H,V	5	WA
29.9	1025	H,V	5	IRA
29.9	1025	H,V,V,V'	5	H
29.9	1025	H,V	5	WA
29.9	1025	B	1.166*	WP
29.9	1025	H,V	5	IRA
39.4	1350	H,V	5	WA
43.3	1480	H,V	5	H
62.3	2130	H,H',V,V'	5	H
90	3080	H,H',V,V'	5	H
KT-31				
1.72	23.5	P	5	H
2.06	28.4	B	1.166*	WP
2.06	28.4	H,P,V	5	H, WA
2.49	34	H,P,V	5	H, WA
3.0	41	B	1.166*	WP
3.0	41	H,P,V	5	H, WA
3.62	49.5	H,P,V	5	H, WA
4.3	58.8	H,P,V	5	H, WA
4.3	58.8	B	1.166*	WP
5.2	71.1	H,P,V	5	H, WA
6.25	85.5	H,P,V	5	H, WA
6.25	85.5	B	1.166*	WP

TABLE C.2 (Cont'd)

Scaled Radius, λ	Radial Distance, Ft.	Measurement	Gage Depth Ft.	Gage Type
7.5	102.5	H,V	5	WA
7.5	102.5	B	5	H
10.8	144	H,P,V	5	H, WA
10.8	144	B	1.166*	WP
15.9	178	H,P,V	5	H, WA
15.9	178	B	1.166*	WP
23	314	H,P,V	5	H, WA
23	314	B	1.166*	WP
39.6	542	H,P,V	5	H, WA
39.6	542	B	1.166*	WP
98.2	1340	H,V	5	WA
KT-41				
1.72	23.5	P	5	H
2.06	28.4	B	1.166*	WP
2.06	28.4	H,P,V	5	H, WA
2.49	34	H,P,V	5	H WA
3.0	41	B	1.166*	WP
3.0	41	H,P,V	5	H, WA
3.62	49.5	H,P,V	5	H, WA
4.3	58.8	H,P,V	5	H, WA
4.3	58.8	B	1.166*	WP
5.2	71.1	H,P,V	5	H, WA
6.25	85.5	H,P,V	5	H, WA
6.25	85.5	B	1.166*	WP
7.5	102.5	H,V	5	WA
7.5	102.5	P	5	H
10.8	144	H,P,V	5	H, WA
10.8	144	B	1.166*	WP
15.9	178	H,P,V	5	H, WA
15.9	178	B	1.166*	WP
23	314	H,P,V	5	H, WA
23	314	B	1.166*	WP
39.6	542	H,P,V	5	H, WA
39.6	542	B	1.166*	WP
104	1480	H,V	5	WA

Notes:

(1) The scaled radius, λ_R, is defined as

$$\lambda_R = R/W^{1/3}$$

where R is the radial distance in feet from ground zero and W is equivalent energy in pounds of TNT. W for JANGLE nuclear shots has been arbitrarily taken as 1.0 KT of TNT (2×10^6 pounds).

(2) Radial distance of measurements from ground zero in feet.

(3) Symbols used identify the type measurement as follows:

- b peak air pressure (velocity method)
- B air blast as a function of time
- F transient displacement fiducial markers
- H horizontal radial accelerometers
- P hydrostatic earth pressure
- q first earth motion arrival time
- Q shear shaft stations
- S shock pin stations
- T transverse accelerometers
- V vertical accelerometers

Notes to Table C.2 (Cont'd)

An apostrophe (') after the letter symbol indicates a "back-up" gage.

Numbers after the letter symbols Q and S indicate the following:

1 station on south line (S20°W)
2 station on west line (N70°W)
3 station on east line (S70°E)
4 station on southeast line (S55°E)

(4) Depth of gage in feet. Those column entries marked with an asterisk (*) indicate height above ground surface in feet.

(5) Symbols used in this column designate the type of gages as follows:

A Schaevitz accelerometers
BJ special blast switch (BHL)
BS special blast switch (SC)
ERA Engineer Research Associates accelerometers. A mark (+) after the symbol indicates location in the structures area.
GE General Electric vacuum switch types FA15 and FA6
If interferometer (self recording buck gage)
N hydrostatic pressure gage in oil filled neoprene bag.
PB Bendix pressure gage type T TP-9
PS pendulum seismic switch (DEMB)
WA Wiancko accelerometers
WP Wiancko pressure gages
Wd wooden black and white targets for transient displacement photography.

APPENDIX D

RADIOACTIVITY AND BIOMEDICAL MEASUREMENTS INSTRUMENTATION

D.1 GENERAL

The principal items of test instrumentation for Program 2 projects and station locations or areas of operation are outlined in the following paragraphs.

D.2 PROJECT 2.1a

Scintillation counters, with 4 pi detectors mounted 28 inches above ground, were employed for measurement of gamma radiation intensity as a function of time and distance. A pattern of 27 stations for the surface shot and 29 stations for the underground shot, Figures D-1 and D-2, was used. Close in stations, marked Double Stations, had a second detector which popped up into position after passage of blast wave.

D.3 PROJECT 2.1b

Five droppable gamma radiation telemetering units, AN/USQ-1, were placed on ground mounts on a NE radial line for each shot, at distances 1000, 1250, 1500, 2000, and 3000 feet from zero. Receivers, AN/ARR-29, on a P2V aircraft and at ground station monitored from 0 to + 15 minutes. Subsequent test air drops of AN/USQ-1 units in both craters were made.

D.4 PROJECT 2.1c-1

Three C-47 type aircraft were directed over a pre-set grid pattern at average altitude of 600 feet several hours after detonation. Scintillation gamma detectors and atmospheric-conductivity equipments were employed to assess the pattern and relative intensity of ground contamination.

D.5 PROJECT 2.1c-2

A P2V aircraft equipped with ionization chamber detectors AN/ARR-4 and a B-17 equipped with phosphor-photomultiplier detectors type F-1 were employed to evaluate these equipments for rapid aerial survey of ground gamma radiation field intensities.

D.6 PROJECT 2.1d

AN/PDR-T1B survey instruments, calibrated with gamma rays from an equilibrium radium source, were used for gamma radiation field intensity measurements. Data includes general area survey after each shot and post test survey of crater and lip intensities.

D.7 PROJECT 2.3-1

Total gamma radiation dosage measurements were made using a number of photographic films of graduated sensitivity placed in National Bureau of Standards type film badge holders. Film dosimeters were exposed 3.5 feet above ground at all Program 2 project stations and in foxholes, tanks, and some structures.

D.8 PROJECT 2.3-2

Standard two-man foxholes instrumented with gamma film dosimeters were constructed at 500-foot intervals on a NE radial line from 2000 to 5000 feet for both shots. In addition one man foxholes and 6-inch diameter soil pipes similarly instrumented were located at 3000 and 4000 feet distance on the same radial line. All openings were 48 inches in depth with film dosimeters placed at zero, 16 inches, 32 inches, and 48 inches depth.

D.9 PROJECT 2.4a

Photographic film packets were used to study beta ray energies and the ratio of beta to gamma ray ionization of residual contamination from both shots. A total of 46 film stations was set up for each shot along three radial lines, extending to 12,000 feet on a N line and 6000 feet on a NE and a NW line.

Energy dependent dosimeters (modified Landsverk Model L-50 100-r dosimeter and Model L-66 2-r dosimeter) and energy dependent survey meters (modified Tracerlab-type SU-1E "Cutie Pies") were employed to assess the effective gamma ray energy over the period from 5 hours to several days after detonation. The surface shot stations were located on south, NE and NW lines at distances from 700 to 3200 feet. The underground shot stations were placed from 1800 to 3000 feet along a south radial line.

D.10 PROJECT 2.4b

Sets of spherical lucite spheres of graduated wall thickness, instrumented with Sievert ionization chamber, phosphate glass and film in a central cavity, were set out to assess the variation in quality of gamma radiation with depth in unit density material. For the surface shot stations were located on a SW line at distances of 750, 850, 950, 1050, and 1170 yards. For the underground shot, stations were located in a line 10 degrees south of west at distances of 500, 600, 700, 800, and 1000 yards.

D.11 PROJECT 2.4c

Scintillation counter gamma ray spectrometer equipment truck-mounted was used to assess the degraded gamma radiation field spectrum. Measurements were made in the vicinity of a number of Project 2.1a stations (Figure D.1 and D.2) on several successive days after each shot.

D.12 PROJECT 2.5a-1

Particle collection equipment was placed 7 feet above ground at 46 stations in a broad pattern to determine concentration and size distribution of active particles in the near ground aerosols. Station pattern close-in is that of Project 2.1a, Figures D.1 and D.2, with additional stations in the NE (downwind) quadrant at 11,000, 14,000, 20,000, 30,000, and 50,000 feet. Filter samplers were located at all stations for gross sampling of aerosols. Several electrostatic precipitators were similarly employed. Cascade impactors, conifuges and particle separators were used to obtain size graded samples. Continuous air monitors and radiological air samplers provided aerosol activity versus time records and provided samples as a function of time.

D.13 PROJECT 2.5a-2

Differential fall-out collectors used to assess time rate of fall-out and thermal precipitators for near ground aerosol sampling were placed at all stations shown in Figure D.3 except as indicated. One hundred or more fall-out collection trays were placed out for each shot in the pattern of Figure D.4.

D.14 PROJECT 2.5a-3

No field instrumentation. Individual active particles were isolated from fall-out and crater samples for physical and radiochemical study.

D.15 PROJECT 2.6a

Remotely controlled weasels equipped with core and surface sampling devices and a television monitoring system were used for early sampling of the crater lip debris. A mobile power and control station was installed in a 2½ ton K-53 truck. Entry was initiated during the first hour after detonation along an upwind radial access road for each shot.

D.16 PROJECT 2.6c-1

Laboratory radiochemical studies.

D.17 PROJECT 2.6c-2

Laboratory radiochemical studies.

D.18 PROJECT 2.6c-3

A line towing rocket with sampling nose was tested as a technique of remote sampling. The rockets were fired into crater and lip after each shot from a truck mounted launcher at ranges of 1000 feet.

D.19 PROJECT 2.7

Mongrel dogs and sheep were exposed about 3 feet above ground at distances of 2500, 5000 and 8000 feet during each shot. A few animals were placed in standard foxholes at the 2500-and 5000-foot distances. All exposures were in the NE (downwind) quadrant.

D.20 PROJECT 2.8

Large fall-out samples were collected at distances from ½ to 10 miles in the NE quadrant for soil and particle study. Tubs and oil-cloth sheets were used as collectors.

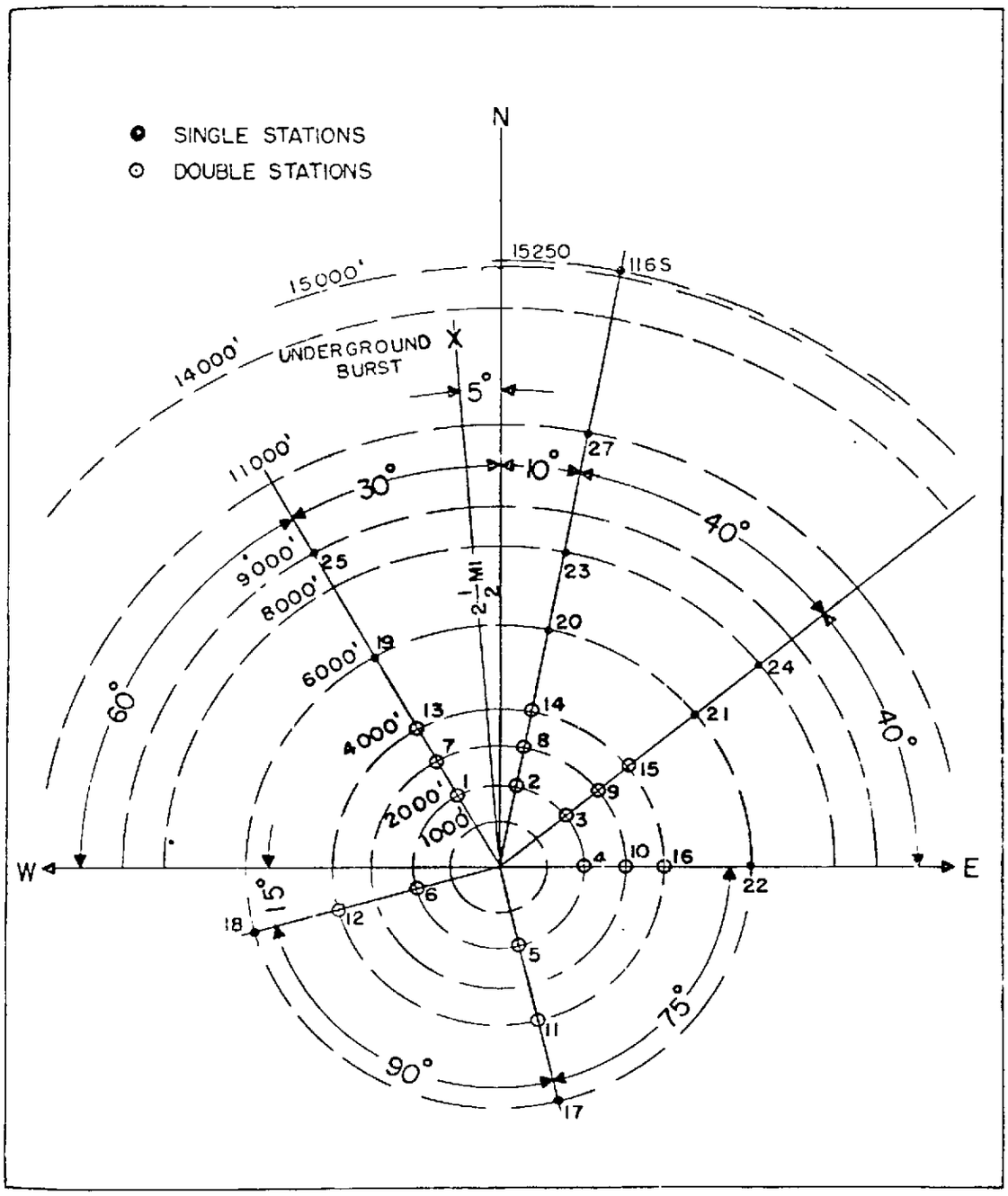

Fig. D.1 Scintillation Counter Station Pattern, Surface Shot

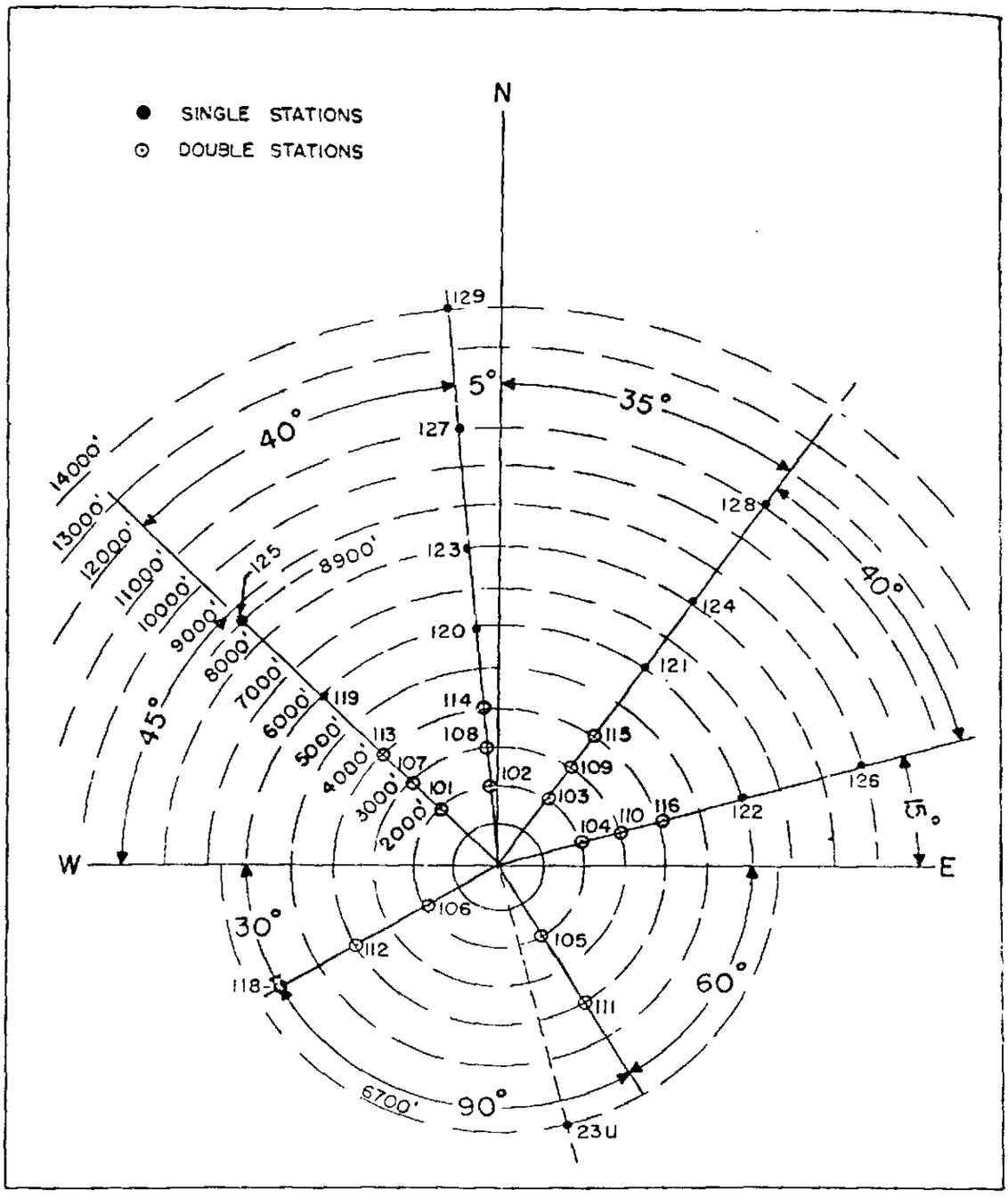

Fig. D.2 Scintillation Counter Station Pattern, Underground Shot

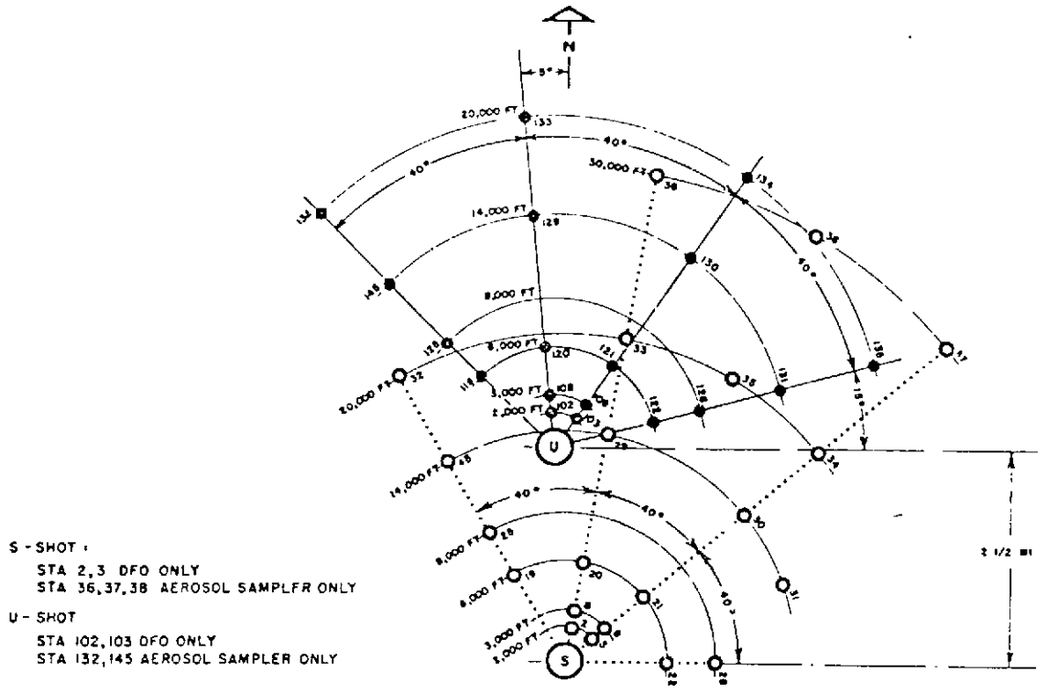

Fig. D.3 Thermal Recipitator and Differential Collector Stations

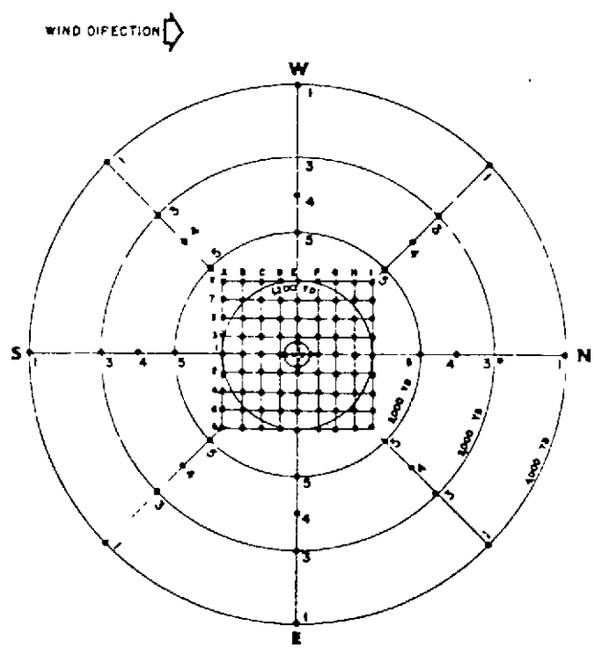

Fig. D.4 Fall-out Collector Pattern

APPENDIX E

STRUCTURES TESTS

E.1 GENERAL

The structures test program of Operation JANGLE included 65 major structures or structural elements. The tests were divided into 26 structural test projects, a project for certain soils studies, and a project for the measurement of transient loading and response of the structures. In addition, measurements of permanent gross displacements were made. Table E.1 lists the structural test projects and Figure E.1 shows the array of the test structures around ground zero.

TABLE E.1

Structural Test Projects

Project	Agency	Description	
3.1a,b	Bureau of Yards and Docks	Light steel frame buildings with corrugated metal siding, 40' x 100'. At 4000 and 10,000 feet from zero.	
3.2a,b,c	Bureau of Yards and Docks	Tripod type antenna towers, 100' high. At 2900,3000 and 3100 feet from zero.	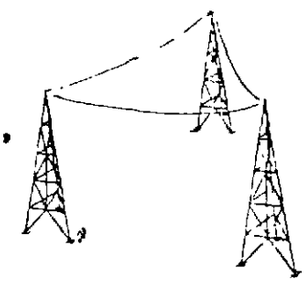
3.2d,e	Bureau of Yards and Docks	Cantilever type antenna towers, 100' high. At 2900 and 3100 feet from zero.	

TABLE E.1 (Cont'd)

Project	Agency	Description	
3.3	Office, Chief of Engineers	1/5 size model of heavy steel column target structure 9' x 12' x 6' high. At 504 feet from zero (see 3.7 for prototype).	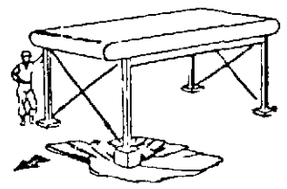
3.4	Office, Chief of Engineers	Reinforced concrete shear wall target structure 33' x 52' x 16' high. At 441 feet from zero.	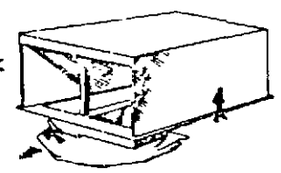
3.5	Office, Chief of Engineers	Reinforced concrete column target structure 11' x 14' x 16' high. At 504 feet from zero.	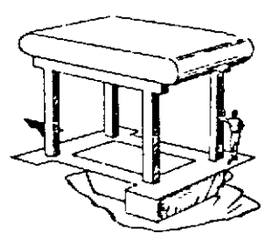
3.6	Office, Chief of Engineers	Three-bay heavy steel column target structure 11' x 47' x 16' high. At 441 feet from zero.	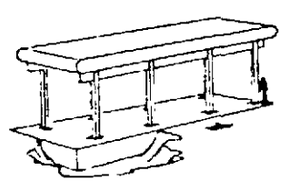
3.7	Office, Chief of Engineers	Single-bay heavy steel column target structure, 24' x 36' x 21' high. At 504 feet from zero.	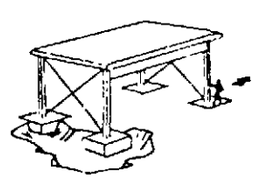

TABLE E.1 (Cont'd)

Project	Agency	Description	
3.8a,b	Office, Chief of Engineers	Single-bay light steel column target structures, 24' x 36' x 21' high. At 630 and 882 feet from zero.	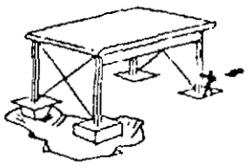
3.9a,b	Air Materiel Command	Reinforced concrete retaining walls, one with loaded face toward zero and one with loaded face away, 12' high. At 900 feet from zero.	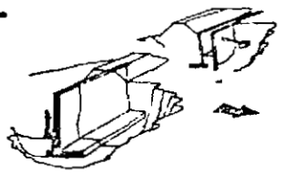
3.10a, b,c	Air Materiel Command	Single-bay, 2-story light reinforced concrete building frames with brick curtain walls, 25' x 27' x 30' high. At 900 feet from zero.	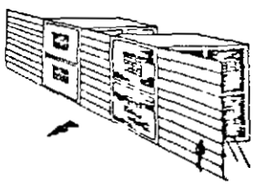
3.11	Air Materiel Command	14" and 18" reinforced concrete pavement slabs, 10' x 150'. At 500 feet from zero.	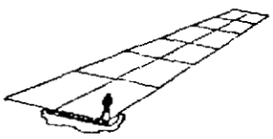
3.12a, b,c	Bureau of Yards and Docks	Precast, prestressed concrete slabs, 20' x 60' x 6" thick. Reinforced concrete slabs 6" x 12" thick, 10' x 60'. At 1200 feet from zero.	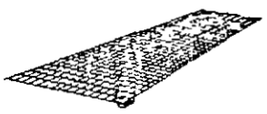

TABLE E.1 (Cont'd)

Project	Agency	Description	
3.13	Office, Chief of Engineers	Buried reinforced concrete box, 25' x 25' x 17' high, open top and bottom, front and rear walls 5' thick. At 238 feet from zero.	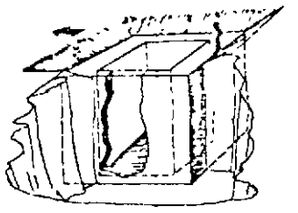
3.15a,b	Bureau of Yards and Docks	Thin-walled rigid frame buried buildings. Precast concrete construction, 20' x 40' x 14' high. At 750 and 1000 feet from zero.	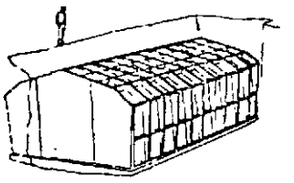
3.16a,b	Bureau of Yards and Docks	Thin-walled circular arch rib buried buildings. Precast concrete construction 20' x 40' x 10' high. At 750 and 1000 feet from zero.	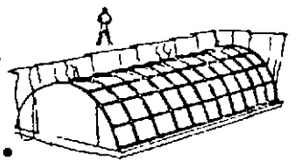
3.17a,b	Bureau of Yards and Docks	Thin-walled dome-shaped buried buildings. Precast concrete construction, 22' diameter at floor x 10' high. At 750 and 1000 feet from zero.	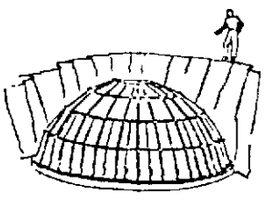
3.18a,b	Bureau of Yards and Docks	Prestressed concrete buried fuel tanks. Precast stave construction, 10' diameter x 8' high. At 750 and 1000 feet from zero.	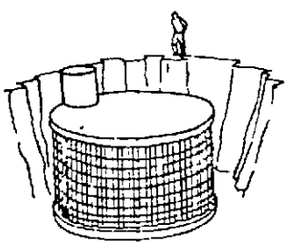

TABLE E.1 (Cont'd)

Project	Agency	Description	
3.19	Air Materiel Command	Unloaded concrete footings and 6' concrete cubes, buried. Located adjacent to several structures	
3.20a_1, a_2	Air Materiel Command	Free standing brick walls, 16' long x 11' high. At 900 and 1050 feet from zero.	
3.20b	Air Materiel Command	Brick wall with superimposed load, 16' long x 11' high. At 1050 feet from zero.	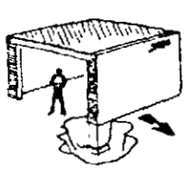
3.20c_1, c_2	Air Materiel Command	50' high brick chimneys. At 750 and 1050 feet from zero.	
3.21a_1-f_1 3.21a_2-f_2	Air Materiel Command	Two arrays of buried square boxes, open at top and bottom. Reinforced concrete and steel construction, between 8' and 20' square with 4" to 8" walls of reinforced concrete and one of 12 gage steel. One array at 725 and one at 850 feet from zero.	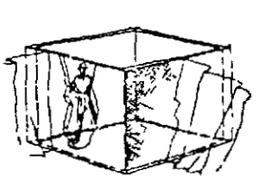

TABLE E.1 (Cont'd)

Project	Agency	Description	
3.23a_1, a_2	Air Materiel Command	Circular section reinforced concrete tunnels, 6' in diameter with 5" wall.	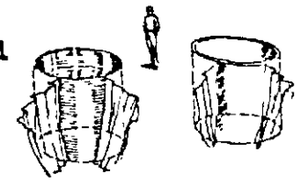
3.24a_1, a_2	Air Materiel Command	Friction pile clusters. 3 timber piles 20' long in each cluster. At 475 feet from zero.	
3.26a-e	Bureau of Yards and Docks	Water, sewer, air, steam and electric lines, all underground. Extended between 600 and 1800 feet from zero.	
3.27	Air Materiel Command	Two-foot concrete cubes, buried. Located adjacent to several structures	

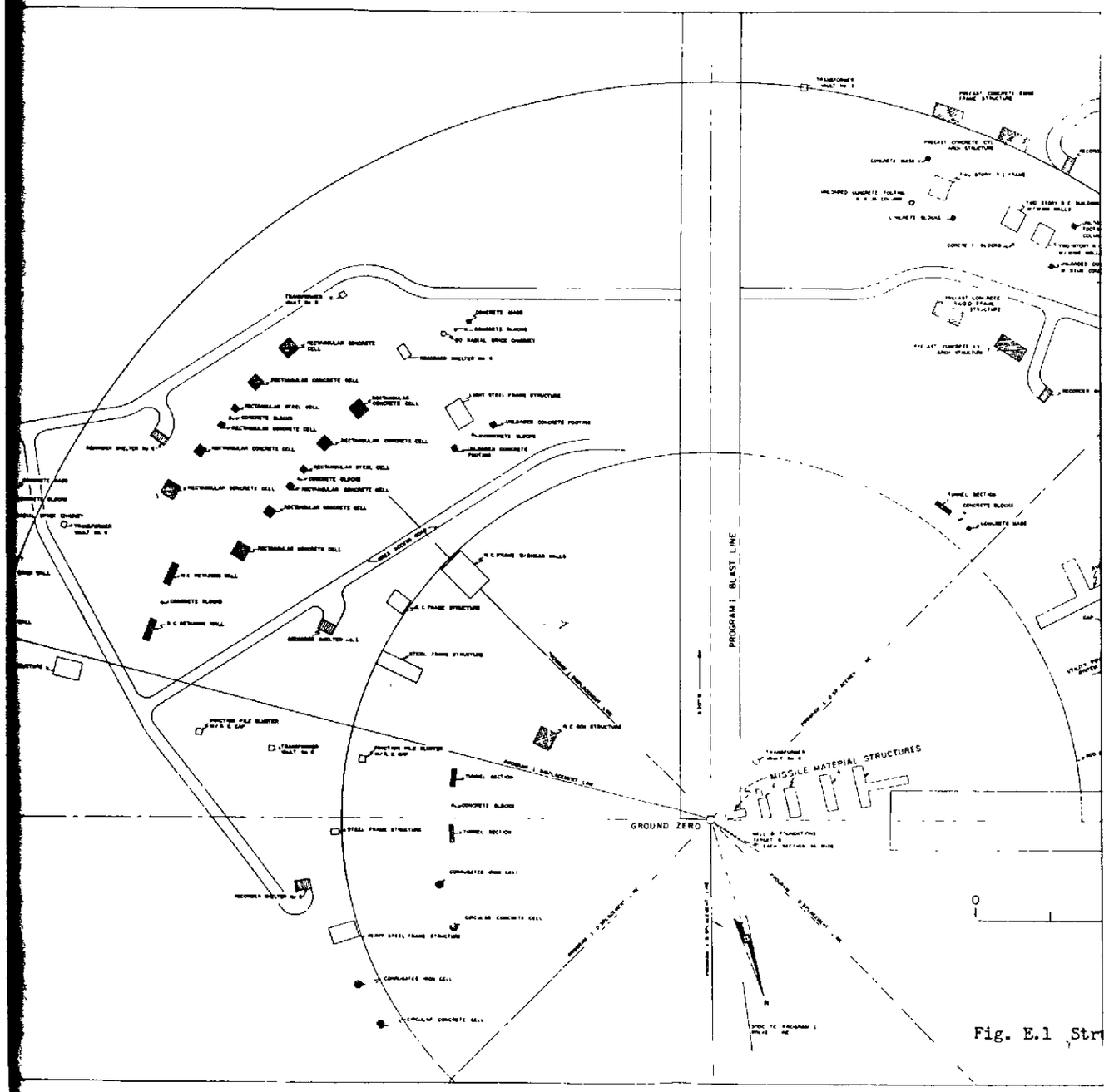
PROGRAM I BLAST LINE
MISSILE MATERIAL STRUCTURES
GROUND ZERO

Fig. E.1 Str